NASA TECH BRIEFS®

Welcome to your Digital Edition of *NASA Tech Briefs, Imaging Technology, and Motion Control and Automation Technology*

Included in This June Edition:

NASA Tech Briefs

Click Here

Imaging Technology

Click Here

Motion Control and Automation Technology

Click Here

How to Navigate the Magazines:

At the bottom of each page, you will see a navigation bar with the following buttons:

Arrows: Click on the right or left facing arrow to turn the page forward or backward.

Introduction: Click on this icon to quickly turn to this page.

Cover: Click on this icon to quickly turn to the front cover.

Table of Contents: Click on this icon to quickly turn to the table of contents.

Zoom In: Click on this magnifying glass icon to zoom in on the page.

Zoom Out: Click on this magnifying glass icon to zoom out on the page.

Find: Click on this icon to search the document.

You can also use the standard Acrobat Reader tools to navigate through each magazine.

June 2014 www.techbriefs.com Vol. 38 No. 6

NASA Tech Briefs®

ENGINEERING SOLUTIONS FOR DESIGN & MANUFACTURING

SAE INTERNATIONAL

Industry Roundtable: 3D Printing

Space Station Air Scrubber Purifies Homes

Create the Future Design Contest 2014

Last Chance to Enter!
See page 8

Imaging Technology

Motion Control and Automation Technology


MOST PREFERRED DISTRIBUTOR
RATED #1
Source: 2013 Most Preferred Distributor, Distributor Customer Evaluation Study, North America, May 2013, UBM Electronics
THE TOP BRANDS from THE TOP DISTRIBUTOR
1.800.344.4539
DIGIKEY.COM
Digi-Key® CORPORATION
1,000,000+ PRODUCTS IN STOCK | 650+ INDUSTRY-LEADING SUPPLIERS | 3.6 MILLION PARTS ONLINE
Digi-Key is an authorized distributor for all supplier partners. New products added daily. © 2014 Digi-Key Corporation, 701 Brooks Ave. South, Thief River Falls, MN 56701, USA
ecia ecsn member CEDA
Free Info at http://info.hotims.com/49746-701

Technologies of the Month

Sponsored by yet2.com

For more information on these and other new, licensable inventions, visit *www.techbriefs.com/techsearch*

Reseatable Pressure Relief Valve Prevents Leaks

DuPont

A new technology prevents leaks in low-pressure (less than 50 psi) relief valves. To form a tight seal, the valve spring compresses the valve's O-ring between two planar mating surfaces. Both the valve seat and the sealing surface of the valve head are oriented substantially perpendicular to the valve axis. A pressure differential increases the extent of compression between the resilient valve seal and both sealing surfaces.

The resilient valve seal is an annular O-ring that deforms to a predetermined extent into sealing engagement against both sealing surfaces. When the pressure of a fluid within the vessel exceeds the desired spring biasing force, the valve face lifts from the valve seat to relieve pressure within the vessel. Applications include lab glassware and gloveboxes, or vacuum commercial operations where the content environment must be rigorously controlled.

Get the complete report on this technology at:
www.techbriefs.com/tow/201406a.html
Email: nasatech@yet2.com
Phone: 781-972-0600

Sounding Technology Analyzes Reservoir Beds

Laser Consult

A novel technology investigates reservoir beds of oil, gas, freshwater, and thermal water deposits. The system, which uses electromagnetic frequency broadband sounding, gathers information to a depth of up to 7,000 meters. For effective operation on deposits, the technology draws up scientifically substantiated references for the allocation of injection wells.

The sounding system discloses and identifies mineral types; nonconventional hydrocarbons/shales; and dynamic changes, including the process of mass movement. Using a helicopter or small airplane, deposits in swamps, mountains, and other hard-to-reach places can be explored, and a system information model can be constructed. The method is ecologically safe, and searches are achieved in abnormal operation conditions, including crystalline shield, salt beds and pillars.

Get the complete report on this technology at:
www.techbriefs.com/tow/201406b.html
Email: nasatech@yet2.com
Phone: 781-972-0600

TechNeeds — Requests for Technologies

TechNeeds are anonymous requests for technologies that you and your organization may be able to fulfill. Responding to a TechNeed is the first step to gaining an introduction with a prospective "buyer" for your technology solution.

Fabrics with an Inherent Thickness

A foam shape must be replaced with a knitted, woven, or nonwoven fabric that derives its thickness from the geometric structure of its components. The current application uses polyurethane foams that range from millimeters to 2 cm thick. The foams offer little or no ventilation in a situation where air circulation can be critical. New materials at the fiber level must be used to create a light fabric with a build-in structural thickness and loft. Possible solution areas include mathematical models of knitting matrices and nonwoven manufacturing techniques.

Respond to this TechNeed at:
www.techbriefs.com/tn/201406c.html
Email: nasatech@yet2.com
Phone: 781-972-0600

Sterility Verification of a Flowing Liquid

A client seeks a device capable of detecting contamination in a liquid flow. The system needs to detect non-liquid particles, bacteria, yeasts, mold, and/or spores in a continuous liquid stream. Any proposed sensing methodology must not physically interact with the liquid flowing in the interior of the channel. In operation, the detection system should report any contamination; the nature of the contamination can be determined later. A proposed solution need not identify the specific contaminant. An optical or light-based system is desired, but a variety of technologies may be acceptable if they do not require the fluid flow to be sampled directly.

Respond to this TechNeed at:
www.techbriefs.com/tn/201406d.html
Email: nasatech@yet2.com
Phone: 781-972-0600

TECH BRIEFS®
ENGINEERING SOLUTIONS FOR DESIGN & MANUFACTURING

June 2014 • Vol. 38 No. 6

FEATURES

SOLUTIONS

(Solutions continued on page 6)

8


74


80


DEPARTMENTS

NEW FOR DESIGN ENGINEERS

SPECIAL SUPPLEMENT

Follows page 40 in selected editions only.

Contents *continued*

PRODUCT OF THE MONTH

The USB-2404-UI from Measurement Computing (Norton, MA) is designed for multipurpose testing.

74

ON THE COVER

The 3D Printer in Zero-G Technology Demonstration payload, seen here undergoing final flight certification testing at NASA's Marshall Space Flight Center, will launch soon to the International Space Station. Designed and built by Made in Space, it will be the first 3D printer to fly in space. Learn about this one-of-a-kind application, and find out how executives at leading 3D printer companies are dealing with an explosion in both technology and customers in the Industry Roundtable beginning on page 14.

(Photo by Emmett L. Given, NASA MSFC)

SCALEXIO

SCALEXIO® — Software Configurable and Scalable Test System

Testing aerospace systems for different programs and variants leads to increased investments in test systems — unless you have dSPACE SCALEXIO.

Thanks to SCALEXIO's scalability and software reconfigurable hardware, you can change your entire system input and output channel configuration without making expensive hardware changes.

Cut costs! Increase Efficiency!

dSPACE SCALEXIO

Embedded Success dSPACE

Free Info at http://info.hotims.com/49746-706

A Step Up for R2

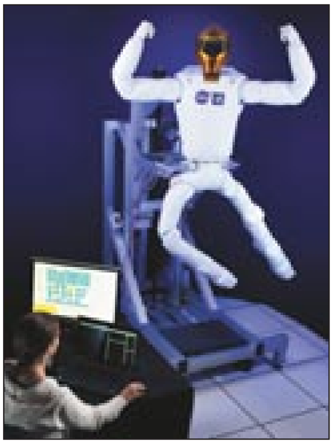

Robonaut 2 with his climbing legs. (NASA)

The lower limbs for the humanoid Robonaut 2 (R2) are aboard the International Space Station (ISS) awaiting attachment by a station crewmember to R2's torso, which arrived on the ISS in February 2011 during the last flight of the space shuttle Discovery. That event signaled the first human-like robot to arrive in space to become a permanent resident of the laboratory. Jointly developed by NASA and General Motors, R2 showcases how a robotic assistant can work alongside humans, whether tasks are done in space or on Earth in a manufacturing facility.

R2 now consists of a head and a torso with two arms and two hands. With the addition of the climbing legs, the robot can augment its chief role: to help astronauts by taking over some of their duties on the space station. But before R2 is up and running with its new limbs, there's some assembly required.

"We've got a number of upgrades we're doing," said Ron Diftler, Robonaut Project Manager at NASA Johnson Space Center. "In sending up the legs, we also have to change things inside R2's body." That includes new computers, new wiring, mechanical assembly, and interfacing the legs to R2's main processor. "We see about 20 hours of ISS crew time to do the task, following detailed procedures and done over at least a month," Diftler said.

Right now, R2's torso, head, and arms are secured to a stationary base, so crewmembers take tasks to the robot. But getting a "leg up" on mobility extends the jobs R2 can perform. "We call them the 3 Ds: the dull, dangerous, and dirty," Diftler noted. "That's what robots are for. The astronauts are highly capable individuals that should not have to do all the tasks that require a human-like hand."

Watch Robonaut 2's climbing legs in motion on Tech Briefs TV at www.techbriefs.com/tv/robonaut-legs. For more information on Robonaut2, go to: http://robonaut.jsc.nasa.gov.

Jet Fuel from Sunlight

The European Union-funded Solar chemical reactor demonstration and Optimization for Long-term Availability of Renewable JET fuel (SOLAR-JET) project has successfully demonstrated the production chain for renewable kerosene obtained directly from sunlight, water, and carbon dioxide, potentially revolutionizing the future of aviation.

The SOLAR-JET project demonstrated an innovative process technology using concentrated sunlight to convert carbon dioxide and water to a so-called synthesis gas (syngas). This is accomplished by means of a redox cycle with metal-oxide based materials at high temperatures. The syngas, a mixture of hydrogen and carbon monoxide, is finally converted into kerosene by using commercial Fischer-Tropsch technology.

Although still at an early stage of development, the processing of syngas to kerosene is already being deployed by companies, including Shell, on a global scale. This combined approach has the potential to provide a secure, sustainable, and scalable supply of renewable aviation fuel, and more generally for transport applications. Fischer-Tropsch derived kerosene is already approved for commercial aviation.

Visit www.solar-jet.aero to learn more.

> Last Chance to "Create the Future"

The 12th annual "Create the Future" Design Contest, sponsored by COMSOL and Mouser Electronics, along with Intel® and Analog Devices, closes for entries on July 1, 2014. If you haven't submitted your entry, go to www.createthefuturecontest.com today for your chance to receive global recognition and a Grand Prize of $20,000 for your new product idea. Entries can be submitted in seven different categories. Don't miss your chance to "Create the Future." Visit www.createthefuturecontest.com to submit your entry today.

Editor's Choice

The Lunar Organic Waste Reformer (LOWR) converts organic waste from human space exploration outposts into useful methane and oxygen products. It reduces risks associated with handling organic wastes while recycling waste into products that otherwise would be imported from Earth. In addition, LOWR can be used for converting terrestrial organic waste into fuel for power generation. Find out more in the article on page 54.

> Next Month in NTB

The July issue will feature special coverage on Data Acquisition & Sensing, as well as new electronics products on the market.

CONNECT WITH NTB

facebook.com/NASATechBriefs

linkedin.com/company/tech-briefs-media

twitter.com/NASATechBriefs


Agilent's Electronic
Measurement Group
Keysight
Technologies

Dr. Mary Ann Meador, Senior Research Scientist, Glenn Research Center, Cleveland, OH

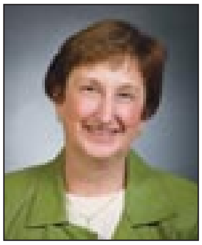

Dr. Mary Ann Meador, Senior Research Scientist at NASA Glenn, guides projects that will synthesize new types of aerogels. Her research has focused on the design and development of new polymers for a variety of applications, including high-temperature composites.

***NASA Tech Briefs*: What are aerogels used for?**

Dr. Mary Ann Meador: Aerogels are low-density solids with a high degree of porosity — 85 to 98%. Different than foams, aerogels have extremely small pores, on the nanometer scale. This makes them 2 to 5 times better insulators than foams, since gas phase heat conduction is very poor. Since they are comprised mostly of air, they also have very low dielectric constants, and hence have application as low-dielectric substrates for devices such as lightweight antennas. Aerogels also have very large internal surface areas, which means they could also be used as sensor platforms. However, the main application is as insulation for aerospace, housing, and construction, or high-performance clothing.

NTB: What are the weaknesses of previous aerogels?

Dr. Meador: The issue with aerogels is their fragility. They have a lot of interesting properties. Because of the way they're made, they have very small pore sizes; that leads to really good insulation qualities, and also very low thermal conductivities, low dielectric, and high surface areas. Because they also have typically been very fragile, it's difficult to put them into use as a monolithic material.

NTB: What were your biggest challenges when creating a polyimide aerogel?

Dr. Meador: With the polyimides, our goal was to improve the mechanical properties so that you would retain all the interesting properties of aerogels, but add the mechanical integrity. We actually were working on a project to design a flexible insulation for inflatable aerodynamic decelerators for Entry, Descent and Landing (EDL). These are essentially large structures that inflate in order to provide drag to slow a spacecraft down, or to slow down another payload to land on the surface of a planet like Mars or even bring things back to Earth. The challenge was to make the aerogel in a flexible form.

The insulation has to be able to withstand certain heat of re-entry, so we chose polyimide as a very-high-temperature stable polymer. Making the aerogel structure from the polymer gives us the ability to make thin films of the aerogel. That's what provides the flexible form of the insulation.

NTB: What are the possibilities with this new flexibility?

Dr. Meador: If you can make a thin film that can now be wrapped around structures, it's a much more conventional way to deliver insulation. Thin films could be used to wrap around a cryotank, to wrap around pipes that are handling cryogenic liquids, or they can be wrapped around things that you want to keep heat in. We think the commercial potential for other types of polymer aerogels would be higher since they may be more cost-competitive with conventional insulation. We are working on polyimide aerogels as an alternative, lower-cost option.

*To read a full transcript of the interview or listen to a downloadable podcast, visit **www.techbriefs.com/podcast**.*

Want to learn more?

Register for a live webcast on NASA Glenn's aerogel technology featuring Dr. Meador on June 19. Go to www.techbriefs.com/webinar214 to register for the free presentation.

NASA Patents

Over the past three decades, NASA has granted more than 1000 patent licenses in virtually every area of technology. The agency has a portfolio of 3000 patents and pending applications available now for license by businesses and individuals, including these recently patented inventions:

Non-Collinear Valve Actuator

U.S. Patent No. 8,322,685

James A. Richard, Marshall Space Flight Center, AL

To regulate the flow of a quarter-turn valve, the weight of a flight system's valve actuator must be reduced. Previous actuators have placed a pressure-actuated piston and return spring system exclusively in line with one another. The weight of return spring systems in the valve actuators, therefore, has depended upon the piston's displacement.

A non-collinear valve actuator includes a primary actuating system and a return spring system. Both systems act on different points of a rotably affixed transmission link, which is one component of a linkage technology responsible for opening and closing a quarter-turn valve. Having the primary actuating system apply force at a greater radial distance than the return spring system increases stroke length while minimizing displacement. By allowing the primary actuating system to undergo longer strokes, the weight of the primary actuating system may be optimized. Furthermore, the non-collinear positioning and diminished displacement reduces the weight of the return spring system and ultimately the weight of the valve actuator.

Ultraminiature Broadband Light Source with Spiral Shaped Filament

U.S. Patent No. 8,264,134

Joseph S. Collura, Henry Helvajian, Michael Pocha, Glenn A. Meyer, Charles F. McConaghy, Barry L. Olsen, and William W. Hansen, Glenn Research Center, Cleveland, OH

White light sources are used to calibrate spectrometers in the visible range. It is desirable, therefore, to have an output source that spans past the visible light spectrum: red, orange, yellow, green, blue, indigo, and violet.

An ultraminiature light source features a generally planar, double-spiral-shaped tungsten filament suspended within a ceramic base. A lid, which is partially transparent, is placed over the ceramic base. The lid may also be coated with dielectric material to selectively transfer specific radiation bands that are selective to the application. The ceramic enclosure includes a reflective bottom, a ledge, and a raised perimeter having a metallic surface. The ledge features metallic surfaces embedded therein for electrical communication with the double-spiral shaped tungsten filament.

Variably Transmittive, Electronically Controlled Eyewear

U.S. Patent No. 8,411,214

John J. Chapman, Louis J. Glaab, Timothy D. Schott, Charles T. Howell, and Vincent J. Fleck, Langley Research Center, Hampton, VA

Specific pilot training and evaluation procedures for instrument flight rating qualification currently involve the use of an opaque hood draped across an aircraft's windscreen. The hood restricts or obscures the student pilot's vision during instrument-only flight sessions. There is a need for a training technique that restricts the pilot's field of view while providing a more realistic and safer training experience.

A flight training and evaluation system includes electronically activated vision restriction glasses that detect the pilot's head position and automatically darken and limit the pilot's ability to see through the front and side windscreens. Thus, the pilot-in-training sees only within the aircraft cockpit, forcing him or her to fly with instruments in the most restricted operational mode.

For more information on the inventions described here, contact the appropriate NASA Field Center's Innovative Partnerships (IP) Office. See page 78 for a list of office contacts.

Check part availability

Industry Roundtable: 3D Printing

It's being called a revolutionary change in the way we design and make products – a disruptive technology that will have far-reaching effects for both engineers and consumers. It's 3D printing, and it is shaping the future of manufacturing. *NASA Tech Briefs* spoke recently with executives at four of the leading 3D printer vendors about what 3D printing is today, what it will be tomorrow, and if it really will change the world.

Our roundtable panel members are Jeff Moe, Founder and CEO of Aleph Objects; Bre Pettis, CEO of MakerBot; Greg Mark, CEO of MarkForged; Conor MacCormack, Co-founder and CEO of Mcor Technologies; and Jon Cobb, Executive Vice President of Corporate Affairs for Stratasys.

NASA Tech Briefs*: 3D printing is being referred to as the next industrial revolution. Is it really on a par with where the personal computer was in the 1980s – on the cusp of being a ubiquitous technology that pervades both our work and home lives, or is that democratization of the technology still years away?*

> "We focus on customer feedback – people looking to print parts with the strength of metal, at their desk. That will enable thousands of engineers to fabricate parts when they need them, without waiting in a long queue for machine time."
>
> *Greg Mark*
> *MarkForged*

Greg Mark: Nobody knows. Technology has a way of sneaking up on you, but it's impossible to predict exactly when that will occur, or how people will use it.

Bre Pettis: We do see the 3D printing industry paralleling the personal computer industry. Thirty years ago, consumers used to ask the question, "why do I need a computer in my home? I have a calculator." Today, everyone has a computer more powerful than we ever dreamed of right in his or her pocket – their smartphone. We see 3D printing going in the same direction.

Jeff Moe: 3D printing technology is a few years away from becoming ubiquitous. Today, we do have customers around the world using our machines, but right now, the 3D printing market reminds me of Linux in the 1990s. For us, ease of use cannot and will not come at the expense of making good hardware.

Jon Cobb: 3D printing could be the next industrial revolution because it has a broader impact. Individuals have the capability to design and print personal products. Embracing this innovative technology will fuel not only a change in the design and manufacturing process, but also distribution.

Conor MacCormack: I relish our industry's challenge of creating a 3D printer for everyone, an ecosystem to support it, and the true democratization of innovation. A new group of users, everyday consumers, are less technically skilled, less driven to master every aspect of 3D printing, but just as interested in the technology's ability to make things they need.

NTB*: There is a new job title in design and manufacturing called "maker." How does that incorporate what the designer and engineer currently do, and what does the "maker" do that is a separate function?*

Cobb: I believe today's makers are what we called "craftsmen" in the past. Makers look at a problem and design a solution. The 3D printer, along with software that is becoming much easier to use, allows the maker to solve his or her own problem, on their own terms, and within their own timeframe.

Mark: I suspect it means different things to different people. In the consumer space, it may be a synonym for "hobbyist." In the industrial space, it may be a synonym for fabricator.

MacCormack: Makers are technically savvy early adopters who have gone online, purchased hobbyist 3D printers, and tinkered with the technology. Many makers are designers and engineers, but not all. These are the people who constantly push the envelope of what the technology can do for them both professionally and personally.

Moe: As the maker movement gets more sophisticated, it follows that companies are creating positions for these types of talented individuals with diverse skill sets. Generally, we understand makers to be inquisitive self-starters who aren't afraid to get their hands dirty. Ultimately, a maker's job function will depend on what companies need.

Pettis: Today, with the help of 3D printing, creative individuals are now being heralded as the new "makers" of our generation. Their talents and skills to move ideas from concept to reality through the process of making are being celebrated. 3D printing brings innovation and iteration to the forefront.

> 3D printing technology is a few years away from becoming ubiquitous. Right now, the 3D printing market reminds me of Linux in the 1990s. For us, ease of use cannot and will not come at the expense of making good hardware.
>
> *Jeff Moe*
> *Aleph Objects*

NTB: *Industry has seen the introduction of 3D printers that use a variety of materials – or multiple materials in one machine. How do manufacturers decide, in many cases, between function and aesthetics when selecting the right machine and material?*

Moe: Manufacturers should not be forced to choose a machine because it comes with a certain proprietary printing material, or is designed to only use one type of printing material. Material developers around the world are consistently innovating and we enjoy bringing their new products to our community. When experimental materials face constraints, developers will introduce new tools and accessories to overcome them.

MacCormack: Users will dictate applications, and applications will dictate material requirements. For example, we selected ordinary paper as the primary build medium for our 3D printers because people couldn't get access to the technology. They demanded much lower cost and ubiquitous consumables,. However, if you want to make an injector nozzle for an engine, the real-world loading will dictate the material and hence the technology.

Mark: We focused on customer feedback — people looking to print parts with the strength of metal, at their desk. That will enable thousands of engineers to fabricate parts when they need them, without waiting in a long queue for machine time.

Pettis: We focus on desktop 3D printing and because of that, we also focus on safe and easy-to-use material that can be used in the office, home, or classroom. We empower individuals to be creative right at their desk.

Cobb: Manufacturers are looking to solve a specific problem. Frequently, 3D printing is seen as a potential solution. 3D printing is similar to many manufacturing processes that are employed today, and these processes can and often rely on secondary processes. The part material takes precedent.

NTB: *While stereolithography (SLA) and fused deposition modeling (FDM) seem to be the most popular 3D printing methods, are there technologies on the near horizon that could become the prominent ones in the future?*

Moe: Today, these technologies appear well positioned for the foreseeable feature. As a flurry of 3D printing-related companies grow out of open-source hardware projects like RepRap, we are seeing comparable growth in related materials, technologies, software, and services. Then again, we never know when the market will surprise us because something new could always be near the horizon.

Mark: Everything has a niche. SLA is really great for jewelry and dental applications. FDM is unbeatable for tooling and structural parts. Objet is great for simulating plastic with overmolding. And carbon filament fabrication (CFF) is great for printing parts with the strength of metal, and the low-friction surface of Nylon. It's also useful to tailor the composite to the application. For example, fiberglass can be used if you want the part to be transparent to RF. Carbon fiber can be used if you want to attenuate RF and provide heat syncing.

MacCormack: I think people believe that all the methods for making 3D objects have already been invented. On the contrary, we're working on new ways to print 3D objects in our R&D labs that, if successful, will really cause a revolution, not just an evolution.

Pettis: MakerBot is currently committed to FDM 3D printing. Our focus is about making 3D printing affordable and accessible on your desktop, and FDM is the safest, most versatile form of 3D printing.

Cobb: I believe all other companies are working to deliver more materials that are well defined in their strength, flexibility, and other properties. I think PolyJet technology gives us good insight into the future where 3D printers can print multiple materials with colors, clear or opaque, and smooth or textured surfaces. In short, it's manufacturing in a box.

NTB: *We're seeing the evolution of the technology in 3D printing machines. What about the evolution on the software side? Are CAD*

> Today, everyone has a computer more powerful than we ever dreamed of right in his or her pocket – their smartphone. We see 3D printing going in the same direction.
>
> *Bre Pettis*
> *MakerBot*

Intro Cov ToC

vendors keeping pace with the necessary software to work with these printers? Is the software keeping up with the hardware?

Mark: The CAD vendors are doing a great job.

Cobb: Software to drive 3D printing is proliferating. Software that is easy to use is becoming available to a wide segment of the population. I believe manufacturers will need to work on developing software that will bridge the design-to-manufacturing process, making it seamless.

MacCormack: Just as the iPod relies on a vast content store from which to buy your music, the 3D printer of the future will be part of a lush ecosystem of content and capabilities. And this ecosystem needs to develop at the same rate as the machines. Elements of the necessary ecosystem include computer-aided design software, which used to be too complex for anyone but designers and engineers. Now a kid can create 3D shapes with a finger on a tablet. We need to refine these capabilities.

> "3D printing could be the next industrial revolution because it has a broader impact. Embracing this innovative technology will fuel not only a change in the design and manufacturing process, but also distribution."
>
> *Jon Cobb*
> *Stratasys*

Pettis: This past year has been especially exciting with all of the software releases that have come out to support 3D printing. We've worked hard to create a 3D ecosystem that makes 3D printing easy and accessible for everyone, and that includes our own software that drives the 3D printing process.

Moe: We seeing rapid development on the software and hardware sides of the 3D printing market. The most exciting developments have been in the Free Software community, where programs like Blender, Slic3r, and FreeCAD, are competing head-to-head with costly closed-source, proprietary alternatives.

***NTB**: It has been estimated that the market for 3D printing equipment will grow from about $1.5 billion this year to $4 billion in 2025. What does it look like for new entrants to the 3D printing market in the next 5 to 10 years? Are the larger printer companies more likely to continue acquiring the smaller players, or is there room in the market for more diversity?*

Mark: I would suspect larger companies will continue to acquire the smaller

ones. And smaller companies should be accepting of this reality.

Cobb: I believe there will continue to be consolidation in the market as larger companies look to smaller organizations to complete or expand their current product lines — not too much different than what is happening in social media today. This does not preclude companies being started that will serve very distinct market.

MacCormack: I believe there is definitely room for more diversity in the industry, and users will continue to demand it in order to achieve greater innovation. The true essence of "democratization of innovation" means that everyone can now participate more than at any time in the past with the help of 3D printers, and this will enable innovation to grow in an exponential way.

Moe: There will always be room for more diversity in the 3D printing market, not only manufacturing printers themselves, but also in printing materials, parts, and accessories; training and education; writing software; designing and modeling; and much more. The future of 3D printing is bright, and we are eager to do our part to innovate and share our knowledge with the community.

Pettis: 3D printing has been around for 25 years and has had only a handful of major players in the industrial sector. Today, there are more companies entering the market. This just helps further the appeal of 3D printing, and helps communicate its power to change work, play, and lives.

> "I relish our industry's challenge of creating a 3D printer for everyone, an ecosystem to support it, and the true democratization of innovation. It's part of the personal quest I've been on for most of my life – to revolutionize the way we design, innovate, and communicate."
>
> *Conor MacCormack*
> *Mcor Technologies*

RESOURCES

Aleph Objects (LulzBot printers)
http://info.hotims.com/49746-122

MakerBot
http://info.hotims.com/49746-123

MarkForged
http://info.hotims.com/49746-124

Mcor Technologies
http://info.hotims.com/49746-125

Stratasys
http://info.hotims.com/49746-126

(Continued on page 22)

A Revolution That's Made in Space

The 3-D Printing In Zero-G experiment is scheduled to launch to the International Space Station (ISS) in August, and will be the first demonstration of 3D printing in space. The printer, designed and built by Made in Space (Moffett Field, CA), will be able to print parts from files sent to the crew on the ISS. We recently spoke with Michael Snyder, Director of R&D for Made in Space, and Niki Werkheiser, 3D Printing in Zero-G Project Manager in the Technology Development and Transfer Office at NASA's Marshall Space Flight Center (Alabama).

NASA Tech Briefs: *How does the printer differ from a commercial 3D printer?*

Michael Snyder, Director of R&D for Made in Space. (Emmett Given/ NASA MSFC)

Michael Snyder: We started off doing simulated flights in the zero-g parabolic aircraft with the ambition to modify commercial printers to work in microgravity. Through a couple days of testing, we realized that the things we'd end up modifying to make the systems work were pretty substantial. It ended up being a lot better for us to build it from the ground up because of the differences from microgravity to Earth gravity. The process itself is basically the same. There was no "eureka" moment in terms of the process being totally different. The mechanics are slightly different, and those slight differences cause substantial defects in the prints.

We'll be able to email parts to space as soon as the printer is installed in the glovebox. We'll be in our offices in Silicon Valley, be able to hit "send," and the part file will be on the printer in a matter of seconds.

NTB: *How are NASA and Made in Space working together on this project?*

Niki Werkheiser: Made in Space, although they are making the first 3D printer in space, is interested in the longer term and creating an industry. Enabling space exploration is the ultimate goal. To enable exploration, the key first step would be to manufacture and have independence from Earth-based launches – to manufacture the part you need on demand. All of the flight certification and mission testing for the printer is occurring at NASA, and we're packing it so it's safe for launch.

NASA's Niki Werkheiser holds a 3D printed Cubesat structure, one of the many potential applications that an in-space manufacturing capability will provide. (Emmett Given/NASA MSFC)

The goal is to take a plastic part made out of the feedstock materials and recycle it back into filament. That will be a very exciting day in space when you can do that, because then you're actually showing the first concept of true independent sustainability. Imagine a day when we can take old food packaging and recycle it back into feedstock material. It's not that far off.

NTB: *Are there other applications for this printer?*

Snyder: We see this technology being very useful for a wide variety of applications – not just based on space. We're in conversations with a lot of people in pretty much every industry and government arm you can think of. It's really exciting and this is relatively brand new — thinking of this technology as more than just a toy. We can really revolutionize how things are made and how quickly they can be made. Imagine in war, your Humvee breaks down but you have a printer. You can fix your Humvee and be back on the road in a matter of hours instead of waiting for people to come help you.

Werkheiser: The Navy is very interested in its use in submarines. Obviously, it's very remote, like the space station, and we've been working together with Made in Space with these entities. Ultimately, to develop the technology, our endpoint applications may be different, but there is overlap in the core set of capabilities we both need to see developed.

NTB: *This project will reduce the distance goods will need to go, and reduce launch costs?*

Snyder: Absolutely. That's what we set out to do is disrupt the supply chain and make it more convenient, eventually eliminating the need for launch vehicles. When you're out exploring places like Mars, you won't have the capability you have on the station. Imagine going to Mars and having feedstock that you can transform into backup environmental control systems or refrigerators. You can do that with the same material and not have to store spares, which reduces mass.

Right now, this technology is capable of doing great things, and it needs to be viewed the same way we view a drill press or a CNC machine. It's actually better because of the extended capability it gives you. It will be a matter of time before people finally open their eyes fully and realize how much this changes everything.

For more information, visit ***www.nasa.gov/mission_pages/station/research/experiments/1115.html*** *or* ***www.madeinspace.com***.

Free Info at http://info.hotims.com/49746-718

Lithium-Ion Batteries Critical to Mars Spacecraft

Lithium-ion batteries
Yardney Technical Products
East Greenwich, RI
401-471-6599
www.yardney.com

On November 18, 2013, the Mars Atmosphere and Volatile EvolutioN (MAVEN) spacecraft was launched into space to begin its ten-month journey to Mars. The spacecraft is being powered by a combination of solar arrays and two advanced, space-qualified, 28-Volt, 55-Ah Yardney lithium-ion batteries.

The MAVEN spacecraft was launched on an Atlas V-401 rocket, which also includes 12 Yardney Silver Zinc batteries (booster main 2, FTS 4, and Pyro 6). The lithium-ion batteries have additionally powered the Mars Rover, Phoenix Mars Lander, and other satellites.

The MAVEN's solar arrays produce 1,150 Watts of energy to power the spacecraft and its payload. The spacecraft has several scientific instruments to study solar winds, magnetic field, and other characteristics of the Martian upper atmosphere. The lithium-ion battery stores extra energy at times when demand is low, provides extra power when demand is high, and is used for load leveling and transient suppression in the power system.

For Free Info Visit http://info.hotims.com/49746-116

EZVI Technology Cleans Up Contaminants at Kennedy Space Center

Jacobs Engineering Group
Pasadena, CA
www.jacobs.com

CORE Engineering and Construction
Winter Park, FL
www.core-encon.com

A groundwater technology developed at Kennedy Space Center was used to treat subsurface contaminants near one of the center's buildings: the Reutilization, Recycling and Marketing Facility (RRMF).

The RRMF was constructed in the late 1960s for the storage and recycling of a variety of equipment and chemicals. Over the course of nine days, the center's Remediation Program injected Emulsified Zero-Valent Iron (EZVI) into an area of about 2,200 square feet, to a depth of 27 feet below ground surface. The target was the chlorinated solvent tetrachloroethene, also known as PERC, which had been historically released into the environment.

Remediation Project Manager Anne Chrest of Kennedy's Center Operations Directorate led the cleanup efforts. Workers

Workers with Jacobs Engineering Group and CORE Engineering and Construction used more than 9,000 gallons of EZVI to treat subsurface contaminants near the RRMF at Kennedy Space Center. (NASA/Anne Chrest)

EZVI directly treats the contaminant source without mobilizing contaminants.

with Jacobs Engineering Group and CORE Engineering and Construction used more than 9,000 gallons of EZVI in the treatment area. The site will be monitored for several years, ensuring that cleanup objectives are achieved. Groundwater samples will be collected over time.

Invented by Jackie Quinn, a NASA environmental engineer, EZVI currently is one of several available groundwater remediation technologies that can treat chlorinated solvent source material, known as dense nonaqueous phase liquids (DNAPLs). The liquids are denser than water and do not dissolve or mix easily in water. The EZVI process places nanoscale zero-valent iron particles into a surfactant-stabilized, biodegradable, oil-in-water emulsion. The emulsion is then injected into the contaminated zones.

For Free Info Visit
http://info.hotims.com/49746-115

Real-Time Minimization of Tracking Error for Aircraft Systems

Direct adaptive control looks at errors and decides if and when corrections are needed.

Ames Research Center, Moffett Field, California

In many cases when an aircraft/spacecraft vehicle encounters a failure (such as a jammed control or loss of a part), there are still enough redundant actuation mechanisms to safely maneuver the vehicle. However, most pilots/autonomous systems are unable to adapt to the altered configuration and learn to control the damaged aircraft in the very short time available for safe operation. Fortunately, the flight computer may have the necessary information as well as bandwidth available to learn the new dynamics and determine mechanisms to control the vehicle quickly. The flight computer needs an intelligent controller that flies the vehicle with the baseline controller during normal conditions, and adapts the design when the vehicle suffers damage. Using information about the vehicle from all the available sensors, the system determines whether the vehicle is damaged. Direct adaptive control (DAC) looks directly at the errors, and updates the control law accordingly. This technology looks not just at the tracking error, but rather its characteristics over time to determine whether the controller needs to be adapted or left alone. This is typically fast and meets the timing considerations for aircraft/spacecraft system implementation.

This technology presents a novel, stable, discrete-time adaptive law for flight control in a DAC framework. Where errors are not present, the original control design has been tuned for optimal performance. Adaptive control works towards achieving nominal performance whenever the design has modeling uncertainties/errors or when the vehicle suffers substantial flight configuration change. The baseline controller uses dynamic inversion with proportional-integral augmentation. On-line adaptation of this control law is achieved by providing a parameterized augmentation signal to a dynamic inversion block. The parameters of this augmentation signal are updated to achieve the nominal desired error dynamics.

If the system senses that at least one aircraft component is experiencing an excursion and the return of this component value toward its reference value is not proceeding according to the expected controller characteristics, then the neural network (NN) modeling of aircraft operation may be changed.

This work was done by John T. Kaneshige, Kalmanje S. Krishnakumar, and Nilesh V. Kulkarni of Ames Research Center; and John Burken of Dryden Flight Research Center. ***For more information, download the Technical Support Package (free white paper) at www.techbriefs.com/tsp under the Physical Sciences category****.*

NASA invites companies to inquire about partnering opportunities. Contact the Ames Technology Partnerships Office at 1-855-627-2249 or ARC-TechTransfer@mail.nasa.gov. Refer to ARC-16235-1.

Detecting an Extreme Minority Class in Hyperspectral Data Using Machine Learning

Automated classifiers can detect surface sulfur in orbital remote sensing observations.

NASA's Jet Propulsion Laboratory, Pasadena, California

Orbital remote sensing provides a powerful way to efficiently survey targets for features of interest in inaccessible regions of the Earth as well as on other planets. One such feature of astrobiological relevance is the presence of surface sulfur deposits, which may be present on icy moons such as Europa. All hyperspectral instruments face the difficult task of spectral feature selection (finding the spectral bands that matter), especially those that operate in previously unstudied arenas encountered in planetary missions. This software demonstrates how manually annotated labels can enable automated feature discovery that boosts science return.

This work evaluates the ability of automated classifiers to detect sulfur in remote sensing observations by the Hyperion spectrometer on the EO-1 (Earth Observing-1) spacecraft. A data-driven machine learning solution was required because it is not possible to reliably detect sulfur in hyperspectral data by simply matching observations to sulfur lab spectra, as is common for in-situ mineral imaging. Several methods (manual and automated) were evaluated to select the most relevant attributes (spectral bands) for successful sulfur detection.

Data was taken from an Earthly analog for Europa: a northern island where bioactivity has produced surface sulfur deposits on ice. This software uses machine learning algorithms to automatically discover the best spectral features that discriminate interesting spectra from uninteresting surrounding spectra such as observations of ice, rock, and exposed sulfur deposits. Unique aspects of this study include ground validation using terrestrial sulfuric ice springs, modern machine learning feature detection using a Support Vector Machine (SVM), and real-time execution onboard the EO-1 spacecraft. A primary technical innovation is the ability to handle a severe imbalance between extremely rare positive

examples (sulfur deposit locations) and a plethora of negative examples.

The experimental results show that a classifier can be trained to successfully detect sulfur-bearing pixels in data collected by the Hyperion instrument onboard EO-1 while accommodating the particular computational challenges and constraints imposed by the onboard environment. The best results were achieved by using Recursive Feature Elimination (RFE) to select the 12 most discriminative bands (a limitation imposed by the EO-1 hardware), modeling the problem using four classes by decomposing "sulfur" into "bright sulfur" and "dark sulfur" populations, and employing Pair-Wise Expectation Maximization (PWEM) to filter out likely mislabeled items from the training set. Automated feature selection is effective on this problem. RFE tended to select bands similar, but not identical, to those chosen manually by an expert, and RFE's bands often yielded higher accuracy performance, as well as a smaller number of false positive detections.

This work was done by Lukas Mandrake, Kiri L. Wagstaff, and Umaa D. Rebbapragada of Caltech for NASA's Jet Propulsion Laboratory. For more information, contact iaoffice@jpl.nasa.gov.

This software is available for commercial licensing. Please contact Dan Broderick at Daniel.F.Broderick@jpl.nasa.gov. Refer to NPO-46564.

KSC Spaceport Weather Data Archive

John F. Kennedy Space Center, Florida

The Spaceport Weather Data Archive provides a fully searchable database of weather data gathered at Kennedy Space Center and the Cape Canaveral Air Force Station. Weather data includes wind, temperature, and humidity data from a surface meteorological tower network; upper air soundings from both weather balloons and radar wind profilers; and data from the extensive rain gauge network. Not only can the user easily retrieve data and download it, but the user can also view graphically the weather data on a map overlay. For example, the user can enter search criteria to view all lightning strikes ending at a particular date/time, and graphically see the lightning strikes color-coded based on elapsed time for the prior seven hours. A unique feature of the software is the capability to invoke an automated playback for cloud-to-ground lightning events on a geographic overlay for a selected date and time interval.

This innovation separates the public-facing Web application from the KSC/CCAFS internal Web application software, and has eliminated ftp downloads. The look and feel has been designed to be similar to current state-of-the-art weather research Web sites, and provides common, standardized interfaces for the various weather data types. The archive has been designed for the handling of new data for automated quality control (empty files, duplicate data, reasonableness verification, and validity checks).

The data are updated every 60 minutes for certain instruments, and as frequently as every 15 minutes for oth-

ers. Data is available 24/7 over a publicly accessible Web site. The data is used by researchers to validate launch commit constraint criteria, and to ensure safe operations for workers at KSC. The site provides links to technical publications and other resources, and allows data to be downloaded for further investigation.

This work was done by Francis Merceret and Jennifer Wilson of Kennedy Space Center; and Barbara Kaysen, Philip Gemmer, Timothy Ritter, Daniel Strohschein, Ryan Arnold, Evan Bonnett, Jothimani Nallasamy, Aldwin Ebuen, Daniel Krainas, Terence Tully, and Brice Crossley of Abacus Technology Corporation. ***For more information, download the Technical Support Package (free white paper) at www.techbriefs.com/tsp under the Information Technology category.***

KSC-13803

Visualizing Acquisition, Processing, and Network Statistics Through Database Queries

NASA's Jet Propulsion Laboratory, Pasadena, California

Given a date range, the UAVSAR MySQL database is queried to evaluate data acquisition, processing status, and network performance, and uses the Google Charts API to dynamically return images of pie and bar charts to visualize processing and network statistics. The MySQL database is populated with relevant data that includes processing status, as well as network performance (ping and sample file downloads). Then, using the open Google Charts API, the metrics are displayed for any desired date range.

This innovation is meant to be a flexible method to display metrics based on MySQL database entries. Given a date range and various other search criteria, this software queries the UAVSAR MySQL database for data acquisition, processing, and network statistics. These are visualized in a Web browser using HTML, CSS, JavaScript, Perl, and the Google Charts API. The data acquisition and processing information are automatically populated into the database once new data is acquired or processed. The network performance information is populated by running a script that checks the network uptime and download rate.

This type of interface for processing metrics and network statistics would be valuable to any task that reports processing metrics, or any task that is partnering with, via the Internet, a data center that receives and distributes the processed data.

This work was done by Sarah L. Flores, Wayne W. Tung, Yang Zheng, and Bruce D. Chapman of Caltech for NASA's Jet Propulsion Laboratory. For more information, contact iaoffice@jpl.nasa.gov.

The software used in this innovation is available for commercial licensing. Please contact Dan Broderick at Daniel.F.Broderick@jpl.nasa.gov. Refer to NPO-47889.

Simulating Data Flow via Multiple Secure Connections

Goddard Space Flight Center, Greenbelt, Maryland

A software simulator was developed to simulate data flow from the Interface Data Processing Segment (IDPS) to the Science Data Segment (SDS) for the NPOESS Preparatory Project (NPP) via multiple Secure FTP (sftp) connections. The simulator is a multithreaded Java program that handles the continuous sftp transfer of large amounts of data with some error-handling capabilities built in.

The simulator takes one orbit of data and pushes it via sftp to user-defined locations. Users have the option of specifying the number of sftp connections and the number of minutes between each orbit.

All data file names are updated with proper time-stamps simulating different orbits of data. A corresponding CRC (Cyclic Redundancy Check) file is creat-

Low Noise Preamplifiers

Voltage Preamplifier

- 1 MHz bandwidth
- 4 nV/√Hz input noise
- 100 MΩ input impedance
- Gain from 1 to 50,000
- RS-232 interface
- $2595 (U.S. list)

SR560 Low-Noise Voltage Preamplifier

The SR560 is ideal in applications where noise matters — like low-temperature or optical detection measurements. The SR560 offers a true-differential (or single ended) front-end, configurable high/low pass filtering, and rechargeable batteries that provide up 15 hours of line-free operation. With a microprocessor that 'sleeps' except when the instrument's setup is changed, no digital noise will contaminate your low-level analog signals.

Current Preamplifier

- 1 MHz bandwidth
- 5 fA/√Hz input noise
- 1 pA/V maximum gain
- Adjustable DC bias voltage
- Line or battery operation
- $2595 (U.S. list)

SR570 Low-Noise Current Preamplifier

Designed for low-noise signal recovery experiments, the SR570 Current Preamplifier is the industry's standard. It offers current gain up to 1pA/V, configurable high and low pass filtering, and input offset current control. The SR570 can be powered from the AC line or its built-in batteries, and is programmable over RS-232. High-bandwidth, low-noise, and low-drift gain modes allow you to optimize the instrument for different applications.

SRS **Stanford Research Systems, Inc.**
1290-D Reamwood Avenue, Sunnyvale, CA 94089

Phone: (408)744-9040
www.thinkSRS.com

Free Info at http://info.hotims.com/49746-733

ed for each HDF5 file so that the data-7ingest software would ingest the data files without issue. The use of the simulator is crucial for testing the interface, load, and performance requirements of the SDS for the NPP.

This work was done by Chiu Wiegand, Jacqueline LeMoigne-Stewart, and LaMont Ruley of Goddard Space Flight Center. For further information, contact the Goddard Technology Transfer Office at (301) 286-5810. GSC-16402-1

Systems and Services for Near-Real-Time Web Access to NPP Data

Software for processing and interpreting S-NPP observations and related data has become publicly available and more readily usable.

Marshall Space Flight Center, Alabama

The recently launched Suomi National Polar-orbiting Partnership (S-NPP) satellite, operated by NASA and the National Oceanic and Atmospheric Administration (NOAA), is providing multispectral global observations over the next several years to support a broad array of research and applications. S-NPP data products consist of a complex set of data and metadata files in highly specialized formats, and the U.S. government's operational ground segment delivers these to users with delays of several hours to a few days.

A growing set of antennas around the globe is capable of receiving S-NPP's continuous, unencrypted data broadcast, and sharing the raw data via the Internet. Furthermore, software for processing and interpreting S-NPP observations and related data has become publicly available and more readily usable.

A suite of software was developed to couple near-real-time S-NPP data feeds with a streamlined, scalable processing chain and geospatial Web services, running in a scalable cloud computing environment. The system provides near-real-time access to data from the Visible Infrared Imaging Radiometer Suite (VIIRS), the Moderate Resolution Imaging Spectroradiometer (MODIS), and other observations. It functions 24/7 to retrieve these data from multiple sources over the Internet, processes them as quickly as possible using a scalable cloud computing environment, and delivers data products and visualizations on demand via standard Web services that can interoperate with a variety of end-user display and analysis tools.

The first component of the system (a Retrieval server) monitors data repositories at several remote S-NPP and Aqua MODIS receiving sites and fetches new satellite data files as soon as they become available. The second component (one or more Processing servers) runs science-validated algorithms on the newly fetched data, and prepares data products and visualizations for Web presentation to end users. The third component (a Map/Data server) draws on these data and visual products, using industry-standard protocols to serve a variety of software clients. Each component is distributed as an integrated machine image, ready to be instantiated on virtual machines in a cloud computing environment. As virtual machines, the three components can be reconfigured easily to monitor different data sources, and to perform different processing workflows on the retrieved data.

One advantage is the use of cloud computing for low-cost entry into full-scale scientific computing and radical scalability to meet wide variations in processing demand at moderate costs. Another is the use of virtual machines capable of running many different workflows, easily reconfigured to fetch, process, and deliver a variety of products from distributed sources.

This work was done by John Evans, Eduardo Valente, Wei Hao, and Samir Chettri of Global Science & Technology, Inc. for Marshall Space Flight Center. For more information, contact Sammy Nabors, MSFC Commercialization Assistance Lead at sammy.a.nabors@nasa.gov. Refer to MFS-33076-1.

CCSDS Telemetry Decoder VHDL Core

Costly ground support equipment can be eliminated.

Goddard Space Flight Center, Greenbelt, Maryland

A flexible Telemetry Decoder Core (TDC) has been designed to decode Consultative Committee for Space Data Systems (CCSDS) encoded telemetry data. The TDC can be used to eliminate costly ground support equipment by placing the telemetry decoding functions in an inexpensive, commercially available field programmable gate array (FPGA) integrated circuit instead of special-purpose printed circuit boards. The TDC can also be used in the design of telemetry systems by enabling end-to-end simulation of these systems' upfront simulation before any hardware is built. The TDC was developed for the Global Precipitation Measurement (GPM) project and because of its success on that project, it will be used to verify telemetry on the Magnetospheric Multiscale (MMS) project.

The TDC has a wide range of flexibility as shown in the figure. A number of options can be enabled or bypassed including: a ½ rate Viterbi decoder, a NRZM Converter, a bit interleaver, a Reed Solomon decoder, pseudo derandomization, and a CRC checker. The Viterbi decoder can be either hard or soft decision and can resync itself based upon a user-configurable bit error rate (BER). The TDC also does frame synchronization and can detect standard pseudorandom patterns PN7, PN15, and PN23. It can accommodate a dual source system by processing two sets of frame data streams.

This work was done by Thomas Winkert and Omar Haddad of Goddard Space Flight Center, and Iraj Sardari of MEI Technologies. ***For more information, download the Technical Support Package (free white paper) at www.techbriefs.com/tsp under the Electronics/Computers category.*** *GSC-16088-1*

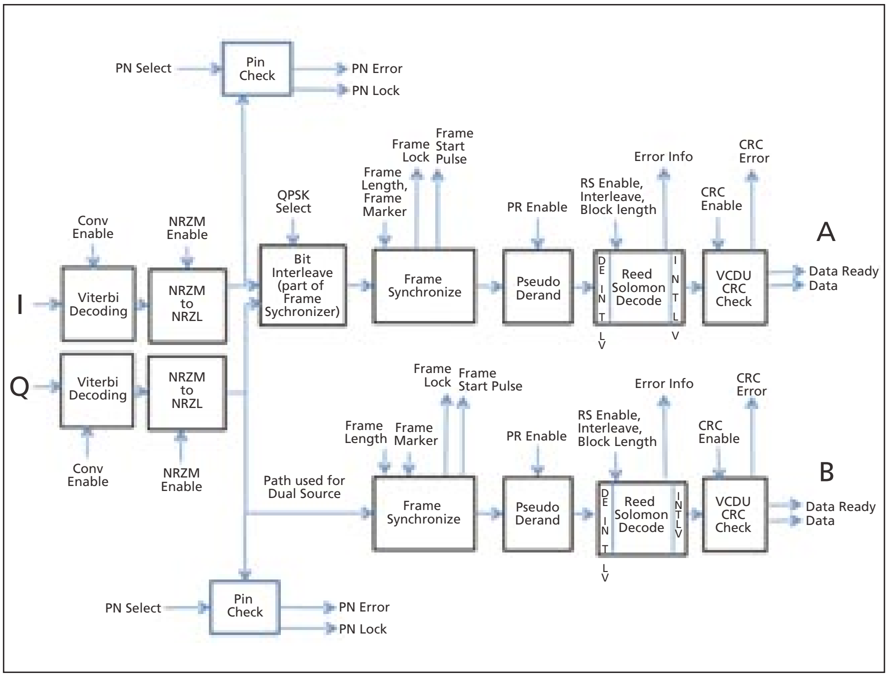

This portable, comprehensive **CCSDS-Compatible Hardware Decoder** was written in VHDL (a hardware description language) and has been developed to verify telemetry data in both simulation and lab environments. Since it is written in VHDL, it can be both simulated easily and ported to lab hardware for verification of telemetry data. The TDC has a wide range of flexibility and can fit into different FPGAs from different vendors.

Intro Cov ToC

Thermal Response of a High-Power Switch to Short Pulses

Simulations are used to calculate temperature changes that occur inside semiconductor switch modules, where measurement is not possible.

Army Research Laboratory, Aberdeen Proving Ground, Maryland

Semiconductor switch modules composed of Super Gate Turn-Off Thyristors (SGTOs) have been evaluated. The switches are intended to handle kiloamp-level currents and may dissipate peak powers measured in megawatts. Recent experiments measured the response of a switch module composed of eight SGTOs to single-short, high-current pulses. Simulations of those experiments were performed to calculate the temperature changes that occur inside the devices, where measurement is not possible. Worst-case operating conditions in which the switches handle several pulses within the space of 4 or 5 seconds (s) also were simulated. Modeling and simulation were performed with SolidWorks 3D modeling software and SolidWorks Simulation computational fluid dynamics software from Dassault Systèmes.

The original switch model includes a module composed of eight SGTO die, lugs and spacers, and base, as well as an aluminum cold plate to conduct heat from the module. In order to reduce the computation time spent in thermal simulations, the original model was simplified, reducing the curves and fillets to a geometry suitable to a rectangular mesh, while attempting to preserve the dimensions and volume of the parts (and materials) for time-dependent thermal calculations. The model was further simplified, and simulation run times reduced, by taking advantage of the symmetry of the model and using one-quarter of the simplified model for simulation. Spacers were eliminated from the model; they have no significant influence on the thermal response of the switch in the timespans studied (see figure).

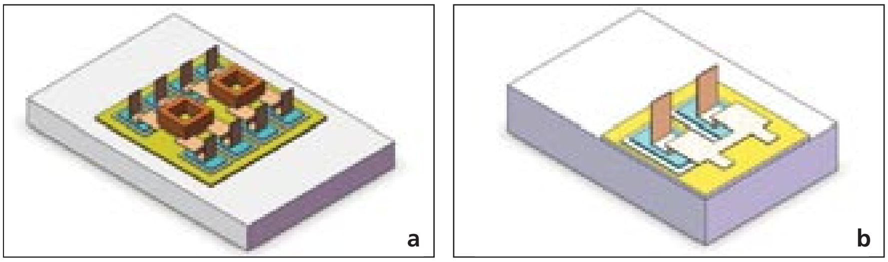

The simplified **Super Gate Turn-Off Thyristor Switch** models in (a) full model, and (b) quarter model. The model was simplified, and simulation run times reduces, by taking advantage of the symmetry of the model and using one-quarter of the simplified model for simulation.

The initial temperature of the model and of the air surrounding it was defined to be 70 °C. The bottom surface of the cold plate on the switch module was also defined to be 70 °C; this served as a sink for heat generated in the SGTOs. The top surface of the circuit board was subject to natural convection, which was included in the simulation by defining those surfaces to have a convection coefficient of 10 W/m^2-K.

The time-dependent thermal inputs for the simulations were derived from measurements of voltage drops and current in the SGTOs made during experimental characterizations performed with the solid-state switch modules. Curves of power versus time were culled from much larger files of data recorded at 0.1-microsecond (μs) intervals. It was assumed that the switch module distributes the power equally among the SGTOs. In the simulation, power was applied uniformly throughout the active part of the die, rather than applying it solely to a junction within the die.

While the active part of the die reached a temperature in excess of 130 °C, that part of the die is covered with a lid, and the observable part of the module has reached a maximum temperature of about 100 °C. Little of the heat in the first pulse has been conducted outside the active die in 35 μs. The "off" time is 1.66 s, at the end of which the die has almost returned to its initial temperature of 70 °C.

Next, how the temperature of the SGTOs rose and fell during a series of pulses was calculated. Two cases were used. The first was five 35- s pulses in a 4-s period, and the second was four 35- s pulses in a 5-s period to see whether or not the temperature of the devices stays within a safe operational range. SGTOs return almost to the original baseline temperature between pulses, and the average temperature rises with each pulse to just over 130 °C. Silicon devices may not operate as efficiently at such temperatures as they do at room temperature, but are not likely to be damaged by such short transits to high temperatures. There still is little sign of heat spreading through the module after 5 s, and visible temperatures are within one degree of those at the peak of the first pulse.

The second set of calculations used a 54-μs-wide pulse as a thermal input to the SGTO switch model. Peak power is 1.5 MW per SGTO, assuming equal distribution of power among the SGTOs in the module. As with the 35-ms pulse case, the thermal effects of a single pulse, a series of five pulses in 4 s, and four pulses in 5 s were calculated. The longer pulse raises the device temperature over 140 °C, about 10 °C higher than the 35-ms pulse.

The effects of 4- and 5-pulse trains with the 54-ms pulse were calculated. As each pulse was applied, the average temperature in the active part of the SGTOs rose to more than 140 °C, and returned almost to the baseline temperature between pulses. The SGTO temperature at the end of the last pulse in both cases was approximately 144 °C.

The model shows a quick rise in the temperature of the SGTOs during the pulse, but peak temperatures are within safe operating limits for Si devices. The heat in the devices dissipates quickly into the surrounding package and into the cold plate to which it is mounted. Heat conduction occurs rapidly enough that the devices' temperature returns very close to their initial temperature within about 1 s after the end of the pulse. Calculations predict that the peak temperatures in the SGTOs will increase little over time when a series of short pulses over 4 or 5 s is applied. This indicates that the switches should be able to withstand repeated cycling at high power levels without sustaining heat-related damage or suffering serious degradation of performance.

This work was done by Gregory K. Ovrebo of the Army Research Laboratory. ***For more information, download the Technical Support Package (free white paper) at www.techbriefs.com/tsp under the Electronics/Computers category.*** *ARL-0164*

Solar Panel and System Design to Reduce Heating and Optimize Corridors for Lower-Risk Planetary Aerobraking

New approach features aggressive load reduction to reduce risk.

Goddard Space Flight Center, Greenbelt, Maryland

This innovation presents a spacecraft aerobraking approach that reduces heating and optimizes corridors, which reduces overall risk. This is accomplished by combining solar panel aspect ratio and edge features with simple spacecraft packaging optimization and integrated thermal-analysis techniques that also allow specifying a more benign temperature corridor.

There has been a perceived general aerobraking risk in early-stage mission designs. The aero-heating of the solar panels during aerobraking in the warmer Venus thermal environment is considered riskier than Mars aerobraking.

Most missions were not optimized for aerobraking, particularly the solar-panel and spacecraft-shape aspect ratio and thermal features. Mars aerobraking had more uncertainty, but lower solar heating rates and more actual mission data. Venus has more solar heating, higher initial temperature conditions, and fewer real-life examples, but less atmospheric change. Lingering aerobraking risks applied to such missions in the early stage required more aggressive early-phase reduction of risks. Older designs did not pursue aggressive solar panel thermal load reduction features, or optimization of temperature, and instead focused on heat rate corridors.

This approach combines multiple new features into one combined solution. The first feature is lower heating from past designs by applying the lowest aspect ratio solar-panel layout, resulting in lowest heating for the solar-panel area required for the mission. A new "picture frame" edge is added to solar panels. The outside 3 to 6 in. (≈7.6 to 15.2 cm) of the panels are directed 45 to 30° into the flow. This reduces heating by an additional 15%. The projected drag surface is increased, which reduces the ballistic coefficient that can be used to either decrease aerobraking duration or increase thermal margin. These edges, which receive higher heat flux, are protected with high-temperature multi-layer insulation.

The new high-temperature solar panel features high-temperature graphite epoxy facesheet and solar array design. The solar arrays are pre-cooled by turning away from the Sun a mission-specific number of minutes before the drag pass. The developed thermal analysis integrated with the trajectory simulation approach is used to fly a temperature corridor instead of a heat-rate corridor, which results in better control of temperatures. This yielded an overall aerobraking approach with shorter aerobraking durations and substantial temperature margins.

This work was done by Charles Baker, Michael Amato, David Steinfeld, and Jeff Stewart of Goddard Space Flight Center; and Jill Prince, Derek Liechty, and John Dec of Langley Research Center. ***For more information, download the Technical Support Package (free white paper) at www.techbriefs.com/tsp under the Manufacturing & Prototyping category.*** *GSC-16407-1*

Low-Cost, Very Large Diamond-Turned Metal Mirror

Reliable plating and diamond-turning technologies produce visible quality mirrors for applications such as semiconductor manufacturing.

Marshall Space Flight Center, Alabama

This innovation is a method for fabricating a low-cost, lightweight, large-aperture mirror by constructing only the mirror substrate by electroforming on a master form machined from plastic foam. Electroformed tubes of the same NiP alloy are installed in the foam mirror substrate master. Installing electroformed NiP tubes in the plastic mirror master before plating on the plastic foam mirror substrate allows the mirror faceplate and the back surface of the mirror to be plated onto the ends of the connecting tubes in the foam plastic. Removal of the foam after plating is complete results in a very stiff and lightweight mirror substrate made only of a single material. The low cost of the electroformed mirror substrate is made possible by very fast production of a master surface made of plastic foam that can be rapidly machined with modern, high-speed machining technology to very good mechanical tolerances in only a few hours.

No expensive and laboriously produced master surface is required for replication as in traditional electroforming of optical mirrors. After the plastic form has been encapsulated with a suitably thick NiP deposit, the plastic is dissolved away with a solvent. This leaves a hollow, electroformed mirror substrate. The excellent diamond machinability of the high-phosphorus nickel allows the electroformed surface to be diamond turned to produce a highly accurate and very smooth optical surface.

The extremely low cutting forces of diamond turning can produce visible wavelength quality optical surfaces without applying any heavy forces to the mir-

ror face plate, as would be the case with conventional optical lapping and polishing processes. The plated-in array of tubular structures allows the interior of the hollow mirror to be open and easily vented in a vacuum. The very low cutting force of diamond turning allows the mirror faceplate to be made very thin to lower the areal density of the mirror. The low cutting force also minimizes the tendency for print-through of the internal support points of the tubular sections connecting the mirror face plate to the mirror back plate.

Excellent visible quality optical figure and surface finish can be produced by diamond turning. Surface finishes on diamond-turned NiP alloy as smooth as 0.6 nm rms have been obtained without any post-polishing of the diamond turned surface. The fast and flexible machining of a very-low-cost, expendable master form made of plastic foam, combined with a proven electroplating process to produce a thick deposit of diamond machinable NiP, results in a process for producing mirror substrates at a cost as small as one-thousandth the cost of comparable one-square-meter beryllium mirror substrate.

This work was done by John Casstevens of Dallas Optical Systems, Inc. for Marshall Space Flight Center. For more information, contact Sammy Nabors, MSFC Commercialization Assistance Lead, at sammy.a.nabors@nasa.gov. Refer to MFS-33035-1.

Very-High-Load-Capacity Air Bearing Spindle for Large Diamond Turning Machines

Marshall Space Flight Center, Alabama

Large-load-capacity oil hydrostatic bearings generate prohibitive amounts of heat in large sizes when run at speeds useful for diamond turning of optical components. The viscosity of air is more than three orders of magnitude less than the thinnest oil; therefore, the frictional heating of large-diameter air bearings is very small and very manageable. A formidable manufacturing problem with large air bearings is that the extremely low viscosity of air requires that the thickness of the bearing film is also very small. This very small bearing clearance of 5–8 micrometers means that the required accuracy of geometry and dimensions of air bearing components is extremely difficult to achieve.

In the case of meter-size air bearing dimensions, the required precision is comparable to high-quality optical components in most cases because exact dimension is required in addition to near-perfect geometry. With current technology, the cost to fabricate, and the time to produce large mirrors, is one of the limiting factors for many missions. Research tools require large-aperture, lightweight optics that will perform well in a space cryogenic environment. Currently, no mirror technology has been demonstrated that meets the mission requirements at an affordable cost.

Diamond turning has been proven to produce highly aspheric optical contours to visible wavelength tolerances with extremely smooth surfaces. Diamond turning has the additional enabling capability to not only produce extremely smooth and accurate optical surfaces, but also mechanical attachment surfaces and datums that allow extremely fast and complex optical components to be quickly and easily aligned. The productivity of diamond turning allows the production of quantities of optical components with exacting duplication of optical surfaces and datums, which allow "snap-together" optical systems.

The large diamond turning machines that have been built all have oil hydrostatic work spindles that fail in diamond- turning very large optical components because of excessive heat generation when this type bearing is made large enough to have the required load capacity for very large optics diamond turning.

The solution to this problem is to make large vertical air bearings with hard metal journals running against porous graphite bearing surfaces. Porous graphite air bearings do not friction weld in the event of the spindle bearing surface contacting the bearing journal surface, and the result is only slight polishing of the graphite surface. The porous graphite flow structure provides extremely uniform flow of the air film, and the tortuous flow path acts to damp the flow-induced dynamic instability that is a severe problem in both oil and air hydrostatic bearings.

This work was done by John Casstevens of Dallas Optical Systems for Marshall Space Flight Center. For more information, contact Sammy Nabors, MSFC Commercialization Assistance Lead, at sammy.a.nabors@nasa.gov. Refer to MFS-32880-1

Intro Cov ToC

Materials & Coatings

Elevated-Temperature, Highly Emissive Coating for Energy Dissipation of Large Surfaces

This coating can be used in high-temperature rocket nozzles, control surfaces, industrial furnaces, and transfer lines.

Marshall Space Flight Center, Alabama

This coating demonstrates high emittance above 80% or better at broad wavelengths within the infrared spectrum. It has shown to have an extremely stable emittance at lower wavelengths within the infrared (IR) spectrum, where energy dissipation is critical at elevated temperatures. The coating has demonstrated increases in surface texturing, and ultimately an increase in emissivity when exposed to temperatures up to 2,050 °F (≈1,120 °C). It is also stable at continuous run, elevated temperatures, and shows no signs of spalling or erosion.

Radiation-cooled nozzles for liquid rocket engines require high emissivity, approaching near black body, in order to properly dissipate energy from the component. A common means of increasing the emittance of metallic components is to perform a high-temperature heat treatment of the material, allowing the surface to oxidize, thus increasing the emissivity. However, an oxidized surface will reduce when exposed to the hydrogen-rich steam from the propellant by-products of liquid hydrogen/liquid oxygen (LH2/LOX) combustion in addition to being reduced when exposed to a hard vacuum environment. Another disadvantage of the high-temperature material oxidation is reduction of the base material properties. Some materials, such as superalloys, require a minimum heat treatment temperature to be obtained; otherwise, the structural properties of the material can be reduced due to carbide precipitation. Additionally, distortion of larger parts can occur at elevated temperatures when performing heat treatment oxidation cycles of the material.

A unique silica-based coating was adapted from industry to meet the emissivity needs of the rocket nozzle. The Cetek coating system is an aqueous-based material that is applied using a handheld sprayer that could be readily adapted to an automatic robot sprayer. Spray application allows even distribution of the coating over the entire surface of the component exposed to both hot gas and the vacuum of space. The coating is applied in a series of air-sprayed layers that combine to produce a total thickness of less than 0.005 in. (127 µm). The thin coating allows for minimal weight impact by increasing the emittance of the surface, ultimately decreasing component temperatures and allowing for reduced weight of the engine component. The cure cycle for the coating consists of an ambient air cure under controlled humidity conditions, followed by oven heating at low temperatures for a period of a few hours.

The development of this coating was necessary to increase the emittance of the surface of the nozzle extension for the radiation-cooled metallic nozzle extension for the J-2X Upper Stage Engine. Because the temperatures of the nozzle wall are dependent upon the radiation effectiveness, emissivity is extremely important. The material properties of the nozzle extension are dependent on the temperature in which they operate. A lower temperature wall (based on emissivity) would allow a higher strength of the base material, and eventually weight savings of the nozzle based on optimization of the design. Thus, a higher emittance for the nozzle results in weight savings for the design and also a design that yields additional thermal margin. This coating successfully completed a series of high-temperature emissivity and durability certification testing and has been shown to survive a rocket nozzle's extreme operating environment through both subscale and full-scale testing.

This work was done by Paul Gradl of Marshall Space Flight Center, Jeff Haynes of PWR WPB, and Naiping Zhu of Cetek Ltd. For more information, contact Sammy Nabors, MSFC Commercialization Assistance Lead, at sammy.a.nabors@nasa.gov. Refer to MFS-32856-1.

Catalyst for Treatment and Control of Post-Combustion Emissions

This oxidation/reduction catalyst can be used in diesel and natural gas applications, and in non-automotive pollution sources.

Langley Research Center, Hampton, Virginia

Emissions from fossil-fuel combustion contribute significantly to smog, acid rain, and global warming problems, and are subject to stringent environmental regulations. These regulations are expected to become more stringent as state and regional authorities become more involved in addressing these environmental problems. Better systems are needed for catalytic control.

In general, existing catalytic converters used for NO_x and He emission control use precious metal (PM) or their combinations as wash coats with various architectures over alumina on ceramic substrates to effect catalytic conversion. Some of the more common are coatings of Pd, Pd/Rh, or Pt/Rh. Existing catalytic converters are less effective for removal of methane HC emissions due to the high light-off temperatures for methane on these catalysts.

The present invention utilizes at least two PMs with at least two different metal-oxides (for example, tin-oxide plus one or more promoters) in a layered matrix to convert CO, HCs, and NO_x to CO_2 and N_2 by oxidation of the first two components (CO, HCs) and reduction of the third (NO_x) in a moderately high-temperature gaseous environment (for example, between about 200 to about 500 °C) containing excess oxygen.

Preparation of ruthenium/platinum-tin-oxide-based catalyst coatings for pellets, beads, granules, fabrics, and especially ceramic honeycomb monoliths can be accomplished by successive layering of the desired components, as follows:

1. A clean, dry substrate is deaerated in a solution containing tin (II) 2-ethylhexanoate (SnEH). The substrate is removed from the solution, and excess solution is removed from the substrate. Residual solution components are evaporated leaving an SnEH layer on the substrate that is thermally decomposed in air to tin-oxide at 300 °C. Several layers are applied in the same manner to achieve the desired loading of tin-oxide.
2. The promoters are added to the catalyst matrix in a similar fashion. For example, an iron oxide promoter is added to an existing tin-oxide-coated substrate by deaerating in an iron nitrate solution, removing excess solution, evaporating the solvent, and finally thermally decomposing the nitrate to oxide.
3. Platinum is added to the coated substrate as above using an aqueous solution of tetraamine platinum (II) dihydroxide or other platinum salt, and then thermally decomposing the salt. Instead of the thermal decomposition, a reductive decomposition can be used. For example, the catalyst-coated substrate is heated in an atmosphere containing a reducing gas, such as carbon monoxide or hydrogen, to induce reduction of the platinum salt to platinum. A similar process can be used to add the second precious metal (i.e., ruthenium), for example, by starting with an appropriate salt, or the mixed PMs may be applied in one step.

The instant catalyst can absorb the NO_x species and convert them to NO. As such, nitrosyl complexation takes place with a noble metal in order to allow it to react with a reducing agent and therefore be converted to nitrogen. Preferred metal-oxide promoters are Fe_2O_3, NiO, and CO_2O_3. The metal-oxide adduct with NO_x is converted to NO on desorption. The NO is subsequently transferred and bound to the PM until reduced by CO and HCs to N_2. The CO and HCs are similarly oxidized by NO or O_2 and SnO_2 at the PM interface site.

The advantages of the present invention include:
- Lower light-off temperatures can enable oxidation of methane emissions to CO_2 for natural gas fueled vehicles at lower exhaust gas temperatures.
- Lower light-off temperatures for CO and HCs enable more efficient catalytic conversion to CO_2 at lower cost.
- A tin-oxide base wash-coat on a ceramic substrate minimizes loss of coating through cracking, peeling, or dusting mechanisms.

- The PM coatings are on the top surface and are enabled to be more efficiently used, thus requiring less PM resulting in lower PM costs.
- The mixed PMs result in a more efficient oxidation/reduction catalyst and may be applied in one step.

This work was done by David Schryer and Billy Upchurch of Langley Research Center. ***For more information, download the Technical Support Package (free white paper) at www.techbriefs.com/tsp under the Materials & Coatings category.*** *LAR-16001-1*

Thermally Activated Crack Healing Mechanism for Metallic Materials

A thin metallic film of a low-melting-temperature healing agent is used.

Langley Research Center, Hampton, Virginia

A thermally activated healing mechanism is proposed and experimentally validated to mitigate crack propagation damage in metallic materials. The protected structure is coated with a thin metallic film of a low-melting-temperature healing agent. To heal or mitigate crack damage, the structure is heated to the melting temperature of the healing agent, allowing it to flow into the crack opening. Once in the crack mouth, the healing agent has two benefits: (1) by adhering to the crack surfaces, the healing agent bridges the crack, reducing the amount of load at the crack tip; and (2) any voluminous substance in the crack mouth causes crack closure (premature crack-face contact during cyclic loading) that also reduces the crack-tip loading.

The technology is a coating that could slow crack propagation in metal aircraft and spacecraft structures. In practice, a structure is coated with a low-temperature healing agent. When a crack is detected, heat melts the healing agent and it flows into the crack. As the temperature is reduced, the healing agent hardens and heals the crack by reducing the crack-tip stress intensity factor through closure and bridging.

Currently, the technology is only applicable for cracks that have reached the surface. It requires an external heat source to heat the coated sheet to 250 to 300 °F(≈120 to 150 °C) and must be processed in a vacuum. The coating has been prototyped on a titanium alloy sheet with an indium-tin eutectic alloy coating. Development continues with the ultimate goal of developing the technology into an in situ healing mechanism that can work automatically with structural health monitoring detectors.

The goal of the technology is to heal cracks in metal on aircraft and spacecraft. Ultimately, the goal for the technology is to incorporate smart coatings that will enable truly self-healing materials, which would provide enormous safety and maintenance benefits. Falling short of the ultimate goal of true self-healing properties, the technology would still have value as an in-shop repair tool.

This work was done by Stephen W. Smith, John A. Newman, Robert S. Piascik, and Edward H. Glaessgen of Langley Research Center. ***For more information, download the Technical Support Package (free white paper) at www.techbriefs.com/tsp under the Materials & Coatings category.*** *LAR-17681-1*

Subsurface Imaging of Nanocomposites

Applications include sensors and actuators, aerospace structures, and tissue infusion in medical areas.

Langley Research Center, Hampton, Virginia

A nondestructive method that is based on modified atomic force ultrasonic microscopy (AFUM) methods has been developed for characterizing nanomaterials. The technology allows imaging and quantifying of material properties at the surface and subsurface levels. The technology reveals the orientation of nanotubes within a composite structure and offers the ability to determine subsurface characteristics without destroying the nanomaterial structure. The method is widely applicable for basic nanomaterials characterization, including distribution and orientation of particles in a nanocomposite, localized elastic constants and changes in elastic constants, adhesive surface properties, sound velocity, and material damping coefficient.

The technology is:

- Nondestructive: Previous methods require destructive sampling.
- Ubiquitous: A wide range of materials characterization for nanomaterials is enabled.
- Elegant: Design is based on modifications to commercially available atomic force ultrasonic microscopy (AFUM) hardware.

The manufacturing of nanocomposites produced by the embedding of nanostructural constituents into matrix materials has placed increased demands on the development of new measurement methods and techniques to assess the microstructure physical property relationships of such materials. Although a number of techniques are available for near-surface characterization, this new method allows assessment of deeper (subsurface) features at the nanoscale.

This new scanning probe microscope methodology is called resonant difference frequency atomic force ultrasonic microscopy (RDF-AFUM). It employs an ultrasonic wave launched from the bottom of a sample while the cantilever of an atomic force microscope engages the sample top surface. The cantilever is driven at a frequency differing from the ultrasonic frequency by one of the contact resonance frequencies of the cantilever. The nonlinear mixing of the oscillating cantilever and the ultrasonic wave at the sample surface generate difference-frequency oscillations at the cantilever contact resonance. The resonance-enhanced difference-frequency signals are used to create amplitude and phase-generated images of nanoscale near-surface and subsurface features.

The technology offers wide-ranging market applications such as functional nanocomposites for aerospace structures, biomedical uses such as infusion of tissue with nanoparticles, verification of drug delivery to tissue targets, and sensors/actuators.

This work was done by John Cantrell and Sean Cantrell of Langley Research Center. For further information, contact the Langley Innovative Partnerships Office at (757) 864-8881. LAR-17440-1

Self-Healing Glass Sealants for Solid Oxide Fuel Cells and Electrolyzer Cells

Operational requirements are 600 to 1,000 °C for thousands of hours.

John H. Glenn Research Center, Cleveland, Ohio

A solid oxide fuel cell (SOFC) is an electrochemical device that converts chemical energy into electrical power. A solid oxide electrolyzer cell (SOEC) operates in a reverse mode of SOFC, and produces O_2 and H_2 gases. SOFCs are being developed for a broad range of applications including portable electronic devices, automobiles, power generation, and aeronautics. The salient features of SOFCs are all-solid construction and high-temperature electrochemical reaction-based operation, resulting in clean and efficient power generation from a variety of fuels. SOFCs of two different designs, tubular and planar, are currently under development. Planar SOFCs offer several advantages such as simple manufacturing and relatively short current path, resulting in higher power density and efficiency. However, planar SOFCs and SOECs require hermetic seals. Various glass and glass-ceramics based on borates, phosphates, and silicates are being examined for SOFC seals. Silicate glasses are expected to perform superior to the borate and phosphate glasses as sealing materials.

Planar SOFCs and SOECs require hermetic seals along the edges of each cell and between the stack and gas manifolds to separate and contain fuel and oxidant within the cell and to bond cell components together. The requirements for SOFC and SOEC sealing materials are severe since the cells will operate at 600 to 1,000 °C for thousands of hours, with sealing materials exposed to both oxidizing and reducing conditions.

Quaternary silicate glasses containing MgO, CaO, Al_2O_3, and SiO_2 have been identified as seal materials for SOFCs and SOECs. These glasses are free of the detrimental constituents such as boron and alkali metals. A representative glass composition in this quarternary system has been prepared by melting the constituents together. Properties of these quarternary silicate glasses are appropriate for use as hermetic sealing materials at operating temperatures of these devices. Seals made out of these glasses will be self-healing as operating temperatures of SOFC and SOEC are higher than the softening point of these glass sealants.

Physical, thermal, mechanical, and electrical properties of these glass sealants are compatible with those of other SOFC and SOEC components: electrolyte, cathode, anode, and interconnect.

This work was done by Narottam Bansal of Glenn Research Center. ***For more information, download the Technical Support Package (free white paper) at www.techbriefs.com/tsp under the Materials & Coatings category.***

Inquiries concerning rights for the commercial use of this invention should be addressed to NASA Glenn Research Center, Innovative Partnerships Office, Attn: Steven Fedor, Mail Stop 4–8, 21000 Brookpark Road, Cleveland, Ohio 44135. Refer to LEW-19100-1.

Micromachined Thermopile Arrays with Novel Thermo-electric Materials

Goddard Space Flight Center, Greenbelt, Maryland

Future missions to outer planets will have stringent limits on payload mass. Thermal imaging instruments to map planetary surfaces will be part of those payloads, and, consequently, will have to be compact and low mass. For thermal instruments, another key requirement will be state-of-the-art, highly sensitive detectors. Thermopiles are prime candidates for high-resolution thermal mapping in the far-infrared (17- to 250-μm wavelength) spectral range. Thermopile detector arrays can be made to be very lightweight and compact. Furthermore, they require very few ancillary components (e.g., readout electronics, optics, amplifiers), which can add to instrument volume and mass. The implementation of thermopiles on these missions is likely because they (1) generate an output voltage that is proportional to the incoming radiation within the spectral range being mapped; (2) do not require an electrical bias or an optical chopper; (3) have negligible 1/f noise; (4) are radiation hard; and (5) have a reported specific detectivity of 1 × 10^9 cm·$Hz^{1/2}$/W at room temperature.

The focus of this work is to fabricate thermopiles using unique semimetallic materials developed in the Detector Development Laboratory (DDL). Novel semimetallic materials, which have been developed for other projects, were evaluated in terms of a thermoelectric figure of merit, as candidate thermopile materials. Intermetallic thermopiles, which have high Seebeck coefficients and, consequently, high detector sensitivity, require highly specialized fabrication techniques and are susceptible to aging. Semiconductor thermopiles have a limited operating range and are susceptible to high radiation environments. An alternative approach can address these issues, but, in the former case, they are not radiation hard, or in the latter case, they are unstable to environmental conditions (temperature, oxygen). The advantage of using semimetallic materials is that they are radiation hard and their thermoelectric properties do not change appreciably in the temperature range of interest.

This work was done by Ari Brown, Emily Barrentine, and Shahid Aslam of Goddard Space Flight Center. ***For more information, download the Technical Support Package (free white paper) at www.techbriefs.com/tsp under the Materials & Coatings category.*** *GSC-16837-1*

Low-Cost, High-Performance MMOD Shielding

Relatively inexpensive fiberglass fabric is proposed in place of costlier materials.

Lyndon B. Johnson Space Center, Houston, Texas

High-performance micro-meteoroid and orbital debris (MMOD) shielding can be constructed from low-cost, off-the-shelf materials. The advantage in using this innovation is in achieving considerable reduction in both cost and mass of the shielding necessary to protect spacecraft from hypervelocity MMOD particle impacts. For instance, in a typical application of this technology for a visiting vehicle used to transport cargo to the International Space Station (ISS) over ten years, an estimated $330,000 is saved (at the time of this reporting) in using a less-expensive MMOD fabric over conventional materials, and an estimated 2,000-kg mass is reduced from the MMOD shielding using the materials and techniques described here compared to conventional means.

Micro-meteoroid and orbital debris shields typically contain relatively expensive ceramic fabrics. For instance, the majority of the MMOD shields on the ISS US Laboratory module contain six layers of ceramic cloth. The purposes of the ceramic fabric in MMOD shields are to break up the incoming MMOD particle or hypervelocity projectile, and cause the debris resulting from the break-up to disperse laterally before impacting subsequent layers of the shield. Ceramics have excellent dynamic properties to achieve good projectile breakup, for either high-density orbital debris particles or lower-density meteoroid particles, by creating relatively high shock pressures in the impacting projectile. Analytical evaluation of various potential materials was conducted to determine which material has suitable characteristics for MMOD protection. Based on these evaluations and cost estimates, materials that could provide suitable MMOD protection at lower cost were identified.

Using inexpensive fiberglass fabric in place of the more expensive ceramic cloth is currently used to protect the SpaceX Dragon commercial cargo vehicle from MMOD particles. This innovation will likely be used on future inflatable modules, and is being considered by Orbital Sciences for use on the Cygnus commercial cargo vehicle. Other future spacecraft can also use this technology in their MMOD shields.

This work was done by Eric Christiansen and Dana Lear of Johnson Space Center, and Frankel Lyons and Bruce Davis of Jacobs Technology. ***For more information, download the Technical Support Package (free white paper) at www.techbriefs.com/tsp under the Materials & Coatings category.*** *MSC-25250-1*

Mechanics/Machinery

Head-Mounted Display Latency Measurement Rig

This technique can be used to characterize systems for product improvement by virtual/augmented reality display manufacturers.

Langley Research Center, Hampton, Virginia

The device and method are used to quantify end-to-end latency of head- or helmet-mounted display with head tracking systems in a laboratory or in situ. All commercial or custom head-mounted display systems that track the user's head for the purpose of virtual or augmented reality applications encounter positional display errors due to system latency. A basic head-mounted display (HMD) with head-tracking system is comprised of (1) a near-to-eye display, (2) the head-tracking system, (3) one or more symbology or image sources, and (4) the display/image processor. Each element, and the communication among them, contributes a portion to the total latency. HMD system latency manifests as erroneous alignment of the virtual and real surroundings as the head is slewed, and is known to induce simulator sickness and other physiological issues. Therefore, minimal system latency is a design goal to reduce these physiological symptoms. The overall latency budget is the sum of time required to measure the dynamic head position, communicate the position to the display processor, compute the scene based on the position, integrate imagery, and render the scene to the display.

The Head-Mounted Display Latency Measurement Rig (HeLMR) device (see figure) consists of a 3D-printed, anatomically approximate human head that is able to "wear" all available commercial and custom HMD systems. A high-speed camera is installed in place of the eye(s) in the correct image plane location. The head is mounted on a precision rotary stage that moves the head in a left-right-left "No-No" fashion at a precise angular rate. The device's native geo-referenced virtual image is rendered and aligned to overlay a real-world reference. Static and dynamic lasers are used for reference to aid the alignment. The head is moved and tracked dynamically while the high-speed (300 fps) video image from the camera shows the angular skew of the virtual-to-actual image due to the system latency. A snapshot image is captured and the angular difference of the virtual image to the actual image is measured with computer-aided design software. With the error angle measurement and the precision rate information, the total system latency is calculated. The HeLMR device/method quantifies the end-to-end latency of the entire system and can be mounted on a synthetic torso for in situ measurements of flight simulators or other applications.

Initial testing was conducted on a custom HMD for a lunar lander application. As with a standard tracking HMD system, symbology (e.g., terrain, attitude, guidance) is rendered that is referenced to a world coordinate system. As the head is slewed, the symbology is misaligned with the surrounding terrain due to the system latency. This head tracker system uses a hybrid combination of optical and inertial sensors where both the display and tracker are mounted to clear-lens glasses with a head-borne weight of 4 oz. (113 g). The total system latency of the lunar HWD system was measured to be 67 milliseconds with detailed lunar terrain rendering, and 33 milliseconds without terrain. This indicates that the latency is content-dependent in addition to several other factors, including the display update rate. This system is novel with the ability to non-intrusively quantify system latency and has been successfully used on several HMD systems. The apparatus combines precision COTS equipment in a unique arrangement, enabling the measurement of a difficult-to-quantify parameter.

This work was done by Kevin Shelton, Randy Bailey, Trey Arthur, Steve Williams, Lance Prinzel, Lynda Kramer, Denise Jones, and Kyle Ellis of Langley Research Center. ***For more information, download the Technical Support Package (free white paper) at www.techbriefs.com/tsp under the Mechanics/Machinery category****. LAR-17884-1*

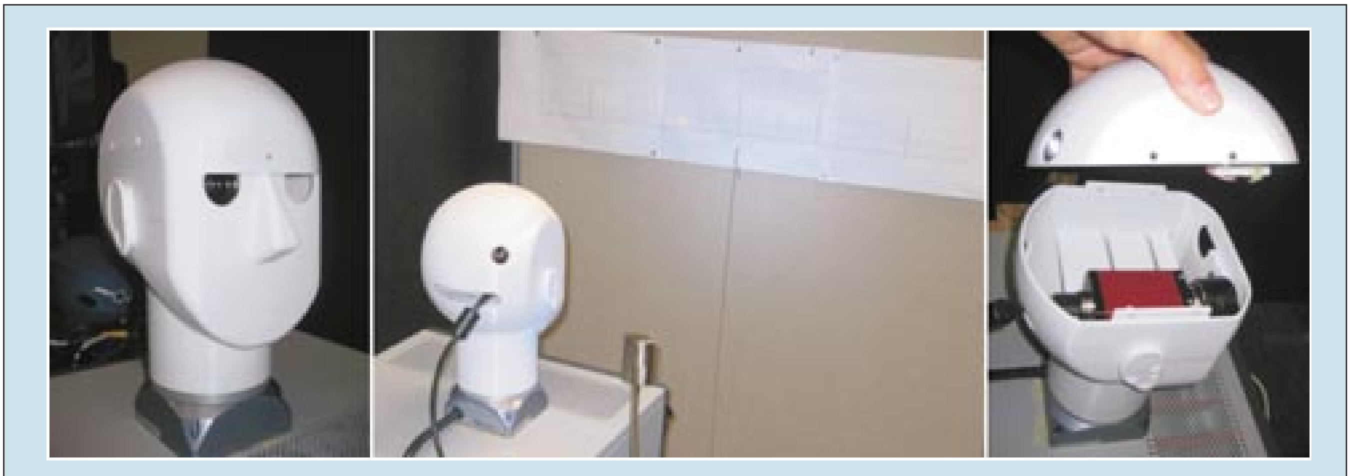

The **HeLMR System** consists of the head, camera, rotary stage, stage controller, and dc light source.

Workspace-Safe Operation of a Force- or Impedance-Controlled Robot

This technology can be used for automatic control of a robot that may come into contact with an object or operator in its workspace.

Lyndon B. Johnson Space Center, Houston, Texas

Precise motion control of a robot by controlling its various robotic manipulators may be organized by the required level of task specification. The levels include object-level control, which describes the ability to control the behavior of an object held in a single or a cooperative grasp of the robot; end-effector control, which is control of the various manipulators such as robotic fingers and thumbs; and joint-level control. Collectively, the various control levels achieve the required mobility, dexterity, and work task-related functionality.

This invention relates to the automatic control of a force- or impedance-controlled robot in an operating environment in which a robotic manipulator of the robot may come into unexpected direct physical contact with an object and/or an operator within its workspace.

A method of controlling a robotic manipulator of a force-or impedance-controlled robot within an unstructured workspace includes imposing a saturation limit on a static force applied by the manipulator to its surrounding environment. Should the robotic manipulator unexpectedly contact an object in its workspace, the static force applied by the manipulator is limited. Upon contact, the robotic manipulator proceeds with its assigned task without "fighting" through the object after the object is encountered.

The control strategy also may include automatically executing a predetermined dynamic reflex upon a threshold contact force with the object. The dynamic reflex alleviates any inertial impulse of the contact that is not already addressed by the saturation-limited static force. The dynamic reflex can rely on either dynamic modeling or exteroceptive sensing in order to detect the contact.

The controller provides a control strategy for the robot using an algorithm. The control strategy provides a static compliance phase at all times, and may also provide an additional dynamic reflex phase to help ensure the safe operation of the robot. The controller may be a server or host machine with one or more microprocessors or CPUs. Individual control algorithms resident in the controller may be stored in ROM (read only memory) or other suitable memory and automatically executed to provide the control functionality.

This work was done by Philip Strawser of Johnson Space Center; John Yamokoski and Brian Hargrave of Oceaneering Space Systems; and Muhammad Abdallah of General Motors Corp. ***For more information, download the Technical Support Package (free white paper) at www.techbriefs.com/tsp under the Mechanics/Machinery category.*** *MSC-25121-1*

Cryogenic Mixing Pump with No Moving Parts

The pump is self-priming and can efficiently pump two-phase fluid.

John H. Glenn Research Center, Cleveland, Ohio

Refueling spacecraft in space offers tremendous benefits for increased payload capacity and reduced launch cost, but the problem of thermal stratification in long-term storage tanks presents a key challenge. To meet this challenge, a reliable, compact, lightweight, and efficient cryogenic mixing pump was developed with no moving parts. The pump uses an innovative thermodynamic process to generate fluid jets to promote fluid mixing. This thermodynamic process eliminates moving parts to generate pumping action. Inherent to its design, the pump is self-priming and can efficiently pump two-phase fluid. The device will significantly enhance the reliability of pressure control systems for storage tanks.

In thermal stratification, vaporized hot spots develop inside the storage chamber, elevating pressure and creating an overpressure hazard. Mechanical mixing to de-stratify the fluid and create a uniform bulk temperature in microgravity is an effective approach for controlling the pressure inside a large propellant tank. Reliable operation at cryogenic temperature is a challenge for pumps because no lubricants can be used. Pumping a saturated cryogenic fluid poses several unique challenges for a mechanical pump. Existing pumps for cryogenic fluid transfer require a high degree of subcooling at the pump inlet to prevent pump cavitation or de-priming.

The thermodynamic process is well known and has been previously used to develop heat pumps and refrigeration devices. This innovation applies this scientific principle to two-phase room-temperature and cryogenic refrigerants to produce pumping from cyclic pressurization and depressurization of the fluid through a thermal process. The thermodynamic process enables efficient use of the heat absorbed during the depressurization step to thermally raise the cryogen pressure during the pressurization step, thus minimizing the net heat input to the cryogen due to the pumping process.

On the pressurization process, the pumping chamber heats the cryogen, increasing pressure within the pump. The increased pressure displaces some of the fluid within the pump.

On the cooling cycle, the pumping chamber cools the cryogen. The vaporized cryogen in the pumping chamber then condenses, creating a suction pressure within the pump that draws in addition fluid. Check valves are used to ensure that the fluid is one-directional for efficient pumping.

This work was done by Weibo Chen and Adam Niblick of Creare Incorporated for Glenn Research Center. ***For more information, download the Technical Support Package (free white paper) at www.techbriefs.com/tsp under the Mechanics/Machinery category.***

Inquiries concerning rights for the commercial use of this invention should be addressed to NASA Glenn Research Center, Innovative Partnerships Office, Attn: Steven Fedor, Mail Stop 4–8, 21000 Brookpark Road, Cleveland, Ohio 44135. Refer to LEW-19140-1.

Seal Design Feature for Redundancy Verification

The technology may be of interest to designers of high-altitude aircraft and submarine vessels.

Lyndon B. Johnson Space Center, Houston, Texas

NASA has requirements for redundant seals to protect human-occupied cabin atmospheres, as well as fluid and gas systems in space vehicles exposed to the harsh environments. Comparable requirements have been passed down to the International Space Station (ISS) Program, and are now levied on the Orion Multi-Purpose Crew Vehicle (MPCV).

The purpose of this invention is to allow independent verification of redundant critical seals, which are seals through which leakage would constitute a catastrophic or critical failure. The problem, in the case of the Orion Crew Module (CM) side hatch, is access to the seals. In most cases with other hatches, access to the seals does not present the same problem because the area where the seals are located can easily be bagged with plastic material and tape. Bagging the area creates a containment volume for a trace gas around the entire perimeter (inside and outside) that allows ease of seal leakage verification using a mass spectrometer leak detector (MSLD) per requirements.

In the case of the CM side hatch, seals are not accessible from either side, and are buried deep in the configuration when the hatch is closed. In the case of the Shuttle Orbiter, side hatch seal leakage verification was performed by pressurizing between the redundant seals, and performing a leak decay test. This verified that both seals together met the leakage requirement; however, it did not meet the requirement to verify each redundant seal path independently as required by the Orion requirement version levied to the program by NASA and thus was the driver for this invention. The leak rate specification is much smaller for the Orion vehicle than the Shuttle Orbiter or any other manned vehicle in NASA's history, and cannot be verified accurately by performing a leak decay test.

In this invention, a two-beaded silicone rubber molded seal with a metal substrate retainer is used and the interstitial area between the two seal beads is connected to the leak detector (MSLD) via the test port connector on the CM Hatch Service Panel. The outer area of each seal bulb is shrouded by a helium environment that is contained by the following features designed into the seal retainer, which is the core of the invention:

1. A series of machined through holes called conductance passageways in the metal seal retainer that are connected to one another by conductance grooves encompassing the entire outer perimeter of each seal bulb.
2. An elastomeric material is permanently adhered to the outer corners of the metallic seal retainer. When the hatch is closed, the elastomeric material is compressed together creating a containment dam and thus a

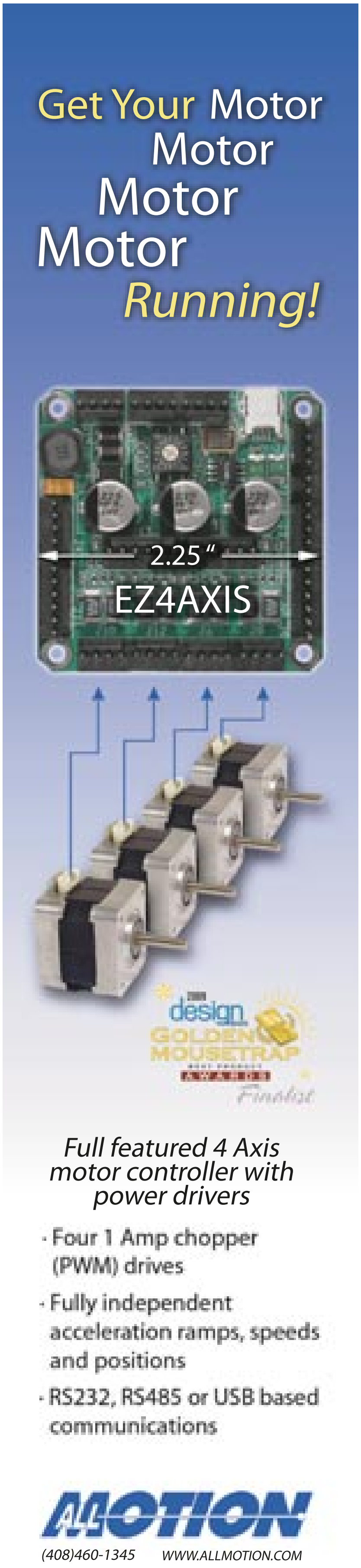

containment area for the helium trace gas.

This containment volume is evacuated and then back-filled with helium to facilitate the test of each seal bead. The volume between the seal beads is evacuated by the MSLD, which quantifies any leakage across that seal bead. The same process is then repeated for the other seal bead.

Similar type seals (with redundant seal beads mounted in metal retainers) are currently used in other human-rated space vehicles, and do include design features such as leak test ports and conductance grooves within the seal interstitial area to accommodate redundant seal verification. Now with the added features that this invention brings, a common leak test method known as the Helium Leak Test, Vacuum Method – Hood Test can be employed to not only verify the redundancy of the seal, but actually quickly quantify the leakage rate of each seal path independently.

This work was done by Doug Harrison of Lockheed Martin Space Systems Co. for Johnson Space Center For further information, contact the JSC Technology Transfer Office at (281) 483-3809. MSC-24680-1

Dexterous Humanoid Robot

This robot can replace human workers in dangerous, life-threatening conditions.

Lyndon B. Johnson Space Center, Houston, Texas

A humanoid robot has been created that includes a torso, a pair of arms, a neck, and a head. The torso extends along a primary axis and presents a pair of shoulders. The pair of arms movably extends from the shoulders. Each of the arms is fully jointed. The neck movably extends from the torso along the primary axis, and has at least one neck joint. The head movably extends from the neck along the primary axis. The head has at least one head joint. The shoulders are canted toward one another at a shrug angle that is defined between each of the shoulders such that a workspace is defined between the shoulders.

In another aspect of the invention, a human robot is created as described above, but also includes a pair of hands and a skin layer. Each of the hands includes at least five fingers such that each hand has at least 12 degrees of freedom (DOF). The skin layer substantially covers the robot. The multiple DOF provide the robot with a level of dexterity required to manipulate standard tools and assembly components. The robot may also be configured to achieve strength and sensing levels that are consistent with manipulating substantial tools and hardware. The hands may be strong enough to solidly grasp heavy payloads, e.g., 20 pounds (≈9 kg) and the like, with the hands in any orientation. The arms, the hands, and the fingers may also be configured to have force control, or the dexterity to manipulate flexible materials, small objects, human tools, etc.

Each robotic joint contains and/or is driven by one or more actuators, e.g., joint motors, linear actuators, rotary actuators, and the like. As a result, the robot is configured to perform significant work. Specifically, the robot can perform assembly, construction, and maintenance tasks that are currently performed by humans. Additionally, the robot may be configured to be of the human scale, allowing the robot to share the same workspaces that are typically designed for human workers.

This work was done by Robert O. Ambrose, Myron A. Diftler, Scott R. Askew, Robert Platt, Joshua S. Mehling, Nicolaus A. Radford, Philip A. Strawser, and Lyndon Bridgewater of Johnson Space Center; Charles W. Wampler II, Muhammad E. Abdallah, Chris A. Ihrke, Matthew J. Reiland, Adam M. Sanders, and Donald R. Davis of General Motors Corp.; and David M. Reich, Brian Hargrave, Adam H. Parsons, and Frank Noble Permenter of Oceaneering Space Systems. For further information, contact the JSC Technology Transfer Office at (281) 483-3809.

Title to this invention has been waived under the provisions of the National Aeronautics and Space Act {42 U.S.C. 2457(f)} to General Motors Corporation. Inquiries concerning licenses for its commercial development should be addressed to:

General Motors Research & Development Center
30500 Mound Road
Warren, MI 48090-9055
Phone No.: (313) 556-5000

Refer to MSC-24739-1, volume and number of this NASA Tech Briefs *issue, and the page number.*

Tethered Vehicle Control and Tracking System

Kite-like wind energy generation systems can power a generator on the ground.

Langley Research Center, Hampton, Virginia

This innovation can control the flight of a tethered vehicle, in an airborne wind energy (AWE) generation system, through the use of a pan-tilt platform and a visible spectrum digital camera, combined with tracking and control software running on a standard PC.

One of the main technical challenges involved in building a feasible AWE system is developing the control system. It is not sufficient to stabilize the kite — it must be flown in a high-speed crosswind trajectory for power generation. Additionally, the behavior of the kite is highly nonlinear and difficult to model due to flexible structures that assume a shape in response to aerodynamic loads. In this invention, all sensors are kept on the ground, allowing the kite to be as light as possible. A fuzzy logic system was chosen to perform this control task because a reliable model of the kite is unavailable, and the operation of the kite is relatively easy to explain. A commercial, two-line-controlled, ram-air kite was used for developing and testing the control system.

The system uses measurements of the tension in each line, the length of each line, and the estimated position of the kite from a vision-based tracking system as input. It then outputs a commanded difference in length between the lines, as well as an average reel rate for both lines.

A predictor-corrector approach is used to track the air vehicle. The previously estimated position and velocity are propagated to a position estimate. Detecting the air vehicle is accomplished using three algorithms: change in time of brightness, a change in time of hue, and spatial maximum of hue. A pan-tilt platform is used to keep the air vehicle within the camera frame. A fuzzy logic-based controller is used to generate steering and reeling commands for the air vehicle from the position and velocity estimated by the tracking system, as well as the line tension, velocity, wind speed, and direction. Ground-based visual tracking is likely to have higher error in localization compared to a combination of onboard sensors, but has a significant advantage in expense, complexity, and the weight of the air vehicle. A fuzzy controller has advantages in robustness over many other control methods.

This innovation makes use of OpenCV code for some vision processing tasks, Microsoft DirectX and XAudio2 code for communicating with some computer hardware, proprietary libraries for communicating with weather stations, and tension-measuring hardware.

This work was done by David North and Mark Aull for Langley Research Center. ***For more information, download the Technical Support Package (free white paper) at www.techbriefs.com/tsp under the Mechanics/Machinery category.*** *LAR-18246-1*

Intro Cov ToC

Lunar Organic Waste Reformer

Possible applications also include conversion of terrestrial organic wastes into fuel for power generation or into feedstock for chemical manufacture.

John H. Glenn Research Center, Cleveland, Ohio

The Lunar Organic Waste Reformer (LOWR) is a novel technology to convert organic wastes from human space exploration outposts into useful propellant constituents. The LOWR meets NASA's Trash to Supply Gas (TtSG) objective under the Advanced Exploration Systems Logistics Reduction and Repurposing project by integrating steam reformation, methanation, and electrolysis to convert organic waste into methane and oxygen products. At reformer temperatures above 700 °C, oxygenated steam reacts with organic matter to produce a gas mixture largely composed of hydrogen, carbon monoxide, and carbon dioxide. After condensing and removing excess water, the reformer exhaust gases are fed to a catalytic Sabatier reactor where they are combined with supplemental hydrogen at 350 to 500 °C to produce methane and water. The methane product can be liquefied for storage.

Electrolysis of water obtained from the reformer and Sabatier reactors provides the supplemental hydrogen needed for methanation, while simultaneously producing oxygen used during steam reforming. Excess oxygen is stored as a product. The LOWR system design requires minimal feed preparation and results in nearly complete conversion of feeds to valuable products with minimal consumables, resulting in rapid payback. The thermochemical production of hydrogen in the LOWR reformer leads to significantly reduced electrolysis power requirements compared to other waste treatment methods.

The primary application of the LOWR is for conversion of organic wastes from human exploration outposts into valuable propellant components. The LOWR reduces risks associated with handling and storing organic wastes while recycling waste constituents into products that would otherwise be imported from Earth.

Adaptations of the LOWR are suitable for conversion of terrestrial organic wastes into fuel for power generation or into feedstock for chemical manufacture. Such usage would reduce effluents otherwise discharged into the environment while reducing the need for new fuels.

This work was done by Stacy L. Carrera, Robert M. Zubrin, and Mark Berggren of Pioneer Astronautics for Glenn Research Center. ***For more information, download the Technical Support Package (free white paper) at www.techbriefs.com/tsp under the Physical Sciences category.***

Inquiries concerning rights for the commercial use of this invention should be addressed to NASA Glenn Research Center, Innovative Partnerships Office, Attn: Steven Fedor, Mail Stop 4–8, 21000 Brookpark Road, Cleveland, Ohio 44135. Refer to LEW-19093-1.

Digital Laser Frequency Stabilization via Cavity Locking Employing Low-Frequency Direct Modulation

Direct modulation reduces complexity, volume, and mass.

NASA's Jet Propulsion Laboratory, Pasadena, California

This project's goal was to simplify laser frequency stabilization. A simpler system will have many benefits, including reduction of power consumption, complexity, volume, mass, and risk of failure. To implement the Pound-Drever-Hall (PDH) technique requires both RF modulation and demodulation electronics, including an electro-optic modulator, a photoreceiver of sufficient bandwidth to detect the RF modulation fields, demodulation electronics of sufficient bandwidth, and an RF function generator. For a space mission, this equipment can be costly and power-hungry, in addition to the difficulty of being rated to operate in the harsh space environment.

The need for laser frequency stabilization will occur in many planned missions employing multiple lasers on multiple spacecraft (SIM, LISA, GRACE Follow-on, GRACE C). In addition, many laboratory measurements require laser frequency stabilization. This software-based system obviates the need for RF components (modulator, detector, frequency/function generator, and associated electronics), both in the laboratory and on a spacecraft, to perform laser frequency stabilization in a digitally controlled system.

The code-based (digital) technique was demonstrated for laser frequency stabilization to an optical reference cavity without requiring any RF electronics or RF equipment. The process is coded using LabVIEW and employs field programmable gate arrays (FPGAs) for digital input and output from the photoreceiver and laser, respectively. Instead of employing an external phase-modulator driven by a function generator, the digital code directly modulates the laser's piezoelectric transducer (PZT).

This work has shown that high laser frequency stability performance can be achieved using optical cavity references, without the need for the traditional PDH RF electronics. This was demonstrated using digital software codes and control, significantly simplifying the analog electronics. This technique reduces mass and power associated with the RF electronics. This software technique is implemented via hardware that will already exist onboard the spacecraft. This also reduces complexity, power consumption, volume, and risk of failure.

This work was done by Glenn DeVine, Brent Ware, Kirk McKenzie, Robert J. Thompson, William M. Klipstein, William M. Folkner, and Robert E. Spero of Caltech for NASA's Jet Propulsion Laboratory. ***For more information, download the Technical Support Package (free white paper) at www.techbriefs.com/tsp under the Physical Sciences category.***

The software used in this innovation is available for commercial licensing. Please contact Dan Broderick at Daniel.F.Broderick@jpl.nasa.gov. Refer to NPO-48530.

Deep UV Discharge Lamps in Capillary Quartz Tubes with Light Output Coupled to an Optical Fiber

NASA's Jet Propulsion Laboratory, Pasadena, California

Researchers at Jet Propulsion Laboratory have come up with a novel approach to the simplification of the 194-nm light source and optical guidance in mercury trapped ion spectroscopy research. Mercury plasma is generated in a capillary tube with a diameter of a few hundred microns (in contrast to current lamp bulbs with a diameter of 13 mm). The deep ultraviolet (DUV) light from the plasma can be guided directly to the ions held in an ion trap in a vacuum system via a piece of DUV fiber that is fused at the end of the capillary tube.

Argon and isotopically enriched mercury (^{202}Hg) are prepared and sealed in a piece of capillary tube with a diameter of a few hundred microns. The mercury plasma can be generated inside the tube with externally applied RF or microwave power. Coils or surface strip electrodes can be used as a capacitive resonator to sustain the plasma. One end of the tube is sealed, and the other end of the tube is fused with a piece of large-core DUV step-index fiber, where the DUV radiation from the plasma is collected. A gradient-index lens can be manufactured at the output tip of the fiber to deliver the condensed light to the ions. The fiber output can be brought close to the ion trap assembly and coupled through a UV window or fiber feedthrough assembly. Alternatively, the miniature plasma and delivery assembly could be placed entirely in the ion trap vacuum assembly.

This work was done by Robert L. Tjoelker, Eric A. Burt, and Shouhua Huang of Caltech; and Lin Yi for NASA's Jet Propulsion Laboratory. For more information, contact iaoffice@jpl.nasa.gov. NPO-48845

Speech Acquisition and Automatic Speech Recognition for Integrated Spacesuit Audio Systems, Version II

System offers superior performance from prior version, and a number of commercial applications.

John H. Glenn Research Center, Cleveland, Ohio

Astronauts suffer from poor dexterity of their hands due to the clumsy spacesuit gloves during Extravehicular Activity (EVA) operations, and NASA has had a widely recognized but unmet need for novel human-machine interface technologies to facilitate data entry, communications, and robots or intelligent systems control. A speech interface driven by an astronaut's own voice is ideal for

EVA operations, since speech is the most natural, flexible, efficient, and economical form of human communication and information exchange.

The current solution is a Communication Carrier Assembly (CCA)-based audio system. While the close-talking, noise-canceling microphone used in the CCA system can deliver speech signals with high intelligibility, its performance is sensitive to the microphone's distance and orientation to the suit subject's mouth. An integrated audio (IA) system is imperatively pursued. In order to possess similar performance to a CCA, the IA system will consist of multiple microphones that form an array to reduce noise and enhance speech intelligibility.

The developed speech human-machine interface will enable both crewmember usability and operational efficiency. It employs a fast rate of data/text entry, small overall size, and is lightweight. In addition, it frees not only the hands, but also the eyes of a suited crewmember.

The system contains the following key technical components/steps: beam-forming/multichannel noise reduction, single-channel noise reduction, speech feature extraction, feature transformation and normalization, feature compression, model adaptation, ASR (automatic speech recognition) HMM (hidden Markov model) training, and ASR decoding.

Potential applications include in-helmet voice communication for the design of new spacesuits; telecollaboration via multimedia telepresence; human-machine interface for intelligent systems; hands-free, in-car voice communication and processing; mobile phones; military voice communication and speech processing systems; telemedicine and telehealth; multi-party teleconferencing; and acoustic surveillance.

This work was done by Yiteng (Arden) Huang, Sherry Q. Ye, and Yao (Yaron) Zhou of WeVoice, Inc. for Glenn Research Center. ***For more information, download the Technical Support Package (free white paper) at www.techbriefs.com/tsp under the Physical Sciences category****.*

Inquiries concerning rights for the commercial use of this invention should be addressed to NASA Glenn Research Center, Innovative Partnerships Office, Attn: Steven Fedor, Mail Stop 4–8, 21000 Brookpark Road, Cleveland, Ohio 44135. Refer to LEW-18930-1.

Advanced Sensor Technology for Algal Biotechnology

Ames Research Center, Moffett Field, California

Advanced Sensor Technology for Algal Biotechnology (ASTAB) is an integrated package of water quality and algal physiology sensors designed to enable algae growers to increase significantly productivity and efficiency of their operations, optimize harvesting periods, and avoid losses of "batches" of algae through nutrient deficiencies and/or population shifts. This sensor technology is expected to increase process automation and performance in large-scale algal production facilities.

ASTAB is a neutrally buoyant instrument package (e.g., a sphere) that travels around algal growth systems (e.g. photobioreators, raceways, ponds, bags, and tubes) with water flow. The parameters to be sensed and included in the package cover physical, chemical, and biological areas. Position information, and data on physical and biological parameters in the raceway or pond, is transmitted via a wireless network. Wireless connectivity allows for accurate position reporting, which will enable the creation of 3D maps and detect "dead spots."

The data are used to control local automatic devices to make appropriate changes to water quality (e.g. nutrient additions, pH controls). The package will determine a suite of important water quality attributes using conventional techniques, while simultaneously determining the photophysiological state of the algae using PAM (pulse amplitude modulation) fluorometry. PAM fluorometry is an optical technique that provides an immediate assessment of the photosynthetic efficiency (e.g., conversion of light into chemical energy) of algae, or the "health" of the algae. Additionally, the system features solar power, and anti-fouling and/or self-cleaning technologies.

This work was done by Brad Bebout of Ames Research Center. ***For more information, download the Technical Support Package (free white paper) at www.techbriefs.com/tsp under the Physical Sciences category.***

NASA invites companies to inquire about partnering opportunities. Contact the Ames Technology Partnerships Office at 1-855-627-2249 or ARC-TechTransfer@mail.nasa.gov. Refer to ARC-16342-1.

High-Speed Spectral Mapper

NASA's Jet Propulsion Laboratory, Pasadena, California

The Hyperspectral Infrared Imager (HyspIRI) spaceborne mission has two imaging sensors operating in the visible to shortwave infrared (VSWIR) and the thermal infrared (TIR), respectively. The HyspIRI-TIR imaging instrument is being developed for infrared mapping of the Earth in 8 spectral bands with a 5-day revisit time at the equator. The system will have 60-m ground resolution at nadir, 200-mK noise-equivalent temperature difference (NETD) for 300 K scenes, and 0.5 °C absolute temperature accuracy. As the spacecraft moves in its polar orbit, a rotating scan mirror allows the telescope to view a 51° cross-track nadir strip, an internal blackbody target, and space, every 2.1 s. Combining the overlapping strips will yield a 51° (597-km) wide swath below the spacecraft.

The detector array will be 256×256 pixels in size and consist of 13.5-µm cut-off HgCdTe material delineated into 40-µm pixels. Eight spectral filters spanning 4 to 12 µm in wavelength will be assembled into a butcher-block assembly in close proximity to the detector array. Four columns of 256 detectors in each spectral channel will be combined using time delay and integration (TDI) to form a single 256-element-wide strip. A custom readout integrated circuit will provide the high speeds needed for the required 32-µs frame time.

This work was done by Marc C. Foote, Simon J. Hook, and William R. Johnson of Caltech for NASA's Jet Propulsion Laboratory. ***For more information, download the Technical Support Package (free white paper) at www.techbriefs.com/tsp under the Physical Sciences category.*** *NPO-48394*

"Ascent - Commemorating Shuttle" — A NASA Film and Multimedia Project DVD

The production has demonstrated itself not only to be a technical record, but to also serve as an inspirational, motivational, and educational tool.

John H. Glenn Research Center, Cleveland, Ohio

NASA seeks to preserve, and make readily accessible, historical Space Shuttle launch footage to inspire and educate NASA stakeholders both in and outside the NASA family through the dissemination of the Ascent production materials as a DVD, and through both NASA Television and online social media avenues without incurring distribution and media costs.

"Ascent - Commemorating Shuttle" is a NASA technical and documentary film record comprised of engineering footage from Space Shuttle launches. The production uniquely serves as a NASA technical, historical, and public outreach document. Various elements of the completed Ascent project were distributed as a professionally produced DVD, on NASA Television, and viewed by millions as streaming video through YouTube.

The Ascent compilation represents the best shuttle film and high-definition video acquired during the program. As part of the Ascent DVD, viewers can choose from three separate commentary tracks to listen to shuttle engineers, launch trackers, and members of the post-launch film analysis team detail the different technical aspects of the film subject matter. These highly engaging and informative interviews, combined with the film, represent perhaps NASA's only official visual and oral record documenting the complex architecture and the men and women who made shuttle launch photography possible. The project took extensive advantage of both traditional and contemporary methods to reach not only a national, but a global audience for little or no cost to the Agency. Contributing to the success of "boosters" was a collaboration between the Ascent project team and engineers at Skywalker Sound, who mastered a 5.1 Surround Sound audio track for the DVD production — possibly another first for a NASA production.

The production has demonstrated itself not only to be a technical record, but to also serve as an inspirational, motivational, and educational tool. The value and significance of this is perhaps best measured by viewing statistics and feedback comments on the social media sites. Nearly two years after the shuttle program ended, the Ascent project team still receives a steady stream of inquiries about the film.

As a permanent historical record in NASA's video archive, the ascent DVD will provide an easily accessible document of shuttle launch footage capturing the knowledge and lessons of the Space Shuttle and its launch imagery system for future generations.

This work was done by Matt Melis of Glenn Research Center; and Gerald Nolan, Eric Mindek, Hugh Aylward, and Jim Firak of Wyle Information Systems. ***For more information, download the Technical Support Package (free white paper) at www.techbriefs.com/tsp under the Information Technology category.***

Inquiries concerning rights for the commercial use of this invention should be addressed to NASA Glenn Research Center, Innovative Partnerships Office, Attn: Steven Fedor, Mail Stop 4–8, 21000 Brookpark Road, Cleveland, Ohio 44135. Refer to LEW-19059-1.

High-Pressure, Reduced-Kinetics Mechanism for N-Hexadecane Oxidation

NASA's Jet Propulsion Laboratory, Pasadena, California

Combustion of realistic fuels is described by thousands of reactions involving thousands of species. Coupling these detailed chemical mechanisms with turbulence simulations is completely impractical because there is no computer powerful enough to solve the resulting equations.

A reduced-kinetics mechanism has been developed that uses only a few important species to duplicate the detailed mechanism at much lower computational cost. The compact reduced-kinetics mechanism has been developed for n-$C_{16}H_{34}$ oxidation that is based on a local full similarity of the detailed mechanism. The reduced mechanism employs only 20 light species and since the light-species reaction rates are more accurately known than those for heavy species, the present reduced mechanism has a smaller relative error than a reduced mechanism employing reactions involving heavy species.

The model was exercised in the context of a fixed-mass, constant-pressure reactor, and results were obtained over the entire range of equivalence-ratio validity of the detailed mechanism at the high pressures encountered in diesel, gas-turbine, and HCCI (homogeneous charge compression ignition) engines, and at both cold-ignition and hot-ignition temperatures. The results uniformly show excellent accuracy on the temporal evolution of the temperature, the major species mass fraction, and the OH mass fraction when compared to those of the detailed mechanism.

One advantage of the developed reduced kinetics is that it consists of the same 20 species for n-C_7H_{16}, n-$C_{10}H_{22}$, n-$C_{12}H_{26}$, n-$C_{16}H_{34}$, and i-C_8H_{18}, making it easy to use a reduced model for mixtures of species composing a practical fuel.

This work was done by Josette Bellan, Panagiotis D. Kourdis, and Kenneth Harstad of Caltech for NASA's Jet Propulsion Laboratory. For more information, contact iaoffice@jpl.nasa.gov.

The software used in this innovation is available for commercial licensing. Please contact Dan Broderick at Daniel.F.Broderick@jpl.nasa.gov. Refer to NPO-49408.

Method of Error Floor Mitigation in Low-Density Parity-Check Codes

NASA's Jet Propulsion Laboratory, Pasadena, California

Low-density parity-check (LDPC) codes often suffer from an "error floor" in which increasing signal-to-noise ratios do not lead to substantially better error rate performance. Error floors of LDPC codes are often not an inherent problem of the code design, but rather, a limitation of the standard decoding algorithms.

In this new technology, small but critical variations in standard belief propagation decoding algorithms dramatically lower the error floor of LDPC codes, including the set of

AR4JA LDPC codes that are recommended by the Consultative Committee for Space Data Systems (CCSDS), an international standards organization.

A modification of standard belief propagation message passing is made in a special way that allows the new decoder to converge to the correct codeword with a higher probability than was previously possible. The key innovation that leads to the lower error floors, particularly for the rate 4/5 AR4JA LDPC code and for any of the AR4JA codes when used with higher order modulations, is the introduction of a "partial hard-limiter" for decoder messages coming from the check nodes of the decoding graph.

Nearly every space mission NASA flies uses channel codes to protect the reliability of transmitted bits. LDPC codes are the way of the future, as they are contained in the standards not just for civilian space use, but also for terrestrial WiFi, WiMAX, and digital video broadcasting.

This work was done by Jon Hamkins of Caltech for NASA's Jet Propulsion Laboratory. For more information, contact iaoffice@jpl.nasa.gov.

In accordance with Public Law 96-517, the contractor has elected to retain title to this invention. Inquiries concerning rights for its commercial use should be addressed to:

Innovative Technology Assets Management
JPL
Mail Stop 321-123
4800 Oak Grove Drive
Pasadena, CA 91109-8099
E-mail: iaoffice@jpl.nasa.gov

Refer to NPO-48076, volume and number of this NASA Tech Briefs *issue, and the page number.*

X-Ray Flaw Size Parameter for POD Studies

Lyndon B. Johnson Space Center, Houston, Texas

Nondestructive evaluation (NDE) method capability is determined by a statistical flaw detection study called probability of detection (POD) study. In many instances, the NDE flaw detectability is given as a flaw size such as crack length. The flaw is either a crack or behaving like a crack in terms of affecting the structural integrity of the material. Although the crack size relates to structural integrity of the part, it may not be the only factor that affects the flaw detectability for most NDE methods. Crack length, depth, and opening may relate differently to the flaw detectability. Part surface roughness and cleanliness may affect the flaw detectability. The proposed flaw size parameter and the computer application described here give an alternative approach to conduct the POD studies and apply results of the POD study to reliably detect small flaws through better assessment of effect of interaction between various geometric parameters.

Many factors affect X-ray crack detectability. Therefore, crack depth-to-part-thickness ratio is not an accurate way of defining X-ray flaw detectability. Models that relate selected factors such as surface crack dimensions, orientation, part geometry, and technique parameters to film or image contrast for a simulated crack in a plate were developed. A geometric flaw size parameter is intended to be monotonically related to the POD under these conditions. This approach assumes that the flaw size parameter and

Intro Cov ToC

technique requirements, including the detector response calibration characteristics, together provide a complete description of the X-ray flaw detection application, and provide sufficient information for assessment of the NDE capability, i.e., whether the flaw size under consideration can be reliably detected. A simulated contrast model could do the same assessment if correlations are established between the simulated contrast and the actual contrast, and the simulation contrast and the POD.

This work was done by Ajay Koshti of Johnson Space Center. ***For more information, download the Technical Support Package (free white paper) at www.techbriefs.com/tsp under the Information Technology category.*** *MSC-25351-1*

Large Eddy Simulation Composition Equations for Two-Phase Fully Multicomponent Turbulent Flows

The composition probability density function moment variables are based on a new type of filter.

NASA's Jet Propulsion Laboratory, Pasadena, California

Liquid sprays are commonly used to inject fuels into combustion devices, making it important to study multicomponent (MC) two-phase flows in order to reveal their physics. "Multicomponent" is the terminology describing all fuels that are combinations of a myriad of species. Single-component simulations lack a detailed representation of the complex composition and reaction mechanisms of realistic fuels, which can contain hundreds to thousands of species. Some species may be responsible for fuel ignition, other species may be the initiators of soot formation, and yet others may be involved in surface corrosion, all of which demonstrates the importance of being able to track the multitude of species.

A new formulation has previously been developed that mitigates this problem: the fluid equations are deterministic whereas the composition equations are statistic and the composition is described statistically in terms of the molar densities. Thus, instead of tracking individual pseudo-components, this previous study used a statistical model, based on continuous thermodynamics (CT), to represent the composition by means of a probability density function (pdf) having an assumed shape. This approach considerably reduced the computational effort, since to obtain information of the type needed to predict mixing and combustion, it turns out that transport equations for only a small number of the lower moments of the pdf must be solved.

That previous formulation was valid when solving all scales of the flow, in a type of computation called direct numerical simulation (DNS). However, DNS requires very fine grids and is not practical in engineering applications where coarser grids are necessary for computational efficiency. For these engineering applications, the formulation called large eddy simulation (LES) is used instead of DNS. In LES, the larger scales are computationally resolved and the small scales, called subgrid-scales (SGSs), are modeled. A previous study deriving the LES equations showed that the SGS terms identified from the conventional methodology to derive the LES composition equations dominated the activity of all other terms, in contrast to the general assumptions of LES. Therefore, it was clear that a more adept formulation for the composition equations must be found.

In this study, a new set of equations was developed that leads to a formulation respecting the LES assumptions. To derive these LES composition equations, instead of the Favre mass density weighted filtering typically used to filter the equations, vapor partial molar density filtering is used. In this new LES formulation, the composition pdf moment variables are based on a new type of filter akin to, but different from, Favre filtering. For the SGS terms in the pdf composition equations that originate from the advective terms, the predictive capabilities of the dynamic Smagorinsky and the approximate-deconvolution-model-issued SGS models have been evaluated in an *a priori* analysis, and it was found that the latter showed superior capabilities compared to the former LES model for the composition equations.

This work was done by Josette Bellan of Caltech and Michael R. Gloor of Institute of Fluid Dynamics for NASA's Jet Propulsion Laboratory. For more information, contact iaoffice@jpl.nasa.gov. NPO-48002

Scheduling Targeted and Mapping Observations with State, Resource, and Timing Constraints

NASA's Jet Propulsion Laboratory, Pasadena, California

This innovation creates observations of both targeted geographical regions of interest and general mapping observations, while respecting spacecraft constraints such as data volume, observation timing, visibility, lighting, season, and science priorities. This tool, therefore, addresses both geometric and state/timing/resource constraints by using a grid-based approach. These set covering constraints are then incorporated into a greedy optimization scheduling algorithm that incorporates operations constraints to generate feasible schedules. The resultant tool generates schedules of hundreds of observations per week out of potentially thousands of observations.

Using greedy combinatorial optimization with gridded coverage representation, both targeted mapping observations (small geographical regions that can be covered in one or a small number of observations) and general mapping observations (large geographical regions that would take large numbers of observations, e.g. hundreds or more) can be scheduled. Using gridded coverage representation of a planetary surface, which maps all polygons (regions) into sets of points on a grid, makes polygon intersection very fast, and compiles the coverage problem into a set point covering the problem. At this point, the problem can be attacked using one of a set of combinatorial optimization techniques.

This work was done by Steve A. Chien, Gregg R. Rabideau, David A. McLaren, and Russell L. Knight of Caltech for NASA's Jet Propulsion Laboratory. ***For more information, download the Technical Support Package (free white paper) at www.techbriefs.com/tsp under the Information Technology category.***

This software is available for commercial licensing. Please contact Dan Broderick at Daniel.F.Broderick@jpl.nasa.gov. Refer to NPO-47603.

June 2014

IMAGING TECHNOLOGY

The State of the Art in Cameras & Vision Systems

Smart cameras, including the NI 1742 (shown) and NI 1752 from National Instruments, are used to inspect beer bottles on a production line. The strobe light control, image acquisition, analysis, and communication to the sorting machine all happen onboard the smart camera. See page 68.
(Image courtesy of National Instruments)

Blurring the Boundaries:

IP and Machine Vision Cameras Converge

Small and light cameras like the Basler ace are especially well suited for use in robotics applications.

In modern production facilities, users are more frequently combining two different strands of camera technology. Classic machine vision cameras manage inspection tasks and yield management, while network cameras (also called IP cameras) handle process monitoring and bringing production to a standstill when necessary.

In many ways, the two camera breeds are actually similar. Industrial GigE cameras typically work with the same Gigabit Ethernet technology as IP cameras. Both camera types also use the same technical protocols, including TCP/IP and UDP. The similarities, in fact, make the separate technologies — both engineered from the ground up to serve different purposes — easy to combine. Customers now want to implement both camera types to fit their specific applications, and new products are being developed that combine the best features from the IP and machine vision devices.

IP vs. Classic Industrial Cameras

The core differences between a classic machine vision camera and a network (or IP) device come in the areas of image data compression, multi-streaming, and real-time compatibility.

IP cameras are specially designed to work with low bandwidths to ensure that they can fit seamlessly in existing networks without overloading them. The camera is configured via a PC on the network to send a compressed video stream, such as MPEG-4, MJPEG, or H.264. The IP camera primarily provides a strong visual impression on the operator's monitor.

Industrial cameras, by contrast, are engineered to work with large bandwidths and optimal image quality as part of closed image processing systems. While network cameras compress the image data down to a fraction of its original data volume, in an effort to reduce the bandwidth required to transport that data, industrial cameras deliver raw images. The unprocessed images allow users to review even the most minute of details, as is necessary for quality inspections or detail measurements. If image data is missing and the error occurs precisely in that area, leading to a false positive by the inspection system, then the system has failed in its mission.

IP cameras are also capable of multi-streaming, meaning the camera sends multiple streams in different compression formats, such as H.264, MPEG-4, and MJPEG. Each end device then accesses a suitable stream. An operator, for example, can call up a high-resolution MJPEG stream offering strong detailing on his or her monitor, even while a space-saving version in the H.264 format is submitted for archiving. Machine vision cameras work with post-processed data that has already been evaluated, such as production statistics. The devices also optimize equipment performance and adapt the equipment to eliminate recurrent errors. In general, the images are only stored after inspection.

Real-time capability, another functional distinction between the two technologies, means that image capture starts immediately after a trigger signal has been sent to the camera. Image data must be acquired, transmitted, and evaluated within a set timeframe. The requirements

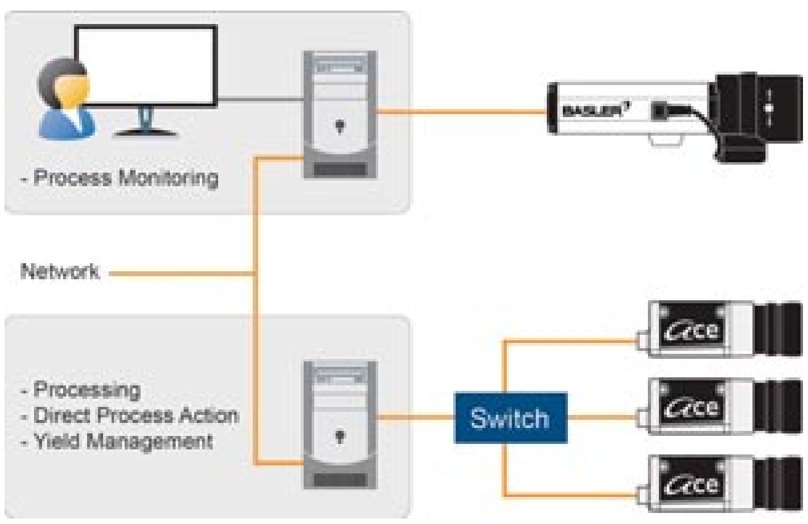

Industrial camera and IP camera systems are typically found within the same production environment, carrying out their own specific tasks.

for the maximum acceptable reaction time between trigger signal and image acquisition can vary from microseconds up to seconds. For industrial cameras, real-time images are a prerequisite. When inspecting components in a production process, for example, the components are transported on the conveyor belts at high speed. For a precise inspection, the camera must acquire the images as quickly as the components are being transported. Timing this precisely requires low latency: a small time delay between receiving the trigger signal and acquiring the image. Further, the time delay must not vary; no jitter can affect the moments of image acquisition. For an application with high image rates (e.g. 300 images per second), the required latency times can only be microseconds.

Similar requirements also exist outside of the factory, especially in traffic applications. In speed control systems, the camera activity must be synchronized with other system components, such as illumination devices. Many classic IP cameras are not real-time capable. In typical surveillance situations, such as monitoring the activity on a banking floor, the user needs an automatically captured, continuous stream of images without the need to trigger a camera. If a camera is set for a frame rate of 30 frames (images) per second, it will internally generate the signals required to initiate an image capture every 1/30th of a second. In some other situations, however, it would be desirable to be able to trigger an image capture at a specific point in time. For example, in a traffic control situation the user may want to trigger an image acquisition immediately after a car passes a sensor on a highway.

Production robots in the automotive industry often combine both camera types: small and light industrial cameras inside the robots, and network cameras for process control.

Converging the Cameras

Despite the different technologies and objectives, many applications are compatible with both types of cameras. There are now even solutions that operate IP cameras and GigE industrial cameras in one single Ethernet-based system using the same software.

The setup is already daily practice in the paper industry. Similar concepts are also in place for steel and foil production. Equipment used for these tasks typically involves numerous sequential process steps spread out over a physical space, including multiple sub-systems that need to pass products like paper webs to one another. IP cameras monitor the individual process steps and the transfer of the product to the next machine. The network devices ensure optimal interplay between all equipment systems, identify threats and sources of disruption, initiate a production stop where necessary, and generally help to optimize the machine configurations. If, for example, problems tend to arise in a given location, then the engineers will know to give that area a closer look. At the same time, classic cameras operate within the individual inline systems and test for quality, completeness, or dimensions.

Additionally, in the world of robotics, machine vision systems have long been used to "teach robots to see." After all, robot arms can only perform their high-precision gripping and positioning maneuvers once cameras and image processing tell them precisely where to move. Small, light industrial cameras, like the Basler ace, are typically used in robots. The devices are ideal for "pick and place" applications: gripping, mounting, and positioning tasks during computer chip assembly. Industrial cameras are also needed for measurement and quality controls of the various product characteristics between and during all production steps.

Safety during the production process is a prime concern for robotics applications. Previously, barriers were built to prevent workers from entering into the danger zones containing the rotating robots. The structures were expensive, cumbersome, and inflexible. IP cameras have changed the situation fundamentally. The network technologies can now be placed around the robots to create a "virtual cage" based on markings on the floor. The camera monitors those marked zones and is authorized to stop the machine if material, or an employee, enters into the robot's working area.

In daily use, the boundaries between the two camera technologies are largely becoming blurred. IP cameras, which classically have served in the monitoring field, are more and more frequently being used in industrial contexts to support process monitoring and production workflows. Camera manufacturers are also offering customers a range of cameras and accessories to ensure an optimal interplay between all components.

This article was written by Eva Tischendorf, Senior Communications Specialist at Basler AG (Ahrensburg, Germany). For more information, visit ***http://info.hotims.com/49746-151.***


INTRODUCING
LINEA™
Single Line Scan Cameras

Defining the Smart Camera

Smart cameras have been used in industrial applications for roughly two and a half decades, but advances in processor technologies have made the devices much more accessible and popular within the past 7 years, especially in areas such as machine vision and surveillance. However, when the term smart camera is mentioned, a wide variety of ideas still come to mind among individuals because there is no widespread agreement upon the definition of what a smart camera technically is. It is generally agreed upon that the basics of a smart camera include not only the image sensor, but also some type of processing chip: a CPU, DSP, FPGA, or other type of processing device (see Figure 1).

Today, however, even an off-the-shelf, point & shoot digital camera has some type of built-in image processing to remove the red eye effect, conduct facial recognition, apply a filter, or perform another type of image processing. So, if the inclusion of a processor along with an image sensor is not the defining attribute of a smart camera, what makes a smart camera "smart?" The key lies in the output.

Unlike most cameras, the primary output of a smart camera is not an image, but a decision or information. Since the image processing or machine vision algorithm is done directly on the smart camera, the image does not need to be passed onto a PC or another device. Instead, the result of the processing can be passed directly to an operator or another device in the system. For example, a smart camera may be selected for use in an in-line inspection system for a manufacturing line. The output of the smart camera could be a pass/fail report over a network to a database, a digital signal triggering a sorting system, or a serial command to a programmable logic controller (PLC).

A smart camera is a decision maker. Still, if you conduct an internet search for a smart camera, you will receive a large variety of results with very different features and appearance options. Let's review some essential properties of smart cameras and how they have progressed:

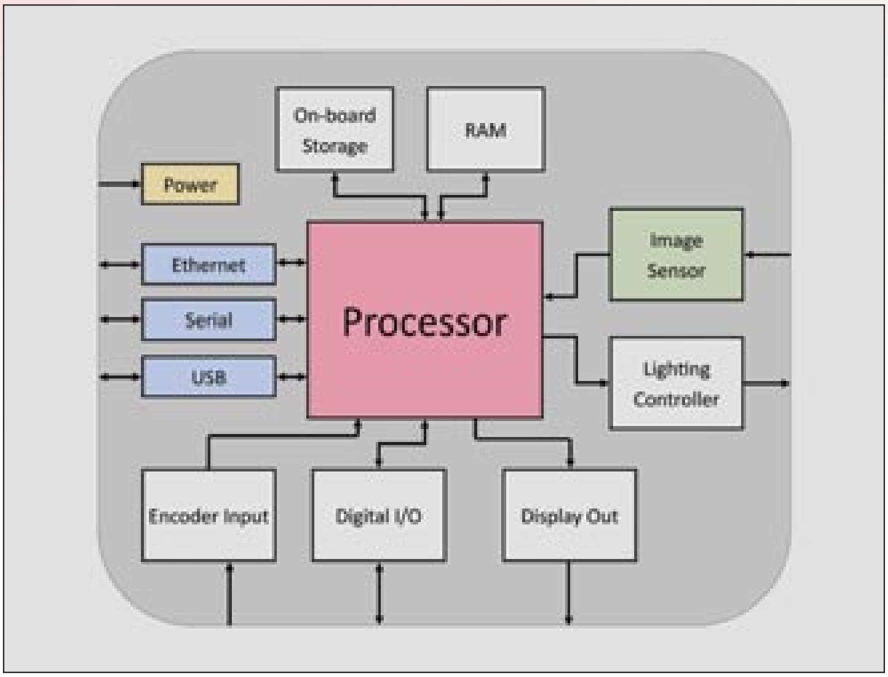

Figure 1. A smart camera typically includes an image sensor, processor, and some type of I/O. Other features can be added, such as direct drive lighting control, industrial I/O, and a display port.

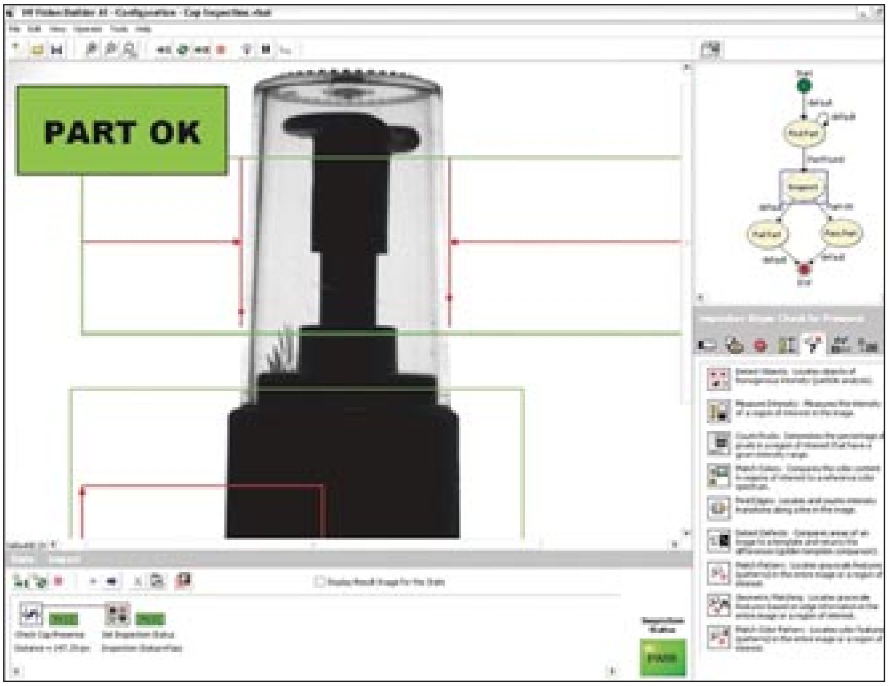

Figure 2. Most smart cameras come with relatively intuitive programming software, reducing the need for an advanced knowledge of programming skills. The program should not only be easy-to-use, but should also be flexible enough to scale to different hardware targets without a complete rewrite.


OVER 30 DIFFERENT CCD & CMOS SENSORS
OVER 100 DIFFERENT GIGE CAMERA MODELS
THOUSANDS OF SATISFIED CUSTOMERS
SEVEN YEARS OF GIGE LEADERSHIP
WE DIDN'T INVENT GigE.
WE PERFECTED IT.
AT BASLER WE KNOW WHAT'S PRECIOUS TO OUR CUSTOMERS. From the time we first championed the development of an industry-wide GigE standard, Basler has driven the GigE innovations that drive business for machine vision customers. We've delivered consistency. Reliability. And high performance—without the high price tag. Basler's rigorous approach to quality assurance has earned us unparalleled customer trust. Every camera we ship is individually tested before it leaves our facilities. That's why we can confidently offer the industry's longest and most comprehensive warranty on GigE cameras. And our commitment to continuous improvement means that every day of the year, every camera in our vast GigE portfolio represents best-in-class value.
There are a quarter of a million Basler GigE cameras in service today. Learn how we guarantee every one is a gem at www.baslerweb.com.
ace
GiGE®
VISION
BASLER
the power of sight
Free Info at http://info.hotims.com/49746-758

Figure 3. Smart cameras like the NI 1772 camera from National Instruments have high IP ratings for protection against environmental exposures like dust and water. Higher IP ratings are beneficial for applications in harsh environments, including outdoor monitoring and industrial vision inspection.

Processor Performance

As previously mentioned, the growing popularity of smart cameras can mainly be attributed to the increase in processor performance over the past decade. A 1 MHz smart camera 15 years ago would have been four times the size and cost of a >1 GHz smart camera of today. Many may be surprised when they realize the processing performance on some smart cameras rival what can be done on PC-based systems. An in-line inspection application, for example, that requires barcode reading, multiple geometric pattern matching, color analysis, line detection, and particle analysis can be done with a yield of over 25 parts per second. Additionally, this type of application can include triggering, lighting control, communication with other devices, and display all within the same compact package. Smart cameras come with a range of available processors, including DSPs, PowerPC-class, and Atom-class. There are also options with a mixed offering, such as a CPU with a DSP coprocessor for certain algorithms.

Size

One benefit to using a smart camera is that multiple components of a vision system are integrated into a single package, resulting in a small size and the potential to save a lot of space. The top-of-the-line, high-performance smart cameras keep getting faster without having to affect size, but the devices are also heading further into the low-end market. Reducing the functionality from an all-purpose smart camera to one that is designed for specific algorithms, such as barcode verification/reading and optical character recognition (OCR), reduces the number of components and complexity. With sizes smaller than 55 x 50 mm and weights of less than 60 grams, these types of smart cameras have been significantly growing in market availability.

Image Sensor

Of course, a smart camera is still a camera and must acquire images. Both CMOS and CCD sensors can be found in smart cameras with resolutions of 5 MP, available in both color and monochrome. Smart cameras are not just limited to area scan anymore. Line-scan smart cameras are also available with frequencies over 10 kHz. While smart cameras do not cover the full range of options as normal cameras, they feature some of the most popular sensors.

A key downfall with smart cameras, however, comes when an application requires multiple image sensors connected to the same processing unit. One way to solve the problem is to synchronize multiple smart cameras, but that can add significant cost and complexity. In these cases, it is best to explore alternatives, such as compact vision systems or PC-based systems.

Software

Most smart cameras today come with relatively simple-to-use software. Advanced knowledge of programming is not required to use the technology, but it is important to keep flexibility and scalability in mind. The investment to learn a new piece of software and write an application should be a somewhat long-term one. That is, the software should scale with application requirements and future projects.

Sensor and processor technologies are advancing rapidly, so the best-case scenario takes place when the smart camera model and software are well integrated, but not exclusive to each other. As a result, if you change smart camera models to a new version or need to move to a different hardware platform, such as a PC or operating system, a complete rewrite of the application or IP should not be required. The operating system running on the camera itself can also be a critical factor as Windows-based smart cameras connected to a plant network may fall under IT restrictions (see Figure 2).

Ruggedness

The level of ruggedness required is dependent upon the environment in which the smart camera is to be deployed. It is important to note that many applications take place in fairly harsh environments. In food inspection applications, for example, the cleaning process washes all parts on the line, including the camera. Smart cameras are available with an IP rating of at least 67, which offers total protection against dust and submersion in water up to 1 m deep (see Figure 3).

Integration

Those who have completed a vision application know that vision is often part of a much larger system. Since the primary output of a smart camera is a decision, result, or some other information beyond an image, most smart cameras have built-in I/O to communicate or control other devices in the system. With industrial automation, the smart camera may need to control actuators to sort products; communicate inspection results to a robot controller, PLC, or

Figure 4. Since the primary output of a smart camera is a decision or some type of signal other than an image, many smart cameras include integrated I/O and communication ports: lighting, digital I/O, serial, Ethernet, and USB buses, as well as display ports for user interfaces.

programmable automation controller (PAC); save images and data to network servers; or communicate inspection parameters and results to a local or remote user interface. With USB and display ports, smart cameras can completely replace PC vision systems where an operator interface is required; the parts are integrated in a single device.

Often, for scientific imaging applications, the vision must integrate with motion stages, data acquisition systems, microscopes, specialized optics, and advanced triggering. As a result, many smart cameras today include I/O such as industrial digital inputs and outputs, encoder inputs for image synchronization, and communication ports.

Models are also available with built-in lighting, however, an integrated light cannot be independently positioned, and the feature is useless if a backlight is used. Built-in light controllers, an available alternative, can modify illumination directly from the smart camera. To effectively communicate to other devices, more and more industrial communication protocols, including DeviceNet, EthernetIP, and serial, are also being supported natively in smart cameras. It is therefore critical to understand how the smart camera will best integrate into an overall system (see Figure 4).

Decision Making

With the capabilities of today's smart cameras, the adoption of these devices continues to grow, and newer technologies are being integrated that could help accelerate the growth. The devices, for example, are moving into the 3D vision space by providing solutions with multiple image sensors integrated into stereoscope or laser triangulation packages. These days, smart cameras can come in all shapes, sizes, and performance levels, but there is still one attribute that still defines them as smart cameras: the ability to perform image processing and make decisions directly on the camera. It is the decision making that makes a camera smart, and with the potential cost savings, ease of integration, and increasing performance, smart cameras are a cutting-edge option for many vision applications.

This article was written by Carlton Heard, Product Engineer – Vision Hardware and Software, at National Instruments (Austin, TX). For more information, visit ***http://info.hotims.com/49746-152****.*

Intro Cov ToC

Indoor/Outdoor Cameras Improve School District's Security

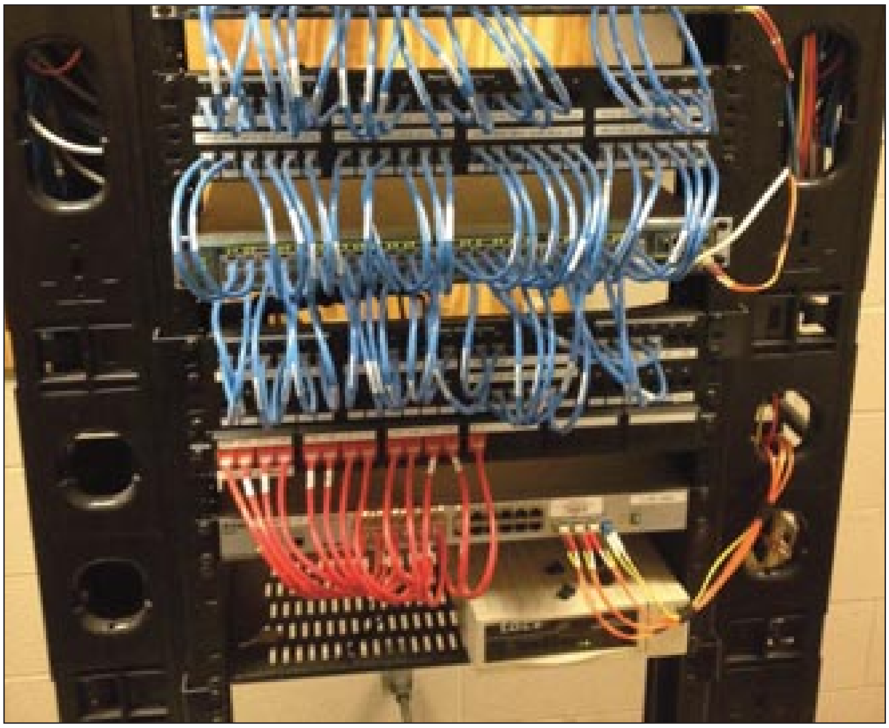

Liberty-Eylau Independent School District utilizes D-Link switches (above) in conjunction with an array of indoor/outdoor cameras and SAN arrays for its surveillance technology.

Located in Texarkana, Texas, Liberty-Eylau Independent School District (LEISD) has been serving communities since 1886. Today, the district has more than 2,700 K-12 students across six schools, including a high school, a middle-intermediate school, an elementary school, a primary school, a pre-K center, and a School of Success.

With safety being a core part of LEISD's vision statement, it is no surprise that district leaders strive to do all they can to ensure the safest school environments possible. In early 2013, however, the district realized that it needed to make some serious improvements to its security infrastructure. According to Matt Fry, LEISD Media Coordinator, 40 analog cameras were being used district-wide, and some campuses were not covered at all.

"The cameras offered some basic coverage outside, but not a lot inside," he said. "Worse yet, they had very poor picture quality and big lag time lapses between frames, so we couldn't really use the video for much. We knew it was time to update to a more modern, digital solution with a lot higher resolution."

Fry took these challenges to the TCEA (Texas Computer Education Association) conference in February 2013, where he met security networking experts from D-Link, a developer and manufacturer of network solutions and IP surveillance, who proposed a follow-up meeting to discuss the district's specific needs.

"We also wanted a system that was scalable so we could take it district-wide, plus provide the ability to do remote monitoring," Fry said.

The Solution

Shortly after the conference, the team brought in a local technology integrator, CMC Network Solutions, and met on site to examine the district's existing network infrastructure and physical layout, while discussing its specific IP surveillance requirements.

"Among other things, the district needed the ability to archive video data for up to 30 days, so they could review incidents after the fact, if necessary," said Scott Broekemeier, Principal at the Plano, TX-based CMC Network Solutions. “After the site survey, we created a custom design that provided the performance, resolution, and coverage they desired.”

Having reviewed bids from multiple providers, LEISD ultimately chose the technology from D-Link: IP cameras, switches, video storage, and access control. The district purchased a complete 240-camera security system that included a mix of D-Link IP indoor and outdoor cameras (most offering Full HD 2 megapixel resolution), as well as D-Link switches, SAN Storage, Video Insight video management software, dedicated VMS servers, and access control products for tighter security at doors and entry points. D-Link Indoor Day and Night Dome IP Cameras also offer integrated mechanical IR filters and infrared LEDs to allow the viewing and recording of video, even in complete darkness.

CMC Network Solutions hosts all of the traffic on a separate VPN network, which does not conflict with the district’s existing data network traffic. Fortunately, CMC was able to use some of LEISD’s existing fiber backbone, which helped keep costs down.

IP Cameras in Action

The solution was installed over the summer, giving the district the surveillance it needed for when the new school year began. The high-definition IP cameras provide higher-quality video images and simplified remote monitoring — even from mobile devices. Additionally, the new solution is making life easier for the local police department.

The Liberty-Eylau Independent School District currently uses over 100 DCS-6113 cameras from D-Link, shown here.

“Officers really like the mobile capability, where they can access video from their phones or tablets and see what’s happening on campus,” said Fry. “One time an officer called because he noticed lights on in the gym after hours. Even though I was out of town, I was able to pull up video images on my smartphone and see for myself, so I could address the situation.”

Thanks to the solution’s centralized management, each campus can keep a watchful eye on its own facility, while administrators at the district office can view video from all six campuses at the same time. The district is already planning to add a few more to provide extra visibility and more zoom on a few additional areas like entry gates.

“This was a huge purchase for our school district; and since we’re using taxpayer dollars, we take that very seriously,” said Fry.

For Free Info Visit ***http://info.hotims.com/49746-153***.

NEW PRODUCTS

Line-Scan Camera

The 3DPIXA 3D line scan color camera from Chromasens (Burlington, MA) employs factory-calibrated stereo engineering. To output both color images and 3D altitude data in real time, the Chromasens 3DPIXA simultaneously captures two images of the same object. Height and shape are calculated using special algorithms running on the GPU.

The cameras are available in two different principle designs: a compact system with a resolution of 15μm / 30 μm and a line frequency of up to 22 kHz, and the 3DPIXA dual system with a resolution of e.g. 10μm and a line frequency of up to 50 kHz. The latter variant inspects at speeds of up to 500mm/s, at 10 μm optical resolution.

For Free Info Visit http://info.hotims.com/49746-140

Frame Grabbers

The PIXCI® EB1mini frame grabber from EPIX (Buffalo Grove, IL) captures from any base Camera Link device. The frame grabber includes trigger input, strobe output, shutter control, bit-packing capability, 64 bit memory addressing, and video rate sequence capture. The XCAP-Lite imaging program, provided with the PIXCI® EB1mini, provides control of image capture, as well as all board functions, through the Capture & Adjust Dialog.

For Free Info Visit http://info.hotims.com/49746-141

X-Ray CCD Cameras

Andor Technology (Belfast, UK) has announced the iKon-M SY and Newton SY series of CCD cameras. The ‘standalone’ detectors offer -100°C deep cooling, optimized for the soft X-ray region. The 200-micron-thick Beryllium window blocks unwanted lower energies and visible wavelengths, with minimal beam hardening. The detectors are integrated and supported in a range of third-party software using Andor’s SDK, including MATLab, LABView, and EPICs.

For Free Info Visit http://info.hotims.com/49746-142

Camera Link Selector

The CLM-602 Camera Link Multiplexer from Vivid Engineering (Shrewsbury, MA) interfaces two Camera Link cameras of any configuration (base, medium, full, 80-bit) to one frame grabber. The CLM-602 incorporates high-speed (85 MHz) interfaces. Multiple camera selection methods are provided, including rear-panel switch settings, Camera Link interface signals (serial or camera control), and an external RS-232 port. The selector is housed in a sturdy, compact aluminum enclosure.

For Free Info Visit http://info.hotims.com/49746-144

New on the MARKET

Product of the Month

The USB-2404-UI from Measurement Computing, Norton, MA, offers simultaneous sampling at up to 100 S/s, per channel, on four 24-bit channels of universal analog input. The device is designed for multipurpose testing, and can measure voltage, current, thermocouples, RTDs, resistance, and bridge-based sensors. The device features a built-in thermistor for cold-junction compensation, and a six-position spring terminal that allows different measurement types to be performed on each channel. It includes channel-to-channel isolation to protect the entire system from harmful voltage spikes and eliminate measurement errors caused by ground loops. It also includes 250 Vrms channel-to-channel and channel-to-ground isolation, and does not require an external power supply. TracerDAQ® software acquires and displays data, and generates analog signals.

For Free Info Visit http://info.hotims.com/49746-120

Product Focus: Test Instruments

Digital Oscilloscope

Rohde & Schwarz, Munich, Germany, has introduced the R&S RTE digital oscilloscope with bandwidths from 200 MHz to 1 GHz, and an acquisition rate of more than one million waveforms per second. The scope features a digital trigger system with virtually no trigger jitter, a sampling rate of 5 Gsamples per second, maximum memory depth of 50 Msamples per channel, and a 10.4" XGA touchscreen. **For Free Info Visit http://info.hotims.com/49746-100**

Electrical Safety Test Systems

Slaughter Co., Lake Forest, IL, offers electrical safety test systems that perform AC Hipot, DC Hipot, Insulation Resistance, and Ground Bond tests. The systems include a 2900 Series Hipot tester and 2600 Series Ground Bond tester. Features include 10 test memory locations for setup, edit, and recall of test settings for different types of DUTs; a milliohm offset feature that allows users to factor out additional lead and fixture resistance; and standard PLC I/O for remote control applications. **For Free Info Visit http://info.hotims.com/49746-101**

High-Voltage Device Testing

Keithley Instruments, Cleveland, OH, has introduced the Model 2290-5 5kV and Model 2290-10 10kV power supplies for high-voltage device and materials testing. Both power supplies have a built-in interlock circuit to disable the output voltage if a high-voltage test fixture's access door is not closed. Front panels provide voltage and current output displays, as well as a third display that shows the user's choice of four settings: output voltage, voltage limit, current limit, or current trip. **For Free Info Visit http://info.hotims.com/49746-102**

Capacitance Manometer

MKS Instruments, Andover, MA, has introduced the a-Baratron® absolute capacitance manometer that is internally heated to 45, 80, or 100 °C. It offers full-scale measurement ranges from 0.1 to 1,000 Torr. The manometer can be configured for both new and existing processing systems, operates on ±15VDC input voltage, and has a standard 0–10VDC analog output signal. **For Free Info Visit http://info.hotims.com/49746-103**

Optical Micrometer

The LS-9000 series multi-axis optical micrometer from Keyence Corp. of America, Itasca, IL, offers a standard sampling rate of 16,000 Hz and repeatability of 1.2 millionths of an inch. Other features are an LED system, HS-CMOS, and no moving parts in its design. Incorporating a custom-designed vibration isolation system within the head, the instrument is able to resist damage from vibration and impact. **For Free Info Visit http://info.hotims.com/49746-104**

Arbitrary Waveform Generator

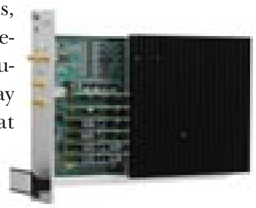

Applicos BV, Heerde, The Netherlands, has announced the AWG18 arbitrary waveform generator that features 18-bit resolution at a 300-Msps data rate. Users may select interpolated oversampling at 600Msps or 1.2 Gsps. The generator has two signal paths: one that starts at DC for time-domain and general-purpose measurements, and one that runs from 10 to 100 MHz for dynamic signal generation in the frequency range. **For Free Info Visit http://info.hotims.com/49746-105**

Varistors

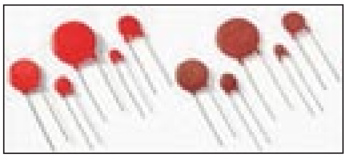

The AUMOV™ Series of low-voltage, high-surge-current, radial-leaded varistors for automotive applications is available from Littelfuse, Chicago, IL. Maximum peak surge current is rated up to 5KA (8/20 s pulse). The varistors offer a voltage range of 16 to 50 VDC and are available in disc sizes of 5, 7, 10, 14, and 20 mm. **For Free Info Visit http://info.hotims.com/49746-107**

Embedded Computer Module

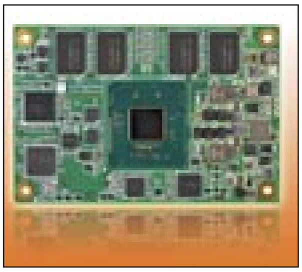

congatec, San Diego, CA, offers the conga-MA3 COM Express Mini Type 10 module based on the Intel® Atom™ E3800 series processors. The module comes in four different Intel Atom processor-based versions ranging from the single-core Intel Atom E3815 with 1.46 GHz and power consumption of 5 Watts, up to the quad-core Intel Atom E3845 with 1.91 GHz and 10 Watts maximum power consumption. **For Free Info Visit http://info.hotims.com/49746-108**

Signal Editing Software

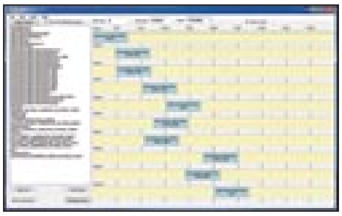

X-COM Systems, LLC, a subsidiary of Bird Technologies, Reston, VA, has introduced RF Editor Version 3.0 graphical signal editing software that provides editing capability for waveforms and waveform segments that have been captured over the air, offloaded from a signal analyzer, or created in programs such as MATLAB. It allows users to manipulate I&Q data files for RF signals of any length. **For Free Info Visit http://info.hotims.com/49746-109**

Mezzanine Connectors

TE Connectivity, Harrisburg, PA, has introduced the Mezalok mezzanine connectors that feature a stack height of 15 mm and a 320 position size, which fills a height gap and adds additional pin density. The connectors are designed for mezzanine cards in rugged applications and are standardized as the interconnect for XMC 2.0 (VITA 61). **For Free Info Visit http://info.hotims.com/49746-110**

Upcoming...

TECH BRIEFS MEDIA GROUP

an SAE International Company

Webinars

Tesla Motors Utilizes Altair HyperStudy to Explore and Optimize Pedestrian Impact Performance

Altair

Tuesday, June 10, 2014, 2:00 pm ET

The design group at Tesla Motors has faced the challenge of meeting legal pedestrian impact requirements and the New Car Assessment Program (NCAP) without affecting the vehicle styling.

This Webinar will introduce the capabilities of Altair's HyperStudy software for use in optimization and design exploration leading into the analysis of Tesla use cases.

Presenters:

Fatma Koçer
Director of Business Development, Math Solutions
Altair

Singai Krishnamoorthi
Technical Specialist and Staff Engineer
Tesla Motors

This 60-minute Webinar includes:

- Live Q&A session
- Application Demo
- Access to archived event on demand

Please visit www.techbriefs.com/webinar212

Making Traceability a Competitive Advantage, Instead of Burden

AEGIS SOFTWARE

Thursday, June 12, 2014, 2:00 pm ET

Traceability has variable and narrow definitions depending on the industry, product, and application.

This Webinar will discuss how a holistic approach to traceability yields invaluable process and product intelligence of such scope and depth that real manufacturing improvement can be achieved by the managers and engineers responsible for the factories.

Presenter:

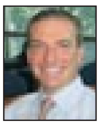

Jason Spera
CEO and Co-Founder
Aegis Software

This 30-minute Webinar includes:

- Live Q&A session
- Application Demo
- Access to archived event on demand

Please visit www.techbriefs.com/webinar213

Aerogels with Improved Properties for Aeronautic and Space Applications

Thursday, June 19, 2014, 2:00 pm ET

Current aerogel products on the market today are silica–based and break down on handling, shedding small dust particles. In contrast, polyimide aerogels are flexible, mechanically robust, and do not shed dust.

You will hear from the manager of NASA Glenn's Technology Transfer and Commercialization Office, who will discuss the innovative work being done at the center.

Presenters:

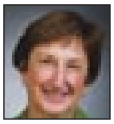

Dr. Mary Ann Meador
Glenn Research Center

Amy Hiltabidel
Technology Transfer Specialist
Glenn Research Center

This 60-minute Webinar includes:
- Live Q&A session
- Application Demo
- Access to archived event on demand

Please visit www.techbriefs.com/webinar214

Differentiated Technologies of Fluid Hoses & Air Springs for Lower Total Cost of Ownership

Tuesday, June 24, 2014, 2:00 pm ET

Today's system designers and operators not only expect quality products, but also expect longer-lasting components that offer long-term value through extended mean time between failures.

In this Webinar, learn how Continental's ContiTech Division offers industrial hoses and air springs that exceed lifecycle expectations, thus lowering the total cost of ownership of automated machinery, capital equipment, and off-highway vehicles.

Presenters:

Peter Tiedemann
ContiTech North America, Inc.
Product Sales Manager – Industrial Hoses, NAFTA Region

Douglas A. Duesing, CFPS
ContiTech North America, Inc.
Product Manager – Industrial Air Springs, NAFTA Region

This 60-minute Webinar includes:
- Live Q&A session
- Application Demo
- Access to archived event on demand

Please visit www.techbriefs.com/webinar215

On Demand! Testing Astronaut-Controlled Surface Robots from the International Space Station

The National Aeronautics and Space Administration (NASA) and the European Space Agency (ESA) are currently developing robots that can be remotely operated on planetary surfaces by astronauts in orbiting spacecraft.

In this Webinar, we summarize the tests that have been done to date, describe the tests that are being prepared for flight, and discuss future directions for our work.

Presenters:

Terry Fong
Ph.D. Director
Intelligent Robotics Group
NASA Ames Research Center

Philippe Schoonejans
Head of Robotics
European Space Agency

Klaus Ehrenberger
Commercial Solutions
Business Development Manager
Hewlett-Packard EMEA
Munich, Germany

This 60-minute Webinar includes:
• Live Q&A session • Application Demo • Access to archived event on demand

Please visit www.techbriefs.com/webinar204

NASA's Technology Transfer Program

NASA's R&D efforts produce a robust supply of promising technologies with applications in many industries. A key mechanism in identifying commercial applications for this technology is NASA's national network of laboratories and business support entities. The network includes ten NASA field centers, and a full tie-in with the Federal Laboratory Consortium (FLC) for Technology Transfer. To explore technology transfer, development, and collaboration opportunities with NASA, visit **technology.nasa.gov**.

NASA's Technology Sources

If you need further information about new technologies presented in *NASA Tech Briefs*, request the Technical Support Package (TSP) indicated at the end of the brief. If a TSP is not available, the NASA field center that sponsored the research can provide you with additional information and, if applicable, refer you to the innovator(s). These centers are the source of all NASA-developed technology.

Ames Research Center
Selected technological strengths: Information Technology; Biotechnology; Nanotechnology; Aerospace Operations Systems; Rotorcraft; Thermal Protection Systems.
David Morse
(650) 604-4724
david.r.morse@nasa.gov

Armstrong Flight Research Center
Selected technological strengths: Aerodynamics; Aeronautics Flight Testing; Aeropropulsion; Flight Systems; Thermal Testing; Integrated Systems Test and Validation.
Laura Fobel
(661) 276-3967
laura.j.fobel@nasa.gov

Glenn Research Center
Selected technological strengths: Aeropropulsion; Communications; Energy Technology; High-Temperature Materials Research.
Kimberly A. Dalgleish-Miller
(216) 433-8047
kimberly.a.dalgleish@nasa.gov

Goddard Space Flight Center
Selected technological strengths: Earth and Planetary Science Missions; LIDAR; Cryogenic Systems; Tracking; Telemetry; Remote Sensing; Command.
Nona Cheeks
(301) 286-5810
nona.k.cheeks@nasa.gov

Jet Propulsion Laboratory
Selected technological strengths: Near/Deep-Space Mission Engineering; Microspacecraft; Space Communications; Information Systems; Remote Sensing; Robotics.
Dan Broderick
(818) 354-1314
daniel.f.broderick@jpl.nasa.gov

Johnson Space Center
Selected technological strengths: Artificial Intelligence and Human Computer Interface; Life Sciences; Human Space Flight Operations; Avionics; Sensors; Communications.
John E. James
(281) 483-3809
john.e.james@nasa.gov

Kennedy Space Center
Selected technological strengths: Fluids and Fluid Systems; Materials Evaluation; Process Engineering; Command, Control, and Monitor Systems; Range Systems; Environmental Engineering and Management.
David R. Makufka
(321) 867-6227
david.r.makufka@nasa.gov

Langley Research Center
Selected technological strengths: Aerodynamics; Flight Systems; Materials; Structures; Sensors; Measurements; Information Sciences.
Kathy Dezern
(757) 864-5704
kathy.a.dezern@nasa.gov

Marshall Space Flight Center
Selected technological strengths: Materials; Manufacturing; Nondestructive Evaluation; Biotechnology; Space Propulsion; Controls and Dynamics; Structures; Microgravity Processing.
Terry L. Taylor
(256) 544-5916
terry.taylor@nasa.gov

Stennis Space Center
Selected technological strengths: Propulsion Systems; Test/Monitoring; Remote Sensing; Nonintrusive Instrumentation.
Ramona Travis
(228) 688-3832
ramona.e.travis@ssc.nasa.gov

NASA HEADQUARTERS

Daniel Lockney, Technology Transfer Program Executive
(202) 358-2037
daniel.p.lockney@nasa.gov

Small Business Innovation Research (SBIR) & Small Business Technology Transfer (STTR) Programs
Rich Leshner, Program Executive
(202) 358-4920
rleshner@nasa.gov

TECH BRIEFS
www.techbriefs.com

Published by .... **Tech Briefs Media Group, an SAE International Company**
Publisher .... **Joseph T. Pramberger**
Editorial Director .... **Linda L. Bell**
Editor, Photonics Tech Briefs .... **Bruce A. Bennett**
Technical/Managing Editor .... **Ted Selinsky**
Technical Writers .... **Shirl Phelps**
Nick Lukianoff
Managing Editor, Tech Briefs TV .... **Kendra Smith**
Associate Editor .... **Billy Hurley**
Production Manager .... **Adam Santiago**
Art Director .... **Lois Erlacher**
Designer .... **Bernadette Torres**
Marketing Director .... **Debora Rothwell**
Marketing Assistant .... **Kaitlyn Sommer**
Audience Development/Circulation Director .... **Marilyn Samuelsen**
Audience Development/Circulation Assistant .... **Martha Saunders**
Subscription Changes/Cancellations .... **nasa@omeda.com**

NASA tech briefs are provided by the National Aeronautics and Space Administration, Innovative Partnerships Program:
Administrator .... **Charles F. Bolden, Jr.**
Chief Technologist .... **David W. Miller**
Technology Transfer Program Executive .... **Daniel Lockney**

TECH BRIEFS MEDIA GROUP, AN SAE INTERNATIONAL COMPANY
261 Fifth Avenue, Suite 1901, New York, NY 10016
(212) 490-3999 FAX (212) 986-7864
Chief Executive Officer .... **Domenic A. Mucchetti**
Executive Vice-President .... **Luke Schnirring**
Technology Director .... **Oliver Rockwell**
Systems Administrator .... **Vlad Gladoun**
Web Developer .... **Karina Adames**
Digital Media Manager .... **Peter Bonavita**
Digital Media Assistant .... **Keith McKellar**
Digital Media Assistant .... **Ranard Miller**
Credit/Collection .... **Felecia Lahey**
Accounting/Human Resources Manager .... **Sylvia Bonilla**
Office Manager .... **Alfredo Vasquez**
Receptionist .... **Elizabeth Brache-Torres**

***NASA TECH BRIEFS* ADVERTISING ACCOUNT EXECUTIVES**
CT, MA, NH, ME, VT, RI, Eastern Canada .... **Ed Marecki**
Tatiana Marshall
at (401) 351-0274
NJ, PA, DE .... **John Murray**
at (973) 545-2132
NY .... **Stan Greenfield**
at (203) 938-2418
Southeast, TX .... **Ray Tompkins**
at (281) 313-1004
Western NY, OH, MI, IN .... **Ryan Beckman**
at (973) 409-4687
MN, ND, SD, WI, IL, KY, MO, KS, IA, NE, Central Canada .... **Bob Casey**
at (847) 223-5225
Northwest, N. Calif., Western Canada .... **Craig Pitcher**
at (408) 778-0300
CO, UT, MT, WY, ID, NM .... **Tim Powers**
at (973) 409-4762
S. Calif, AZ, NV .... **Tom Boris**
at (949) 715-7779
Integrated Media Consultants .... **Patrick Harvey**
at (973) 409-4686
Angelo Danza
at (973) 874-0271
Scott Williams
at (973) 545-2464
Rick Rosenberg
at (973) 545-2565
Reprints .... **Jill Kaletha**
at (866) 879-9144, x168

Advertisers Index

For free product literature, enter advertisers' reader service numbers at www.techbriefs.com/rs, or visit the Web site listed beneath their ad in this issue.

Advertisers listed in bold-face type have banner ads on the* NASA Tech Briefs *Web site — www.techbriefs.com

Supplement to *NASA Tech Briefs*: 2 and 3.

NASA Tech Briefs, ISSN 0145-319X, USPS 750-070, copyright ©2014 in U.S. is published monthly by Tech Briefs Media Group, an SAE International Company, 261 Fifth Avenue, Suite 1901, New York, NY 10016. The copyright information does not include the (U.S. rights to) individual tech briefs that are supplied by NASA. Editorial, sales, production, and circulation offices at 261 Fifth Avenue, Suite 1901, New York, NY 10016. Subscription for non-qualified subscribers in the U.S. and Puerto Rico, $75.00 for 1 year; $135 for 2 years. Single copies $6.25. Foreign subscriptions one-year U.S. Funds $195.00. Remit by check, draft, postal, express orders or VISA, MasterCard, and American Express. Other remittances at sender's risk. Address all communications for subscriptions or circulation to *NASA Tech Briefs,* 261 Fifth Avenue, Suite 1901, New York, NY 10016. Periodicals postage paid at New York, NY and additional mailing offices.

POSTMASTER: Send address changes and cancellations to *NASA Tech Briefs,* P.O. Box 3525, Northbrook, Il 60065.

Home Air Purifiers Eradicate Harmful Pathogens

An air scrubber used in space station plant growth helps you breathe easier at home.

In the 1990s, NASA scientists were thinking of what astronauts would need to survive long-term missions to the Moon and other planets. One important requirement was a dependable source of food, which could be accomplished by astronauts growing their own produce in space-age greenhouses. But cultivating crops in a sealed-off environment results in the buildup of an undesirable gas called ethylene. Plants release the odorless, colorless fume into the air, which has the unfortunate effect of accelerating decay, hastening the wilting of flowers and the ripening of fruits and vegetables.

Mizuna lettuce growing aboard the International Space Station. Ethylene scrubbers are used to remove the gas from the air, keeping vegetables fresh in space.

To address the problem, Marshall Space Flight Center's Space Product Development Program funded the Wisconsin Center for Space Automation and Robotics at the University of Wisconsin to develop plant growth chambers that included an ethylene reduction device. In this "scrubber," air is drawn into tubes coated with thin layers of titanium dioxide (TiO2). When an ultraviolet (UV) light source located in the tubes strikes the TiO2, the ethylene gets converted to water and carbon dioxide, both of which are beneficial for plants.

The ethylene scrubber was first used in 1995 aboard a Space Shuttle Columbia mission, successfully preserving a crop of potato seedlings. Updated versions of the device were subsequently flown on several missions to the International Space Station.

While NASA's main objective was to get rid of ethylene, the scrubbers were capable of purging all kinds of unwanted organic particles from the air. Recognizing its powerful air purification abilities, KES Science & Technology (Kennesaw, GA) licensed the technology from the University of Wisconsin. The company then partnered with Akida Holdings (Jacksonville, FL), which marketed the technology as Airocide.

In 2013, Airocide finally found its way into people's homes when Akida Holdings adapted the technology for home use by developing an eye-catching portable unit with enough power to purge an entire room of pathogens. The Airocide unit is the only air purifier that completely destroys airborne bacteria, mold, fungi, mycotoxins, viruses, volatile organic compounds, and odors. Grocery stores and produce distribution facilities now use it, in addition to a host of wineries, distilleries, and floral businesses. The device has also found its way into refrigerators used for both homes and for distributing food aid to remote towns. In hospitals and clinics, Airocide's germ-killing properties are used to purge the air of harmful bacteria.

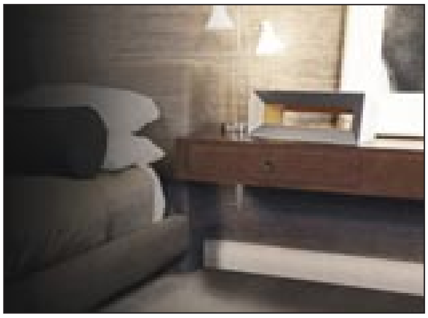

The Airocide home unit can be placed on a flat surface, hung on a wall, or mounted to a floor stand.

The home Airocide unit has a sleek, glossy, rectangular body and can either be mounted on a floor stand or hung on a wall. Airocide works differently from High-Efficiency Particulate Air (HEPA) filters, which are designed to capture particles that are 0.3 microns across and larger. Airocide is simple to operate — just plug it into an outlet, turn it on, and forget about it. The only upkeep required is replacing the reaction chamber, which houses the UV light source, every 12-14 months. There are high- and low-intensity modes, as well as automatic, which alternates from high in the day to low at night.

According to users, the product helps relieve symptoms associated with asthma, allergies, and sinus problems.

*Visit **http://spinoff.nasa.gov/Spinoff2013/cg_4.html** for the full story.*

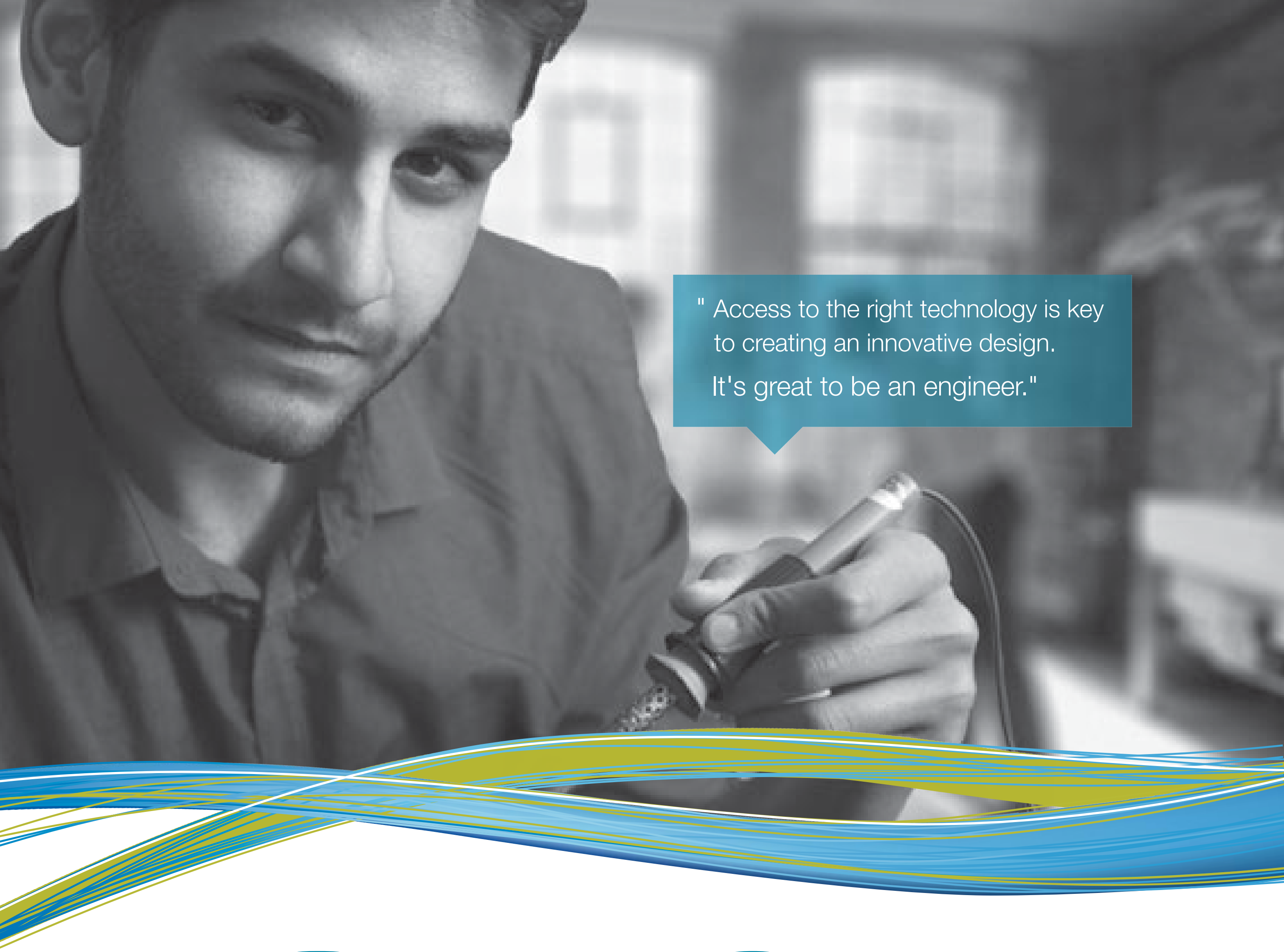
" Access to the right technology is key to creating an innovative design.
It's great to be an engineer."

Agilent's Electronic Measurement Group is becoming **Keysight Technologies**.

Agilent & Our Distributor Network

Right Instrument. Right Expertise.
Delivered Right Now.

Agilent Basic Instruments

May–July 2014

Newark element14

TESTEQUITY

microlease
The experts in Test Equipment management

Agilent Technologies
Authorized Distributor

Check it out.

BUY FROM DISTRIBUTORS

NEW higher frequency waveform generator from Agilent.

Our Featured Distribution Partners make it easy to buy.

PAGE 3

Upgrade to your Ultimate Scope

Get Up to 16 scope applications for the price of 1!

See promos on page 8 or scan QR Code for complete promo listing.

Anticipate __Accelerate __Achieve

Agilent Technologies

Eliminate the uncertainty and generate the signals you expect to see

When your tests demand a precise and predictably shaped signal, can you be sure your signal generator is outputting the signal you expect?

The drawbacks of DDS

Direct digital synthesis (DDS) is a simple and inexpensive method that produces approximations that are acceptably close to the ideal for many applications, which is why lower-cost waveform generators typically use this technology.

However, these signals are indeed approximations, which can create problems with harmonic distortion, jitter, aliasing, and even skipped points in the waveform.

Because DDS generators have a fixed sample clock, if they output one unique point for each sample clock, they would be able to output only one frequency. When a lower frequency is needed, the generator needs to use many clock cycles to output a single point and will repeat points. When a higher frequency is needed and the generator can't output all of the points in waveform memory, it will skip over some points. The higher the frequency, the more points are skipped—and the less the output resembles the signal you expect to see.

Moreover, DDS generators use internal algorithms to determine which points are skipped. These algorithms put a priority the phase of a signal, which results in signals that don't necessarily skip the same samples in every cycle.

True signals with True*form* technology

True*form* waveform generators use proprietary technology that allows waveforms to be expressed with the same shape, regardless of frequency. Designers working with complex waveforms can use True*form* generators to generate signals with complex modulation and abnormalities. Digital waveforms with transients and pulses can be reproduced with the same characteristics every time.

Figure 1 shows an example of the dramatic differences between DDS and True*form* waveforms. Note the three small peaks in the True*form* signal and compare the DDS output; these signal characteristics are distorted or missing entirely.

Dramatic reduction in jitter

Another key benefit of the True*form* architecture is extremely low jitter. Cycle-to-cycle jitter for the new Agilent 33600A Series, for example, is specified at less than 1 ps for all waveforms, including arbitrary, sine, and square waves. That's about 200 times less jitter than DDS-based generators (**Figure 2**).

Missing the point

Figure 3 illustrates the problem of missing points in DDS outputs. At 1 kHz, both generators were able to create an accurate waveform with all seven aberrations, but when the frequency was dialed up to 2 MHz, three of the seven signal features disappeared from the DDS output. At even higher frequencies, the aberrations can be become intermittent or distorted—or all of them can disappear completely.

To learn how to overcome your function generator challenges with True*form* technology, view videos and download free measurement briefs, visit **www.agilent.com/find/trueformTC**

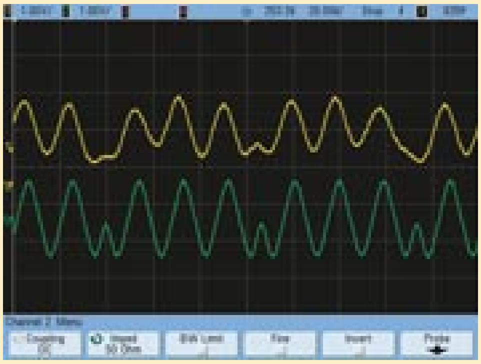

Figure 1:
Signals at the same frequency created by a DDS generator (upper trace) and a Trueform generator (lower trace)

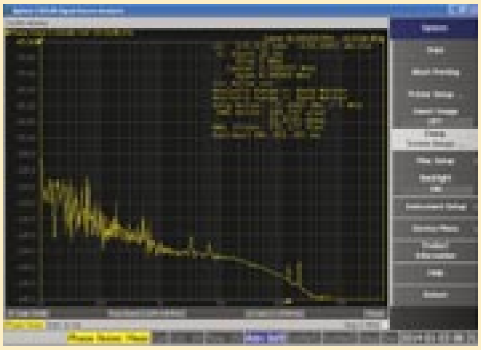

Figure 2:
This 40 MHz sine wave from the 33600A shows less than 800 femto-seconds of jitter.

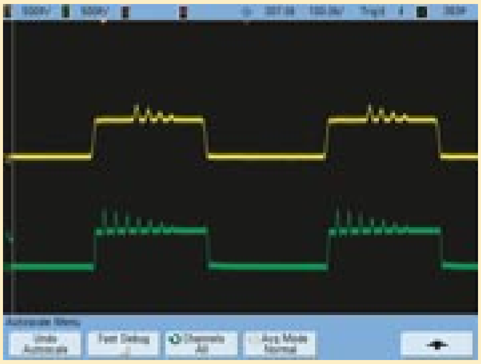

Figure 3:
A DDS generator (upper trace) was unable to output all seven aberrations in this 2 MHz arbitrary waveform.

WAVEFORM GENERATORS
FREQUENCY COUNTERS

High performance, multifunction counters cover the RF and microwave spectrum from 50 MHz to 46 GHz

53200 Series RF and universal frequency counters

- Frequency, frequency ratio, time interval, rise/fall time, phase, and much more
- Histograms, trending, data logging, and built-in math and statistical functions
- 53230A offers: 20 ps single-shot, burst microwave, and continuous gap-free measurements with time stamped edges
- Optional 6 or 15 GHz RF channel
- USB, GPIB and LAN (LXI) connectivity

Model	Key specifications	Price from (US)
53210A	350 MHz RF frequency counter, 10 digits/s	$2,165
53220A	350 MHz universal frequency counter/timer, 12 digits/s, 100 ps	$2,507
53230A	350 MHz universal frequency counter/timer, 12 digits/s, 20 ps	$3,918

Speed, accuracy, and measurement versatility

E4980AL precision LCR meter

- 20 Hz to 300 kHz / 500 kHz / 1 MHz
- Exceptionally low noise at both low and high impedance to improve test quality; 0.05% basic impedance accuracy
- High speed at an affordable price: 12 ms (SHORT), 118 ms (MED), 343 ms (LONG) @ 1 MHz
- 16 impedance parameters
- 100 μV to 2 Vrms, 1 μA to 20 mA variable test signal
- 201-point programmable list sweep

Price from (US): $4,266

General purpose function generators with arbitrary waveform capabilities and high signal fidelity

33200 Series waveform generators

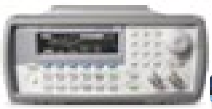

- Sine, square, ramp, triangle, noise, pulse generation with variable edge, DC waveform, AM, FM, and more
- Linear and logarithmic sweeps and burst operation modes
- USB, GPIB and LAN (LXI) interfaces included
- BenchVue software compatibile

Model	Key specifications	Price from (US)
33210A	10 MHz, 1-Ch, 14-bit, 50 MSa/s, 8 K point, 5 MHz pulse (optional arb)	$1,321
33220A	20 MHz, 1-Ch, 14-bit, 50 MSa/s, 64 K point, 5 MHz pulse	$2,487
33250A	80 MHz, 1-Ch, 12-bit, 200 MSa/s, 64 K point, 50 MHz pulse	$4,953

MEASUREMENT HINT

Need to visualize multiple instrument measurements simultaneously? Capture data, screen shots, or system states? Return your entire bench to an earlier state to replicate tests? Remotely monitor and control your bench with a mobile device? You can do it all with Agilent BenchVue. Data capture simplified: Click. Capture. Done.

Validate your most challenging designs with realistic test signals using exclusive Trueform technology

33500B Series waveform generators

- True*form* waveform technology generates signals with the low jitter (<40 ps) and harmonic distortion (<0.04% THD)
- Arbitrary waveforms: 1 M points (16 M optional), sequencing, and embedded editor
- Sine, square, ramp, triangle, noise, DC, AM, FM, PWM, Sum, PRBS, and more
- 16 bits of resolution, 1 mVpp to 10 Vpp
- USB, GPIB and LAN (LXI) connectivity
- BenchVue software compatibile

Model	Key specifications	Price from (US)
33509B (Arb optional), 33511B	20 MHz, 1-Ch, 20 MHz pulse	$1,707
33510B (Arb optional), 33512B	20 MHz, 2-Ch, 20 MHz pulse	$2,607
33519B (Arb optional), 33521B	30 MHz, 1-Ch, 30 MHz pulse	$1,914
33520B (Arb optional), 33522B	30 MHz, 2-Ch, 30 MHz pulse	$2,922
33502A	Isolated amplifier, dual channel, 50 V peak-to-peak	$2,812

Higher frequency with Trueform technology delivers unparalleled signal integrity.

33600A Series waveform generators

- Exclusive True*form* technology generates high-fidelity, gap-free signals with very low jitter and low harmonic distortion
- Arbitrary waveforms: 4 M points (64 M optional), sequencing, and embedded editor
- Sine, square, ramp, triangle, noise, DC, AM, FM, PWM, Sum, PRBS, and more
- 14 bits of resolution, 1 mVpp to 10 mVpp
- USB, LAN (LXI), and optional GPIB connectivity
- BenchVue software compatibile

Model	Key specifications	Price from (US)
33611A	80 MHz, 1-Ch 660 MSa/s arb, 60 MHz pulse	$3,995
33612A	80 MHz, 2-Ch 660 MSa/s arb, 60 MHz pulse	$5,695
33621A	120 MHz, 1-Ch 1 GSa/s arb, 100 MHz pulse	$4,695
33622A	120 MHz, 2-Ch 1 GSa/s arb, 100 MHz pulse	$6,695

Quickly and accurately evaluate your DUTs with precision/low-noise sourcing and easy-to-use GUI

B2900A Series source measure units (SMUs)

- Superior graphical I-V Curve
- High sourcing and measurement resolution (6½ digit)
- Wide output range (210 V / 3 A DC / 10.5 A pulse)

Price from (US): $6,133

B2960A Series low-noise power sources

- Ultra-low noise performance with the external low noise filter (10 μVrms)
- High sourcing resolution (6½ digit, 100 nV/10 fA)
- Innovative sourcing capability such as ARB and DC emulation

Price from (US): $6,133

You need it when? Agilent distribution partners offer expedient delivery.

High performance DC power

Anticipate new demands with high speed, versatility, and accuracy

N6700 low-profile modular power system

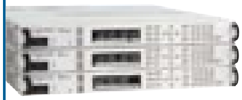

- Ideal DC power supply solution for automated test systems: small, fast, and flexible
- Small 1 U high mainframe (400, 600, 1200 W) with slots for up to 4 programmable DC power modules
- Mix and match the performance you need with your choice of over 30 programmable DC power modules: basic, high performance, and precision (mA and µA); available in 50, 100, 300, and 500 W
- USB, GPIB and LAN (LXI) connectivity
- BenchVue software compatible

Price from (US): $2,627

N6705B DC power analyzer

- Get deep insight into DUT power consumption—without assembling a complex test system
- Integrate up to four DC programmable power modules with DMM, scope, arb, and data logger features; up to 600 W total power
- New source/measure units and application-specific modules for battery-drain analysis, functional test and more
- USB, GPIB and LAN (LXI) connectivity
- BenchVue software compatible

Price from (US): $7,471

6600 Series high-performance DC supplies

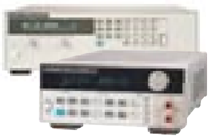

- Fast, low-noise outputs improve measurement accuracy and test throughput
- 40 to 6600 W, single output, up to 120 V, and up to 875 A
- Programmability and built-in V & I measurements simplify test setups
- GPIB connectivity

Price from (US): $2,488

N3300 DC electronic load mainframe

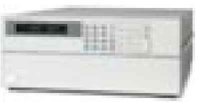

- Stable and accurate: these loads are easy to integrate into your test system
- Automated command list execution reduces workload on system controller
- 1800 W mainframe accepts up to six 150 to 600 W modules for simultaneous testing
- Maximum inputs up to 240 V and 120 A
- GPIB connectivity

Price from (US): $1,833

For applications that require precise, accurate measurements and efficient analysis of AC power

6810B Series AC power sources/ power analyzers

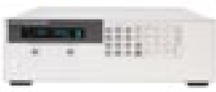

- One-box solutions provide generation, measurement, and AC power analysis by combining the capabilities of a multimeter, oscilloscope, harmonic analyzer, arbitrary waveform generator, and power analyzer
- Available in 375, 750, and 1750 VA models, with 300 Vrms, 3.25 to 13 Arms, and 40 to 80 A peak

Price from (US): $7,610

High value

Solid performance and robust features help you achieve more on lower budgets

N8900 Series autoranging high-power system supplies

- 5 kW and 10 kW basic, single-output, autoranging programmable DC power for ATE applications
- Just the right amount of performance at just the right price
- 18 models that offer up to 1000 V or 340 A
- Easily parallel units to create "one" power supply with 100 kW of power
- USB, GPIB, LAN (LXI) connectivity and analog programming

Price from (US): $7,722

N5700 and N8700 Series system DC power supplies

- Basic, high-power, single-output power supplies
- 45 affordable models in compact 1 U (750 and 1500 W) and 2 U (3.3 and 5 kW) packages
- Up to 600 V or up to 400 A
- Programmability and built-in V & I measurements simplify test set ups
- USB, GPIB and LAN (LXI) connectivity

Price from (US): $2,611

E3600 Series DC power supplies

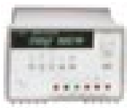

- Output noise as low as 1mVp-p/0.2mVrms
- Tight 0.01% load and line regulation
- Fast load transient response time (<50 µs)
- 30 to 200 W outputs
- BenchVue software compatible

Price from (US): $657

6030 Series basic autoranging DC supplies

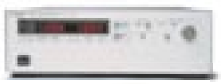

- Autoranging to do the job of multiple power supplies
- 240 or 1200 W output, up to 500 V and up to 120 A
- Programmability and built-in V & I measurements simplify test setups
- GPIB connectivity

Price from (US): $5,338

Agilent offers more than

300 power products to meet your specific needs.

The free *Agilent Power Product Catalog* helps you choose your instrument by the number of outputs, output power characteristics, packaging, special features and application specific solutions.

www.agilent.com/find/highpower

Modular flexibility and universal channels for a wide range of measurements with no external signal conditioning

34970A/72A data acquisition switch units

- Low-cost, 3-slot unit with 6½ digit DMM and built-in signal conditioning
- Choose from 8 plug-in modules, up to 120 1-wire (60 2-wire) channels or 96 cross points
- BenchLink Data Logger software included, optional 34830A BenchLink Data Logger Pro
- GPIB & RS-232 connectivity (34970A) USB & LAN (LXI) connectivity (34972A)—built-in web interface for easy control

Price from (US): $1,745/$2,015

34970A/72A plug-in modules

Model	Key specifications
34901A/02A/08A multiplexers	Up to 300 V, 16, 20, or 40 channels
34903A GP switch	300 V, 20 actuator channels
34904A matrix	4x8 matrix
34905A/06A RF switches	2 GHz dual, 50 and 75 Ω
34907A multi-function	DIO, DAC, totalizer

34980A multi-function switch/ measurement unit

- High performance, 8-slot mainframe with 6½ digit DMM and built-in signal conditioning
- Choose from 21 plug-in modules, up to 1024 1-wire (560 2-wire) channels or 4096 cross pts.
- Optional 34832A BenchLink Data Logger Pro
- GPIB, USB,LAN (LXI) connectivity—built-in web interface for easy control

Price from (US): $2,803

34980A plug-in modules

Model	Key specifications
34921A–34925A multiplexer switch modules	Up to 300 V, 40, 70, or 80 channels
34937A–34939A GP switch modules	Up to 64 channels, 5 A, 300 V
34931A–34934A matrix switch modules	Up to 512 crosspoints per module
34941A–34947A RF & µWave switch modules	Up to 26.5 GHz bandwidth
34950A–34952A system control modules	DIO, DAC, totalizer, frequency period, counter

MEASUREMENT HINT

Configure a low-cost, high-performance RF solution for wireless transceiver measurements by pairing a **N9320B/N9322C** spectrum analyzer with the **N9310A** RF signal generator using a **33500B/33600A** Series waveform generator as its modulation input. You can measure any wireless connectivity device with ASK, FSK, or GFSK modulation across a range of industrial, automotive, and consumer electronics.

Achieve more on a tight budget: Solid performance with robust measurement features

N9330B handheld cable and antenna tester

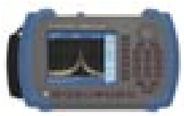

- Frequency range: 25 MHz to 4 GHz
- 3.0 ms/data point sweep time
- VSWR/return loss/cable loss; distance-to-fault
- 4-hour battery life

Price from (US): $5,248

N9340B handheld spectrum analyzer (HSA)

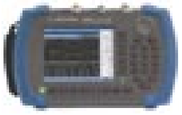

- Frequency range: 9 kHz to 3 GHz
- One-button features: channel power, ACPR, OBW, field strength, spectrum emission mask
- 3 GHz tracking generator: insertion loss, amplifier gain, filter passband
- AM/FM IBOC and xDSL measurement

Price from (US): $8,599

N9320B basic spectrum analyzer (BSA)

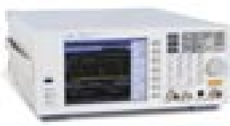

- Frequency range: 9 kHz to 3 GHz
- DANL: -148 dBm with pre-amp on
- RBW: 10 Hz to 1 MHz
- LAN, GPIB, and USB connectivity
- 3 GHz tracking generator
- PowerSuite: channel power, occupied bandwidth, and more
- AM/FM and ASK/FSK demodulation analysis
- Free remote control PC software
- BenchVue software compatible

Price from (US): $8,452

N9322C basic spectrum analyzer (BSA)

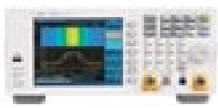

EDN 2013 HOT 100

- Frequency range: 9 kHz to 7 GHz
- DANL: -152 dBm typical, with preamp on
- RBW: 10 Hz to 3 MHz
- 7 GHz tracking generator, built-in VSWR bridge
- AM/FM, ASK/FSK demodulation
- Free remote control PC software
- BenchVue software compatible

5-in-1 RF analyzer

- Spectrum analyzer
- Stimulus and response tester
- Spur and interference analyzer
- ASK/FSK modulation analyzer
- Peak and average power meter

Price from (US): $11,699

Professional performance and compact size for general purpose testing needs

N9310A RF signal generator

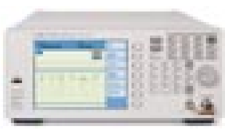

- 9 kHz to 3 GHz CW output, 20 Hz to 80 kHz low frequency (LF) output
- -127 to +13 dBm output level range (max +20 dBm settable)
- - 95 dBc/Hz SSB phase noise
- Extensive analog modulation: AM, FM, phase, and pulse modulation
- Optional IQ modulator, 40 MHz bandwidth
- Up to ± 0.1 ppm aging rate

Price from (US): $7,808

Agilent distribution partners: fast, local response with a direct line to Agilent's test and measurement experts

Benchtop DMMs

Exceptional performance and ease of use

BenchVue software compatible

Model	Description	Features: Digits of resolution	Features: DCV, DCI True RMS ACV/ACI	Features: 2– and 4– wire Ω	Features: freq/ period	Features: diode/ cont	Features: cap.	Features: temp.	Max reading rate at 4½ digits (rdgs/s)	Built-in PC Interfaces	Price from (US)
U3401A	Dual display. Elegantly simple and affordable DMMs with basic capabilities	4½	•	•	•	•			3	None	$497
U3402A		5½							22		$662
U3606A	DMM with built-in 30 W power supply. Halves bench/rack space needed for two instruments	5½	•	•					37	USB, GPIB	$1,258
34450A	Faster measurement speed, ultra-bright OLED with dual display, and basic statistical tools	5½	•	•	•	•	•	•	190	USB, Serial interface (RS-232), optional GPIB	$813
34460A	Display DMM results in ways you never have before and measure with unquestioned True*volt* confidence	6½	•	•	•	•		•	300	USB, optional GPIB and LAN	$945
34461A									1,000	USB, LAN optional GPIB	$1,095
34401A	Industry standard for accuracy, speed, measurement ease and versatility	6½	•	•	•	•			1,000	GPIB	$1,159
34410A	Dual display. Highest throughput of benchtop DMMs, best choice for system use	6½	•	•	•	•	•	•	10,000	USB, GPIB, LAN	$1,404
34411A									50,000		$2,235
34420A	Nano volt/μΩ meter. Very accurate, low-level measurements	7½	DCV only	•				•	250	GPIB	$4,349
3458A	The fastest, most flexible and most accurate multimeter, ideal multimeter for demanding applications	8½	•	•	•				100,000	GPIB	$9,568

Handheld DMMs

Rich features and robust design for real-world conditions

- High-contrast OLED display with 160° viewing angle (U1273AX, U1273A and U1253B)

The U1177A
Infrared (IR)-to-*Bluetooth*® Adapter:
Enables *Bluetooth* connection to ALL Agilent U1200 Series handheld meters. Use with the complimentary Mobile Meter and Mobile Logger, on your Android device to monitor and log data remotely and wirelessly (up to 3 handheld meters).

Agilent U1177A: an electronics industry multiple award winner for 2013.

	U1230 Series	U1240 Series	U1250 Series	U1270 Series	U1210 Clamp Meter Series
Counts	6,000	10,000	50,000	30,000	4,000
AC bandwidth	1 kHz	2 kHz	30 to 100 kHz	100 kHz	2 kHz
Voltage AC/DC	600 mV to 600 V	1 to 1,000 V	50 mV to 1,000 V	30 mV to 1,000 V*	4 to 1,000 V
Current AC/DC	60 μA to 10 A	1 μA to 10 A	500 μA to 10 A	300 μA to 10 A	40 to 1,000 A
Battery life	500 hours	300 hours	72 hours*	300 hours	60 hours
Additional features	Built-in flashlight, continuity alert with flashing backlight, Z_{Low} non-contact voltage detector with V_{sense}*	Switch counter, harmonic ratio, dual and differential temperature measurements*	20 MHz frequency counter, programmable square wave generator*	Low pass filter, AC and/or DC voltage check, low impendance mode offset compensation* Operational down to -40 °C*	Large 2" jaw size, back light with dual display, ACI, ACV/DCV, diode test, R, C, frequency 400 Ω to 40 MΩ resistance 4 to 4,000 μF capacitance*
Connectivity	IR-USB and Infrared (IR)-to-*Bluetooth*				
Price from (US)	**$101**	**$206**	**$390**	**$347**	**$255**

*Specification available on select models only.

Maximum versatility to troubleshoot today's challenges and anticipate tomorrow's needs

U1600 Series handheld scopes

- 5.7-inch VGA TFT LCD display with indoor, outdoor, and night-vision viewing modes
- 3-in-1 instrument: oscilloscope, DMM, and data logger
- Fully isolated channels (U1610A, U1620A)
- Up to 2 GSa/s sample rate and up to 2 Mpts deep memory to zoom in on critical details
- Benchtop-like dual window zoom for more detailed waveform analysis

Price from (US): $1,388

Big scope performance with a small scope price

1000 Series oscilloscopes

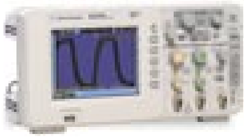

- 50 to 200 MHz, 2 and 4 channel DSO models with up to 20 kpts memory
- 5.7-inch color display offers powerful signal capture and display
- Up to 2 GSa/s sample rate
- 23 automatic measurements, sequential acquisition, mask testing and digital filters provide advanced measurement capabilities
- Accelerate your productivity with an 11-language user interface, USB connectivity, and a standard educator's kit

Price from (US): $520

See the big picture without losing sight of the details

N2820A & N2821A High sensitivity current probes

- Measure currents as low as 50 µA
- Measure currents as high as 5 A
- Measure AC and DC
- Also use as a voltage probe with as low as 3µV sensitivity
- Bandwidth; 3 MHz Zoom-Out Channel, 500 kHz Zoom-In Channel
- Compatible with InfiniiVision 3000X and InfiniiVision 4000X

Price from (US): $2,100/$3,200

For the complete list of available probes: www.agilent.com/find/probes

MEASUREMENT HINT

The **N2820A** 2-channel high sensitivity current probe comes with two parallel differential amplifiers inside the probe with different gain settings. The low gain side allows you to see the entire waveform, the "zoom out" view of the waveform, and the high gain amplifier provides a "zoom in" view to observe extremely small current fluctuations, such as a mobile phone's idle state.

Breakthrough scope technology lets you see more, do more and get more for your money

InfiniiVision Oscilloscopes

- Up to 1,000,000 waveforms/sec update rate
- MegaZoom IV responsive, uncompromised smart memory
- Integrated—5 instruments available in one
- Fully upgradable—bandwidth, MSO, memory, serial analysis, built-in WaveGen function generator, or digital voltmeter
- BenchVue software compatible

2000 X-Series

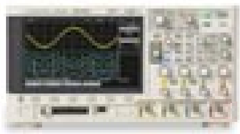

- 70 to 200 MHz bandwidth, up to 1 Mpts memory, DSO and MSO models
- 8.5-inch WVGA display offers 2x the viewing area and 5x the resolution of competitive scopes
- Standard 5 year warranty

Price from (US): $1,258

3000 X-Series

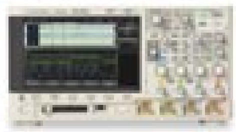

- 100 MHz to 1 GHz bandwidth, up to 4 Mpts memory, DSO and MSO models
- 8.5-inch WVGA display is 50% larger and 3x the resolution of competitive scopes
- Segmented memory optional
- Standard 3 year warranty

Price from (US): $3,222

4000 X-Series

Experience speed, usability and integration

- 200 MHz to 1.5 GHz bandwidth, 4 Mpts smart memory, DSO and MSO models
- 12.1-inch capacitive touch display is 40% larger than competitive scopes
- InfiniiScan Zone touch triggering—if you can see it, you can trigger on it
- Segmented memory standard
- Standard 3 year warranty

Price from (US): $5,611

Gain greater insight with powerful applications

See the complete list at www.agilent.com/find/scope-apps

Description	2000 X-Series	3000 X-Series	4000 X-Series
20 MHz WaveGen	DSOX2WAVEGEN	DSOX3WAVEGEN	DSOX4WAVEGEN2 (2-ch AWG)
3-digit voltmeter	DSOXDVM	DSOXDVM	DSOXDVM
DSO to MSO upgrade	DSOX2MSO	DSOX3MSO*	DSOXPERFMSO
CAN/LIN trigger/decode	DSOX2AUTO	DSOX3AUTO	DSOX4AUTO
I^2C/SPI trigger/decode	DSOX2EMBD	DSOX3EMBD	DSOX4EMBD
RS232/UART trigger/decode	DSOX2COMP	DSOX3COMP	DSOX4COMP
USB full/low trigger/decode			DSOX4USBFL
USB high trigger/decode			DSOX4USBH
USB signal quality test			DSOX4USBSQ

** 1 GHz models require DSOXPERFMSO*

*Get a **FREE** 30-Day Trial License.* **www.agilent.com/find/30daytrial**

Agilent distribution partners: your local connection to Agilent's global technical resources

Agilent Technologies
P.O. Box 3828, Englewood, CO 80112-5910

Higher frequency signals, meet True*form* signal integrity.

Introducing the new
80 & 120 MHz 33600A Series
True*form* waveform generators

SEE PAGE 2

Printed in U.S.A., May 1, 2014

5991-3975ENUS

PROMOTIONS

Special promotions available only through Agilent distributors

Check out these great offers*

RF

Buy a N9310A RF Signal Generator and get a free IQ Modulator.
Ends 6/30/14.

RF Promo FREE 5 Year Warranty.
Ends 9/30/14.

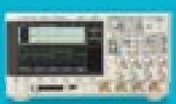

SCOPES

Upgrade to your Ultimate Scope with the InfiniiVision X-Series Application Bundle.
Ends 9/30/14.

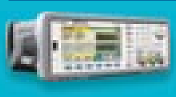

WAVEFORM GENERATORS

Buy a New 33600A Series Trueform Waveform get FREE Waveform Builder Pro License
Ends 8/31/14.

**Certain restrictions apply.*

See our complete list of current promotions.
www.agilent.com/find/promotions

Our Featured Distribution Partners

TESTEQUITY
http://agilent.testequity.com
800-588-3457

Newark element14
www.newark.com/agilent
800.463.9275

microlease
The experts in Test Equipment management
www.microlease.com/agilent
800.432.3424

Agilent Technologies
Authorized Distributor

Anticipate* __*Accelerate* __*Achieve

Find an Agilent distributor today at
www.agilent.com/find/distributor

June 2014

MOTION CONTROL and Automation Technology

HAWE Hydraulics' load-sensing valves are designed for both fixed and variable displacement systems. See page 10a.

Supplement to *NASA Tech Briefs*

www.techbriefs.com/motion

High-Temperature Actuators for Aircraft Propulsion Systems

Future "more electric aircraft" (MEA) will require electric actuation systems for control surfaces and engine controls. Electric motors, drive electronics, and mechanisms are essential elements of aircraft actuation in MEAs that incorporate Electro-Magnetic Actuators (EMAs). High-temperature environments experienced in aircraft applications place demands on actuator components, materials, and insulation systems that dictate the use of new technologies and materials.

High Temperature Electromagnetic Actuator (HTEMA) options for high-temperature aircraft environments include appropriate motor types, drive and control electronics, mechanisms, materials, and construction methods. These options are evaluated to identify candidates that meet the challenges of tomorrow's MEA actuators.

Efforts to design, build, and test a prototype demonstrating a high-temperature, high-reliability class of all-electromagnetic actuator design with minimal/no heat load on aircraft cooling systems are ongoing. Size and weight goals are consistent with the aircraft engine limits. The key technical aspects being addressed include operation in the high temperature and vibration environment, actuator force, power, weight, size, efficiency, speed, stroke, mechanical robustness and reliability, lifecycle cost, failure modes and effects, and maintenance predictions.

Engine nozzle actuation is presently accomplished using fuel as a hydraulic working fluid (fueldraulic actuation) for the current-generation engine actuators. While the nozzle actuation has a low duty cycle, the heat generated is continuous and presents a significant load on the ircraft/engine thermal management system.

An electrically driven actuator can reduce the heat load of the aircraft. The present engine fueldraulic actuators and aircraft fuel systems are highly interrelated, leading to a challenging thermal management problem that has an impact on aircraft performance. Elimination of this fuel heat load reduces the fuel system's thermal issues. High-temperature, electromagnetic actuator component solutions that meet the technology challenges and performance requirements for an actuator system operating engine nozzle actuation have been identified.

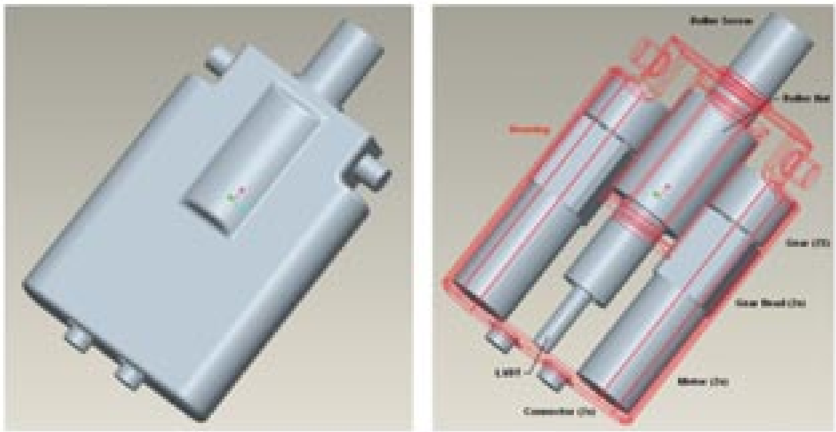

Figure 1: HTEMA actuator package (left) and interior view.

Convergent Nozzle Actuation

The design and development of HTEMA technology for a Convergent Nozzle Actuation System (CNAS) actuator has been completed. The CNAS is the first critical application of the HTEMA technology, providing the power to position the nozzle as required for the pilot-selected engine Power Level Angle (PLA). The CNAS actuators are mounted to the aft end of the engine. Current fueldraulic actuators for the CNAS are limited by the actuator O-ring material. In the CNAS application, fluid temperature limits approach 325 °F and seal temperature limits approach 400 °F. The current engine actuators are able to operate in a temperature environment approaching 325 °F continually and up to 560 °F for transients of 10 seconds by using the hydraulic fluid (fuel) as a means of cooling.

The CNAS actuators have a linear stroke of 4", a combined stall load (for 4 actuators) of 42,000 lbf, and weigh about 52 lbm (actuation system hardware including routing). Envelope goals provided by the AFRL are 11 × 2.5 × 6.5". The power type is 270 VDC.

Key technologies evaluated included motor, insulation, bearings, electronics, gearing, cooling, and signals and sensors for a notional actuator. The best candidates for detailed design and optimization were identified.

The notional CNAS HTEMA employs five actuators, each capable of 10,500 lbs (46.7 kN) of force, producing a total of 42,000 lbs (186.8 kN) with one actuator missing. Given the requirement for an electromagnetic solution, a direct drive actuator was considered first. Aerospace machines typically develop a pressure of 3-5 psi^2 in the air gap due to magnetic

fields. This dictates a gap area of at least 2.1×10^3 square inches is needed to generate the required force. Based on the 5 psi curve, an actuator with an 18" gap diameter has roughly a 2' outer diameter and 3' length. An approximate actuator weight would be greater than 1,000 pounds, which is clearly unacceptable. Given the envelope requirement of 11 × 2.5 × 6.5", an 11"-long machine would have over a 60" diameter, an unacceptable result.

Therefore, the CNAS application requires mechanical advantage to decrease the required electromagnetic actuator force and size, while increasing speed. The Navy investigated electromagnetic actuator replacements for hydraulic cylinders and found planetary roller screws to be a good candidate for rotor-to-linear conversion and mechanical advantage. Typical COTS roller screw ratings indicate a screw diameter in the 30- to 48-mm (~1.2 to 1.9") range is appropriate.

Inclusion of a single-pass, 5 to 1 planetary gear between the planetary roller screw and motor improves this situation. COTS planetary gears show a significant performance advantage for a small weight (<2.8 lbs). Issues with dry lubrication, life, and seals must be addressed in a custom detailed design for this high-temperature application. However, this information is sufficient for trade studies. Assuming a ~3:1 length-to-diameter ratio, the motor weight is less than 12 pounds.

Harmonic drives were considered for higher gear ratios in smaller packages. However, concerns about the ability to back-drive the unit in some failure modes prevented inclusion in the baseline design. Magnetic gearing is also an option but concerns about permanent magnet (PM) demagnetization during flux reversals at high temperature were considered high risk.

Care must be exercised in the lead screw and gear ratio selection if the actuator must be back-driven with the power off. There is a critical angle in lead screws where the unit will act as a friction lock at and below the critical value. Similarly, the gearing will multiply any drag and cogging torques present in the motor, which can also inhibit the ability to back-drive an actuator. It is important to keep this in mind during detailed trades.

Baseline Actuator Concept

The system design includes the following key components and technologies: roller screw, planetary gearing, high-temperature coatings, high-temperature motor materials and insulation system, high-temperature power electronics, and sensors.

Several motor types have been considered with high efficiency and minimal weight and volume. These include surface mount PM, Halbach Array PM, buried magnet PM, and hybrid stepper. Others that do not require PMs include wound rotor DC (brush and brushless), variable or switched reluctance (VR or SR) machines, and squirrel cage induction motors. Trades have identified brushless DC PM and SR machines are of primary interest. Both motors can use sensorless commutation methods. A VR resolver can be incorporated in the design if required for control feedback.

VR motors are robust with simple windings, facilitating application of high-temperature insulation. Because VR motors have no permanent magnets, they do not generate a back Electro Motive Force (EMF) voltage when

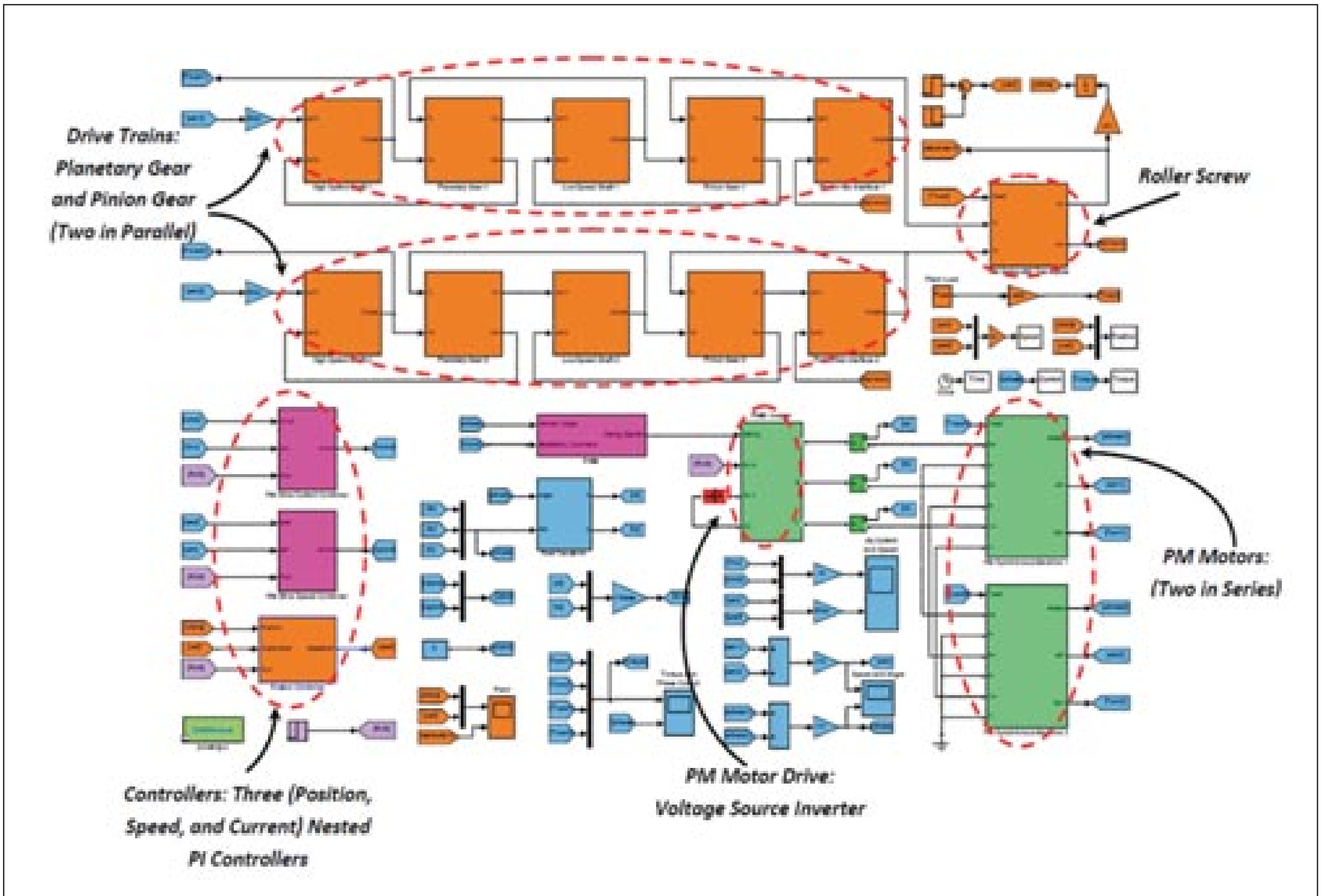

Figure 2: HTEMA representation in Simulink.

unpowered, which may be advantageous in some failure modes.

The PM motor design includes a band to contain the surface-mount PMs. VR machines do not require such containment requirements, but have quite small mechanical gaps that must be maintained over temperature and life. Both machines can be back-driven, with VR machines having an advantage of no back EMF generated when unpowered. This may be an advantage in failure modes and effects analyses (FMEA). Given the motor is used in an aircraft application, high-saturation flux density lamination material is highly desirable.

Brushless DC PM motors provide excellent efficiency with high bandwidth for servo applications. Brushless commutation is appropriate for life, reliability, and maintenance issues. High motor pole count is a big factor in minimizing weight. Maximum slew rate, speed, switching speed, and/or geometry will be the limiting factor, but the higher the number of poles, the better.

Mechanical gears are a mature technology with a long and rich history. When properly designed, applied, and maintained, they can provide long, failure-free performance. In addition, cost and manpower limitations are pushing hardware toward more robust, no-maintenance technologies.

Planetary gears were selected in the baseline design for their power-dense, high-torque transmission capacity and form factor. A COTS gearhead was identified with 5:1 gear ratio in a single pass. Modifications to the COTS gearhead with a 98- 95% efficiency for a single pass and 150,000 to 200,000 hours of life at room temperature to meet the high-temperature environment are anticipated. Flex spline or harmonic drives can also be used if failure modes and effects analyses show their inability to be back-driven is not an issue.

A simulation study of HTEMA was performed based on flow-down requirements. The simulation tool used was Simulink together with its SimPowerSystems (SPS) toolbox from MathWorks. Instead of using SPS library models, custom models were created for the permanent magnet synchronous motor, the motor drive, and some of the mechanical elements. The main reason for creating custom models is that the existing SPS models do not provide the flexibility needed for detailed study of the HTEMA.

As shown in Figure 2, a nested controller structure is used to provide the servo performance. The outermost control loop is the position controller, which generates the motor speed reference used by the speed controller. The speed controller calculates the motor current reference, and the innermost current controller regulates the motor current to follow this reference.

Key elements of the HTEMA have been investigated, and the baseline design meets the space, weight, and performance requirements. Development continues to mature the HTEMA system for the CNAS application, perform detailed design, build and test a prototype unit, and validate analytical models. This work will lead to efforts that transition the HTEMA to military flight-certified hardware supporting future engine upgrades and commercial aviation applications.

This article was written by Gerald Foshage, Richard Young, Yuntao Xu, Edward Wagner, and Dennis Mahoney of RCT Systems (Linthicum Heights, MD); and Alireza R. Behbahani of the Air Force Research Laboratory. For more information, visit ***http://info.hotims.com/49746-320***.

Haydon Kerk™ Linear Actuators...

SOLUTIONS IN MOTION

High performance, precision linear motion technology

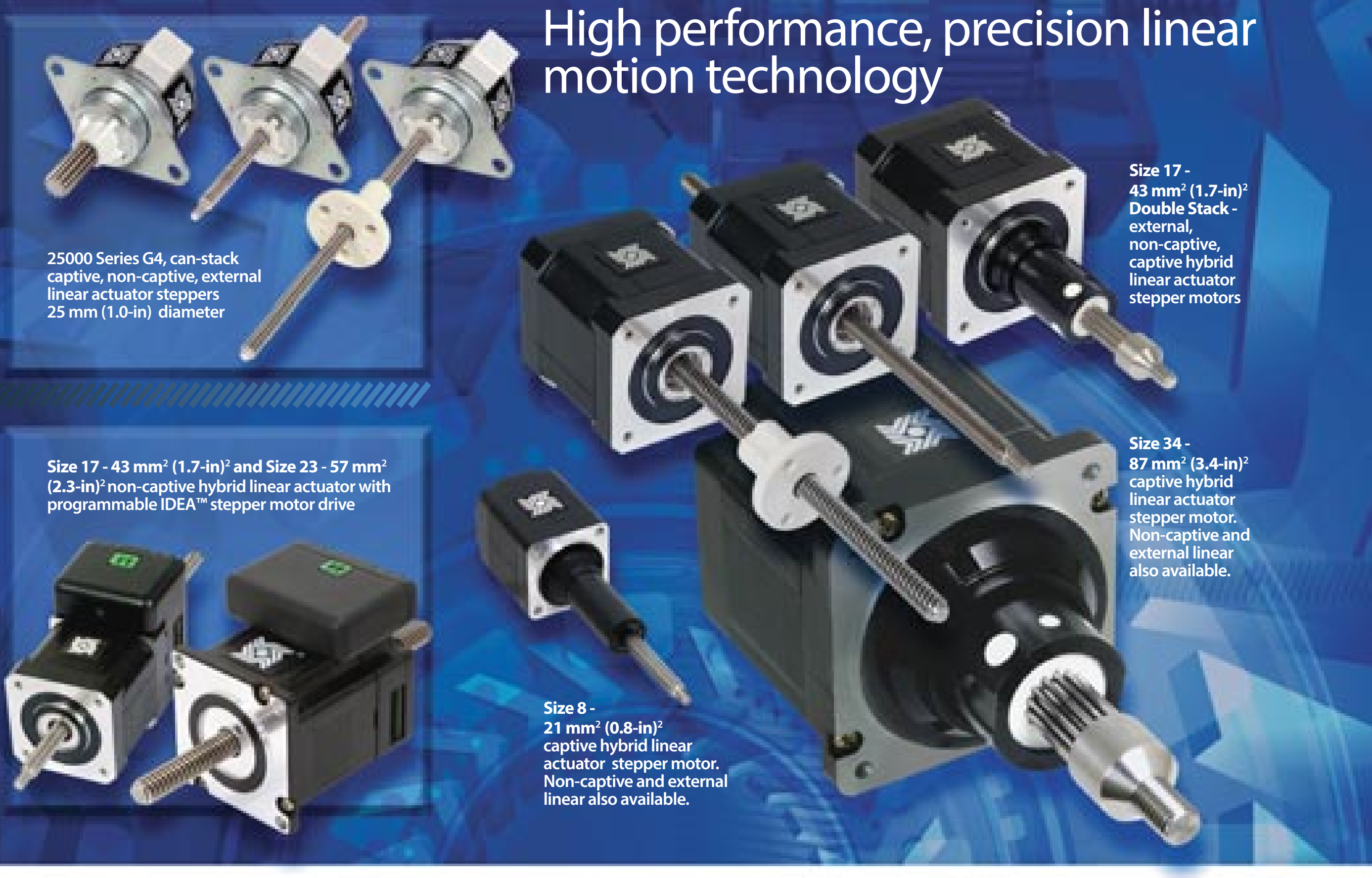

Haydon Kerk Motion Solutions hybrid and can-stack linear actuators continue to offer equipment designers new motion control solutions that provide unmatched performance-to-size ratios, patented technologies and tens of thousands of configuration options.

HYBRID actuators are available Size 8: 21 mm² (0.8 -in.) to Size 34: 87 mm² (3.4-in.) – capable of delivering up to 500 pounds (2224 N) of force. Travels per step range from .001524 mm (.00006-in) to .127 mm (.005-in), with micro stepping capability for even finer resolution. An integrated, programmable IDEA™ Drive is available with Size 17 and Size 23 hybrid motors.

The G4 Series represents the industry's most robust and most powerful **CAN-STACK** linear actuators. The G4 Series offers diameters of 20 mm (.79-in), 26 mm (1-in), and 36 mm (1.4-in). The can-stack product line also includes motors with diameters of 15 mm (0.59-in), 20 mm (.79-in) , 26 mm (1-in), 36 mm (1.4-in) and Ø 46 mm (1.8-in), available with captive, non-captive or external linear lead-screws.

Haydon Kerk Motion Solutions continues to be an innovative motion control technology company with a global network of people, facilities and services dedicated to engineering and manufacturing the world's most advanced linear motion solutions.

For more information: **www.HaydonKerk.com** > Linear Actuators

2D/3D Model Downloads **www.HaydonKerk.com**

Haydon kerk™ Motion Solutions

Call **1.800.243.2715**

AMETEK® PRECISION MOTION CONTROL

Haydon Products Division
1500 Meriden Road
Waterbury, CT 06705 U.S.A.
Telephone: **203.756.7441**
Fax: 203.756.8724

Kerk Products Division
1 Kerk Drive
Hollis, NH 03049 U.S.A.
Telephone: **603.465.7227**
Fax: 603.465.3598

dunkermotoren™ advanced motion solutions · Haydon kerk™ Motion Solutions · PITTMAN® · Windjammer® Brushless Blowers · Nautilair · ROTRON®

Free Info at http://info.hotims.com/49746-773

Probe Positioning System for Antenna Range

Three or more cables provide the desired positioning.

NASA's Jet Propulsion Laboratory, Pasadena, California

In situ measurements of antenna patterns on rovers in a simulated terrain are difficult to make with conventional antenna range techniques. The desired pattern data covers a hemisphere above the antenna of interest, which is close to the ground. This is incompatible with traditional measurements that place the antenna under test on a movable support that tilts and rotates.

The solution is to suspend the probe from three or more flexible cables attached to computer-controlled winches that are supported above the test volume. By varying the length of the cables, the position of the probe can be moved anywhere in the test volume. A separate metrology system can be used to increase the accuracy of knowledge of the probe position and orientation.

The probe carrier, at the junction of the suspension cables, has actuators to alter the probe orientation. Power is supplied by passing current through the suspension cables, or by battery power on the probe carrier. Multiple sets of cables and probe platforms can be used to simulate multiple orbiting assets. The probe can be a transmitter, a receiver, or both, and can be at any frequency that is needed for the test scenario. A calibration reference, for phase and/or amplitude, can be transmitted to the probe carrier by RF, optical, or wired means.

This technology has been used to "fly" a video or film camera over a football stadium, but has never been used for antenna measurements or simulation of moving sources over an area. For low-precision applications, the lengths of the cables can be mathematically transformed into the position of the probe. An external tracking system, using optical or RF means, can be used for higher precision. Closed loop control can be implemented from the tracking system to the winch controllers to allow very precise and repeatable control of the position of the probe.

The cables can be made of any reasonably strong material, although materials with low elasticity (e.g. Kevlar or Spectra) are preferred for precision positioning. Steel cables have been used in the commercial flying camera applications. However, a non-conductive cable has significant advantages for the antenna and RF application, since it does not perturb the RF fields as much as a conductive cable; however, with suitable probe design, a conductive cable may be acceptable. Non-conductive cables improve safety, since the cables won't conduct dangerous voltages or currents, as from an inadvertent contact with some energized conductor or lightning.

Power for the probe is provided either by batteries, solar cells, or other means. If it is desired to use conductive support cables, they can be used to carry power. In this case, the addition of suitable RF absorbing materials may be needed to

Intro Cov ToC

reduce the effect on the measurement accuracies. Control and telemetry signals from the moving probe can be carried by an optical fiber or other wireless means. While three cables are the minimum to provide the desired positioning, the use of more cables can provide a wider range of motion, and can allow positioning of the orientation of the probe.

This work was done by James P. Lux of Caltech for NASA's Jet Propulsion Laboratory.

For more information, download the Technical Support Package (free white paper) at www.techbriefs.com/tsp under the Mechanics/Machinery category*. NPO-44090*

Fluidic Actuators with No Moving Parts

Langley Research Center, Hampton, Virginia

Two new fluidic actuator designs were developed to control fluid flow in ways that will ultimately result in improved system performance and fuel efficiency in toimprove the aerodynamic performance of a variety of vehicles. These flow control actuators, often referred to as fluidic oscillators or sweeping jet actuators, utilize the Coanda effect to generate spatially oscillating bursts (or jets). They can be embedded directly into a control surface (such as a wing or a turbine blade) to help reduce flow separation, increase lift, reduce drag, enhance mixing, or increase heat transfer. Recent studies show up to a 60% performance enhancement (such as increased lift or reduced drag) with fluidic actuators.

One of the actuator designs effectively decouples the oscillation frequency from the amplitude (i.e. mass flow through the actuator). A decoupled actuator can deliver high mass flow rates without changing the frequency, or deliver high- or low-frequency oscillating jets at minimal mass flow rates. The second actuator design enables in-phase or anti-phase synchronization of the oscillating jets. This overcomes issues caused by the random oscillation of individual actuators when they are used in an array of actuators, and has particular benefit for flow-control applications. These new designs will provide better control authority over the fluidic actuator, increased actuator efficiency, decreased mass flow, and improved system performance.

The new actuator designs do not require any additional equipment—oscillations, decoupling, and synchronization are achieved in a passive manner, entirely via internal flow dynamics. Since these actuators have simple and compact structure and do not have any moving parts, they are basically maintenance-free, and highly scalable. They can be manufactured from many different materials and therefore can also be used in harsh environments.

This work was done by Mehti Koklu of Langley Research Center. ***For more information, download the Technical Support Package (free white paper) at www.techbriefs.com/tsp under the Mechanics/Machinery category****. LAR-18089-1/90-1*

Submersible Pressure Transducer for Tank Fluid Level Monitoring

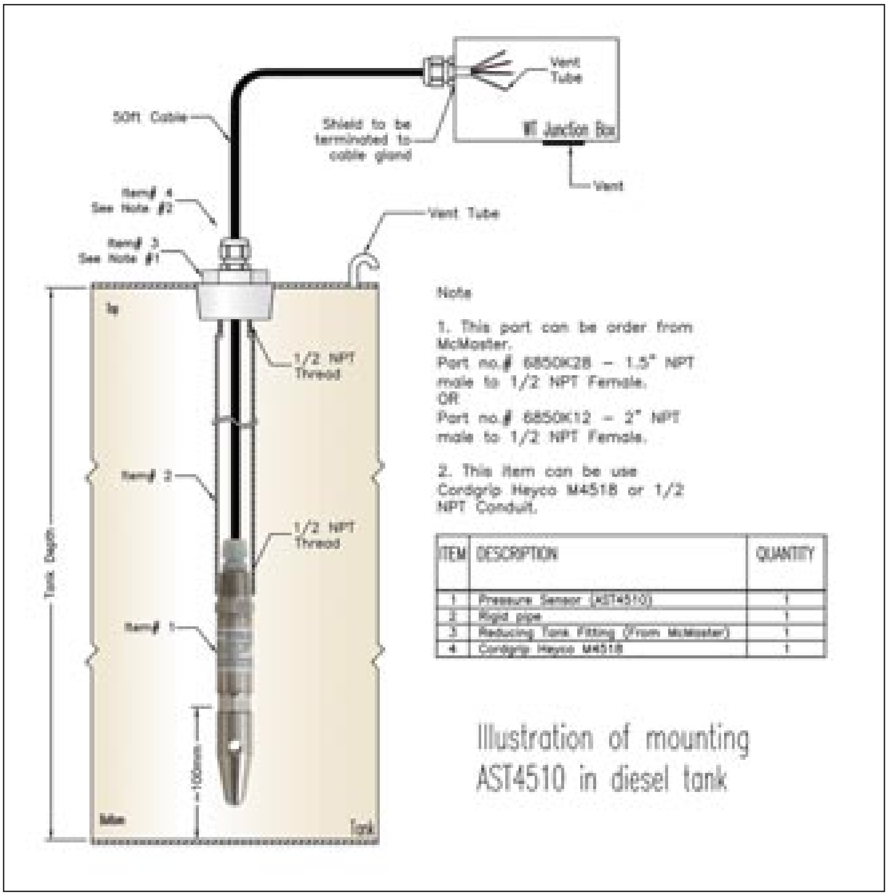

Monitoring the level of liquid can be accomplished through the use of a pressure transducer. The density of the liquid and its height create pressure on the diaphragm of the pressure transducer to generate an accurate and cost-effective level measurement. Generally, pressure transducers can be used for level measurement from 10 inches of water column up to 10,000 PSI (700 bar).

Designed with stainless steel and Hytrel materials, submersible pressure transducers are reliable, cost-effective instruments to measure the level of various liquids including water and diesel. These pressure sensors are an ideal choice for mobile applications such as ships, train cars, or when the tank is transported between locations such as for construction sites, chemical totes for industrial processing, or well site injection chemicals.

A variety of factors should be considered when installing a submersible pressure transducer in a tank. The figure shows one installation method used by American Sensor Technologies for its AST4510 submersible transducer using a rigid pipe. The transducer comes standard with a 1/2" NPT male conduit connection at the base of the cable connection. In tanks that are turbulent due to an inlet/fill pipe or the use of an agitator, the transducer can have rigid plastic or metal conduit installed over the cable to prevent sensor movement within the tank.

The conduit over the cable is mounted to a bung at the top of the tank. Parts that thread onto a 1.5" female NPT bung and have a 1/2" female NPT thread can mate the ridid conduit. The cable exits the tank and is held in place by a cord grip that runs to the control box. The same cable grip can be used at the junction box, ensuring that the vent tube is clear. Depending on hazardous location requirements, this can be in the non-hazardous area with connection to the intrinsically safe barrier. In this example, it is expected that the junction box is properly vented to the atmosphere to prevent water ingress.

In this application, the pressure sensor was installed above the base of the bottom of the tank. As sludge and silt tend to line the bottom of the tank, a height of 100 millimeters was calculated to ensure the process connection did not clog over time. The diaphragm of the transducer is close to the top of the process connection hex, so operators can calculate the offset from when the tank is empty.

Other applications may have the submersible pressure transducer installed directly into an intrinsically safe radio device at the top of the tank. This reduces the cost of the transducer, as less cable and less time are required for the installation. With shorter cable lengths, a voltage output signal with low current consumption is an option if the system is battery operated. Less current consumption means longer battery life and less maintenance.

This article was contributed by American Sensor Technologies (AST), Mount Olive, NJ. For more information, visit ***http://info.hotims.com/49746-322***.

LIN ENGINEERING
The Step Motor Specialists

Why Lin?

Why Every Day More Engineers Choose Lin Engineering

Over the past decade, Lin Engineering has gained a tremendous amount of market share and earned a reputation as the "**Leader in Step Motor Technology**."

Proven Application Support, Performance, and Quality

Unrivaled Application Support

- 98% application success rate
- 95% of prototypes shipped in less than 1 week

High Performance

- Highest torque output
- High accuracy = no skipping steps
- Reduced vibration and resonance

Reliable Quality

- Consistent Performance
- 4.5 Sigma System
- ISO 9001 certified
- Continuous Improvement

Satisfied Customers

Customers in 2004 Customers in 2014

Extensive Product Line & Value Added Services

- Stepper Motors ranging from NEMA 8 to NEMA 34
- The most complete line of high accuracy and low resonance 0.9 degree stepper motors
- Value added options such as: configurable shafts, windings, and cable assemblies
- Stepper Motors for vacuum, laboratory, and wash-down environments

LIN ENGINEERING
The Step Motor Specialists

16245 Vineyard Blvd., Morgan Hill, CA 95037
Tel. (408) 919-0200 - Fax: (408) 919-0201
Email: sales@linengineering.com
Website: www.linengineering.com

Free Info at http://info.hotims.com/49746-776

NEW Products

Drive Kits

Avnet Electronics Marketing (Phoenix, AZ) offers the Zynq®-7000 All Programmable SoC/Analog Devices Intelligent Drives Kit for prototyping motor control applications. Combining the Xilinx® Zynq-7000 All Programmable SoC ARM® dual-core Cortex™-A9 + 28 nm programmable logic with the Analog Devices data converters and digital isolation, the kit enables motor control and dual Gigabit Ethernet industrial networking connectivity. The kit is supported by Simulink®, Embedded Coder®, and HDL Coder™ from MathWorks, allowing engineers to use an integrated hardware/software workflow to prototype on hardware directly from Simulink and deploy into production using the Xilinx Vivado® Design Suite. A pre-built Zynq reference design of Field Oriented Control features Analog Devices Ubuntu Linux framework to provide an infrastructure for designers to build their own control algorithms.

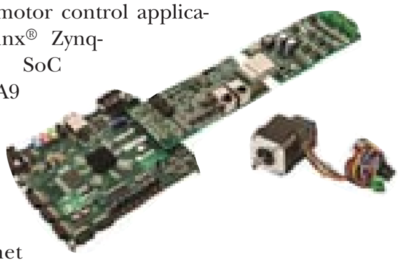

For Free Info Visit http://info.hotims.com/49746-300

Hydraulic Valves

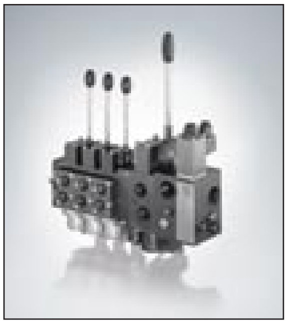

HAWE Hydraulics (Charlotte, NC) offers the PSL/PSV proportional directional spool valve series that can be configured for the hydraulic functions of a silage trailer. These functions include raising/lowering the tailgate or front gate, and operating the scraper floor drive and conveyor drive systems. A modular design permits adjustments via manual, remote hydraulic pilot, or electrical control. The flange-mounted design simplifies plumbing/hose runs, and uses a twin solenoid configuration that reduces wiring and allows for both proportional and on/off operation.

These load-sensing valves are designed to keep the input pressure constant without being affected by the individual work units, enabling independent pressure control between the work sections/functions of the valves. They feature operating pressures of up to 420 bar and maximum flows up to 200 lpm.

For Free Info Visit http://info.hotims.com/49746-302

Step Motors

Applied Motion Products (Watsonville, CA) has announced the HT range of step motors for DC powered drives available with 10' shielded cables. The motors are available in single- or double-shaft versions with additional encoder or encoder and cover options. The motors are suitable for rugged and industrial applications with stepper drives. HT23-598, HT23-601, and HT34-506 are designed for the ST and STR series DC stepper drives. HT23-552/553/554 and HT34-495/496/497 are designed for the STAC5 and STAC6 high-voltage AC stepper drives.

The motors are available with a single shaft or dual shafts. The YAA and ZAA versions include a 2,000-line (8,000-count/turn) optical encoder with differential output signals for noise immunity. The YAC and ZAC versions include a rugged metal housing and 10' strain-relieved, shielded cable. The encoders support position verification, stall detection, and stall prevention.

For Free Info Visit http://info.hotims.com/49746-301

Actuator

NB Corp. (Hanover Park, IL) offers the BG compact, single-axis actuator with a U-shaped integrated slide and ball screw. The actuator's rigid structure can be one-end supported. There are four ball circuits contained in the single block.

For Free Info Visit http://info.hotims.com/49746-317

Motor

The EC-4pole 32 HD motors from maxon precision motors (Fall River, MA) are designed for operation in air or in oil (flooded in hydraulic oil). The power rating depends on the surrounding medium and amounts to 220W in air and, due to the much higher heat flow, 480W in oil. They are designed for ambient temperatures of more than 200 °C and atmospheric pressures of up to 1700 bar. The motors also withstand vibrations of up to 25 grms, as well as impacts of up to 1000 G.

The motors feature high efficiency (up to 89% in air and more than 80% in oil), making them suitable for use in battery operated applications. The motors are used in environments with extreme temperatures, subject to high vibration, or under ultra-high vacuum.

For Free Info Visit http://info.hotims.com/49746-303

Nanopositioning System

The P-736.ZR Large Aperture piezo-Z nanopositioning system from PI LP (Auburn, MA) is designed for imaging and fast focusing applications. It consists of a large-aperture piezo stage and a digital controller. The flexure-guided piezo nanopositioning stages are optimized for high resolution and fast step and settle. The system enables travel ranges of up to 220 µm with sub-nanometer closed-loop resolution. The digital nanopositioning controllers can be switched between focus tracking and closed-loop positioning, and also accommodate fast focus and freeze applications. The system is equipped with a compact digital servo piezo controller, as well as user interfaces such as USB, SPI, RS-232, and real-time analog.

For Free Info Visit http://info.hotims.com/49746-307

Tilt Display Mount

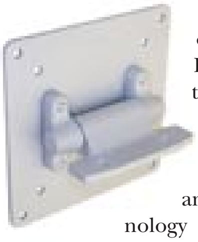

Southco (Concordville, PA) has introduced the T Series Tilt Display Mounts with or without counterbalanced constant torque. The AV-D25 Tilt Display Mount Basic provides tilt positioning for moving and positioning heavy panels and displays. The counterbalanced version provides even lower operating efforts. The T Series enables adjustment of a display's tilt angle and features integrated positioning technology that provides control and customization of operation. It eliminates the need for constant maintenance and readjustment, and enables fingertip positioning.

For Free Info Visit http://info.hotims.com/49746-304

Inclinometer Sensors

Jewell Instruments (Manchester, NH) offers the Emerald Series inclinometer MEMS sensors in a small rectangular package, enabling installation in areas with space constraints. They can withstand up to 500g shock, and offer single- or dual-power input. Custom ranges and bandwidths are available. The inclinometers can be used for industrial and railway applications including wheel alignment, construction equipment, antenna positioning, cross rail management, and tilt safety systems.

For Free Info Visit http://info.hotims.com/49746-306

Rotary Position Sensor

Penny + Giles, a business group of Curtiss-Wright Controls (Christchurch, UK), has introduced the NRH275DR rotary position sensor featuring a low-profile sensor housing and separate permanent magnet assembly. With no contacting mechanical parts that can wear, the sensors can be used in extreme and hostile environments where installation space may be limited. The sensor features a fully encapsulated 12-bit Hall effect sensor system that can withstand high shock and vibration, can operate at temperatures from -40 to 140 °C, and is IP67-rated for dust protection and water immersion to a depth of 1m for 24 hours.

The sensor operates from a 5Vdc regulated supply, and has two independent sensor power supplies and outputs that enable full redundancy. It enables a range of output configurations such as CH1/CH2 angle, output type, and output direction. It also features maximum output signal noise of less than 1mV, which means no additional signal filtering is required on the output signals.

For Free Info Visit http://info.hotims.com/49746-305

Rotary Encoders

HEIDENHAIN (Schaumburg, IL) offers the ExN rotary encoders for Potentially Explosive Atmospheres (ATEX) that feature a 12-mm blind hollow shaft in a sturdy design with increased wall thickness. The encoders are resistant to shock up to 1500 m/s2 (for 2ms), and vibration up to 100 m/s2. The IP 66 encoders handle shaft speeds up to 6000 rpm in a temperature range from -20 °C to 60 °C. The encoders feature ASIC scanning technology, available with EnDat or SSI interfaces for improved signal generation and less interpolation error. The encoders are certified for operation in Zones 1 or 21 of equipment group II (above ground applications).

For Free Info Visit http://info.hotims.com/49746-308

Air Cylinders

Fabco-Air (Gainesville, FL) has announced the OEM NFPA cylinders. The FCQN Series is a repairable NFPA interchangeable cylinder line that comes with magnetic pistons for position sensing. Adjustable cushions at both ends of the cylinders are included as a standard option. Stainless steel tie-rods are incorporated into the cylinder construction, as well as anodized end caps. Each cylinder includes both bottom tapped and end-cap sleeve nut mounting configurations. NFPA mounting is accomplished by adding a detachable NFPA mount to the standard cylinder.

For Free Info Visit http://info.hotims.com/49746-311

Intro Cov ToC

Motion Control Chip

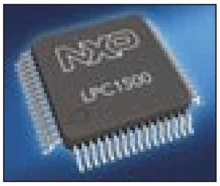

Mouser Electronics (Mansfield, TX) offers the LPC1500 Motion Control Chip from NXP Semiconductor. The flexible controller can drive a variety of different motors including brushless DC, sensored, sensorless, and permanent magnet motors. The integrated circuit is powered by a 72-MHz ARM Cortex M3 core combined with specialized motor control peripherals. Two 12-bit, 12-channel ADCs and a quadrature encoder interface provide support to drive two motors at the same time. The ADCs sample at 2 Msamples/sec, and allow for motor position sensing and speed control. Precision PWM generators provide motor drive control, including stepper motors.

A 12-bit DAC samples at 500 Ksamples/sec, and provides precision voltage control of DC motors. An on-chip temperature sensor monitors system temperature to correct overheating conditions. External control is achieved via a CAN or USB bus; I²C and SPI interfaces are also available. Programming for specific motor control applications can be performed with free microcontroller firmware that provides pre-written motor control code.

For Free Info Visit http://info.hotims.com/49746-309

Motorized Actuators

Newport Corp. (Irvine, CA) has introduced the TRB motorized actuator series that provides motorized linear motion with up to 25 mm travel in a lightweight package. The actuators are designed as a direct replacement to the micrometers found in manual positioners or other applications requiring a linear pushing motion like deformable mirrors, inserters, or delay lines. The actuators are available in stepper and closed-loop DC servomotor versions. They include fixed integrated optical limit switches to prevent component or motor damage. They also provide a base for repeatable referencing and homing. The actuators include test results and are available with 6-, 12-, and 25-mm linear travel.

For Free Info Visit http://info.hotims.com/49746-310

Gearboxes

Lenze Americas (Uxbridge, MA) has introduced g500 gearboxes that enable speed-controlled operation with frequency inverters. They minimize losses, so the motor can generate less energy. The lower level of generated heat increases the overall service life. The gearboxes are designed for total integration with a Lenze Smart Motor, which provides integrated functions for material handling applications, including adjustable speeds between 500 and 2,600 RPM. The helical, helical-bevel, and shaft-mounted helical gearboxes are available in sizes from 45 to 600 Nm constructed in aluminum housings.

For Free Info Visit http://info.hotims.com/49746-312

Speed Controller

Lin Engineering (Morgan Hill, CA) offers the BL-100 intelligent, compact brushless DC speed controller that can be used with a large majority of BLDC motors. It features an input operating voltage of up to +48VDC, and up to 10 amps of continuous current, 20 amps peak. It also features closed-loop control with adjustable P and I values for finer tuning. The controller can be used in either analog or digital modes. The analog mode allows users to adjust speed and direction via the onboard potentiometer or an external potentiometer for higher resolution. The digital mode allows for communication via RS-485 (RS-232 and USB converter cards are available), and comes with a complimentary Graphical User Interface (GUI). The GUI enables users to configure acceleration and deceleration profiles, along with controlling multiple speed controllers through assigned character addresses.

For Free Info Visit http://info.hotims.com/49746-314

DC Motor Controls

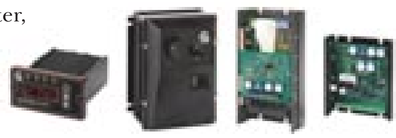

Groschopp (Sioux Center, IA) has introduced brushless DC motor controls for BLDC motors and gearmotors. Designed to provide commutated power and variable speed control, the closed-loop controls provide speed regulation over a range of loads. Features include line and low-voltage options, chassis-mount and NEMA 4X enclosures, and analog and digital options. The brushless speed controls are suitable for use where high torque, high speed, and quiet operation are needed.

For Free Info Visit http://info.hotims.com/49746-327

Linear Position Transmitters

Macro Sensors (Pennsauken, NJ) offers the HSIR Series LVDT linear position transmitters that can serve as level sensors to measure liquid level changes from a few inches to several feet in gauging tank level volumes when configured with a float. In this configuration, a stainless steel float coupled to a nonmagnetic stainless-steel rod is attached to the armature core of the LVDT. The 4- to 20-mA loop-powered position transmitter senses the position of the core and, therefore, the level of the float. Sensitivity to the change in level depends on the length of LVDT.

As water level changes, the float moves up or down, raising the LVDT core along with it. A threaded stainless steel rod that protrudes from the other end of the core carries two jam nuts that are used to adjust the position sensor output at the desired low water level.

Core position is sensed using magnetic induction. Electronics of the LVDT are hermetically sealed inside a stainless steel housing for protection against water and other environmental elements. A Teflon liner inside the bore minimizes any friction to core motion. As there are no springs to fatigue or parts to wear out, the LVDT sensors are nearly friction-free.

For Free Info Visit http://info.hotims.com/49746-313

Motion Stages

Bell-Everman (Goleta, CA) offers the SLS line of ballscrew- and linear-motor-driven sealed motion stages that feature a lip seal design that keeps debris, particulate, and liquid contaminants from gumming up the internal drive and bearing components. Made from a ruggedized polyurethane elastomer, the seal integrates with the stage's anodized aluminum housing. The seal's design allows it to be field-replaceable without disassembling the stage. Linear motor configurations can achieve accuracies of ±4 µm per meter of travel, and bidirectional repeatability of ±2 µm. Ballscrew configurations can achieve accuracies of ±10 µm per meter of travel, and bidirectional repeatability of ±5 µm.

Standard travel lengths are available from 100 to 1,000 mm, with custom lengths to 2,000 mm. Speeds to 4 m/sec for linear motor drives and 0.4 m/sec for ballscrew drives are achievable. Continuous linear force to 300 N is achievable for linear motor drives, and 1,540 N for ballscrew drives. Applications include laser machining, welding, semiconductor, machining, and other contamination-sensitive precision motion applications.

For Free Info Visit http://info.hotims.com/49746-316

Position Sensor

The Micronor MR330 Series fiber optic absolute position sensor system from Micronor (Newbury Park, CA) features 14-bit single-turn resolution. Rotary sensors are offered in two models: Standard MR332 and MRI Safe MR338. The absolute rotary encoder measures absolute angular position from 0° to 360° via programmable 13-bit (8,192 count) or 14-bit (13,950 count) resolution at speeds exceeding 2500 rpm. System firmware also tracks turns up to 12 bits (4096 revolutions). The controller features multiple built-in interfaces: SSI, USB, RS485 Serial, Modbus RTU, two analog outputs (4-20mA and ±10V), and two digital set points.

The position sensor is an all-optical design that resists electromagnetic interference such as lightning, radiation, magnetic fields, and other harsh environmental conditions. It uses an optical technique embedded in a passive sensor and active controller connected by a duplex fiber optic link. The controller transmits a burst of light to the code disk in the sensor that modulates the spectral components of the light based on angular position. The position information is imprinted in the optical spectrum of the light and guided back to the controller for position readout. The sensor requires no electrical power and houses no electronic components.

For Free Info Visit http://info.hotims.com/49746-325

Accelerometers

Meggitt Sensing Systems (Irvine, CA) offers Endevco Models 41A, 42A, and 43A Isotron accelerometers. The general-purpose, single-axis accelerometers feature 10, 25, 100, 500, and 1000 mV/g sensitivities for the 41A and 42A, with 100, 500, and 1000 mV/g for the 43A. Amplitude response of ±5% is 1 to 10,000 Hz. The stud-mounted accelerometers have a 10-32 threaded hole. The Model 41A mounting bottom is a hex with 10-32 top connector; Model 42A mounting bottom is hex with 10-32 side connector; and Model 43A has a cube shape that allows mounting in two different orientations, with the sensitive axis parallel to the connector and 10-32 connector. Optional accessories include cables, adhesive mounting adapter, and signal conditioners.

The Model 45A is a general-purpose, high-sensitivity triaxial accelerometer in a 20-mm cube shape with 500 mV/g (10 g range) and 1000 mV/g (5 g range) options. Amplitude response of ±5% is 1 to 6000 Hz for y- and z-axes, and 1 to 3000 Hz for x-axis. They are also stud-mounted with a 10-32 threaded hole.

For Free Info Visit http://info.hotims.com/49746-318

EtherCAT Drive Modules

ACS Motion Control (Bloomington, MN) has introduced UDMMC compact EtherCAT modules that feature two and four universal drives with ratings of 12 Vdc to 80Vdc, and 2.5A (5A peak) to 20A (40A peak) per drive. Each drive is programmable to control a two- or three-phase servomotor, a DC brush motor, a voice coil motor, and a two- or three-phase step motor. The motor drives address the needs of multi-axis motion applications with limited space.

The safe torque off (STO) cuts the power to the motor without removal of the power source for applications that are required to comply with SIL-3 and PLe safety levels. The four-axis modules can be ordered with mixed current specifications. It is a slave drive that runs under any ACS EtherCAT masters. The MMI Application Studio, a set of software support tools, is provided for configuration, setup, tuning, and diagnostics.

For Free Info Visit http://info.hotims.com/49746-319

Workholding Vice

The RZM Centric Vice from Röhm Products of America (Lawrenceville, GA) provides workholding rigidity and contributes to higher-accuracy 5-axis machining. The vice's design features clamping jaws positioned relatively high, and a horizontal spindle situated at the top of the vice and closer to the jaws. The jaws are shorter and complement the vice's overall compact height of 7.7" to minimize interference.

The double jaw-guidance system moves jaws along their axes to accommodate a range of part sizes without having to remount the jaws. In operation, the first jaw moves along an outside guideway as the second jaw travels on an inside one. This quasi-telescopic arrangement allows for a greater guidance length without placing significant limits on machining operations. When fully opened, the RZM presents little, if any, interference, and its telescoping design allows the jaws to close to the zero point.

For Free Info Visit http://info.hotims.com/49746-326

Motion Controllers

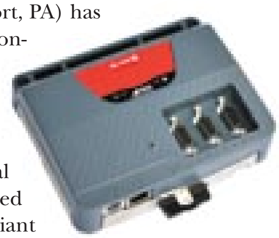

Trio Motion Technology (Freeport, PA) has introduced the MC403-Z motion controller in two versions offering control of two or three axes. The core axis connections can be configured as pulse and direction outputs to drives, or as incremental encoder feedback inputs or simulated encoder outputs. The three-axis variant allows one axis to be set-up as an extended axis where the connection may also be configured as an input for SSI, Tamagawa, or EnDAT absolute encoders.

The controllers feature a 64-bit ARM11 processor, digital and analog I/O count, built-in Ethernet, and the ability to add robotic transformations or synchronize motion with double floating point precision. The controller can undertake linear, circular, helical, and spherical interpolation across all axes, as well as flexible CAM shapes and linked motion. The controller has eight 24 VDC digital inputs including six 20-µsec registration inputs, and four 24 VDC bi-directional I/Os. Two 12-bit analog inputs are included, and an RJ45 Ethernet port is provided for programming and connection of HMI or other devices.

For Free Info Visit http://info.hotims.com/49746-328

Linear Motor Stages

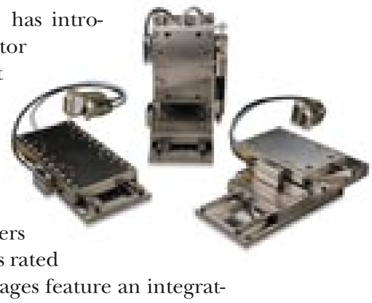

Kollmorgen (Radford, VA) has introduced MMG series linear motor stages in four models that deliver 25-mm, 50-mm, 100-mm, and 150-mm travel. They provide uncompensated accuracy from 6 um to 14 um, and resolution from 1.0 um to 5 nm. Each model delivers repeatability to ±0.4 um, and is rated for 10-kg load capacity. The stages feature an integrated feedback mechanism that eliminates the need for compensation tables or slope correction factors. A standard Z-axis counterbalance kit eliminates the engineering required to integrate a Z option. The stages leverage a standard 3-phase brushless motor to enable control with various drives and controllers. No specialized piezo or proprietary motor/drive technology is necessary. They can be used in constant velocity (CV) or high throughput point-to-point applications, allowing common units to be used.

For Free Info Visit http://info.hotims.com/49746-315

Tool Positioning System

The EPPINGER Trifix® tool positioning system from EXSYS Tool (San Antonio, FL) enables exchanges of both static and driven tooling for multitasking machines. Based on the VDI interface, the system provides positioning accuracy within 10 µm between tool stations, and single-position repeatability of less than 5 µm at a tool length of 3.9" (100 mm). After the user initially aligns the unit in the lathe turret, further adjustment for subsequent tool changes becomes unnecessary. As a result, manufacturers can preset tools off the machine, reducing setup time. Tooling can be mounted with four additional hold-down screws to maximize rigidity in heavy-chipload operations such as milling. Use of the Trifix system does not prevent a facility from using other tooling.

For Free Info Visit http://info.hotims.com/49746-329